UNIVERSITÀ DEGLI STUDI DI MILANO

DEPARTMENT OF PHARMACEUTICAL SCIENCES
Ph.D. PROGRAM IN PHARMACEUTICAL SCIENCES
XXXIII CYCLE

EXTEMPORANEOUS PREPARATIONS IN PERSONALIZED THERAPY: THE DESIGN OF ORODISPERSIBLE DOSAGE FORMS

APPLIED PHARMACEUTICAL TECHNOLOGY
CHIM/09

Ph.D. thesis of:
Garba Mohammed KHALID
Matriculation: R11987

Supervisor: Professor Francesca SELMIN
Program Coordinator: Professor Giancarlo ALDINI

ACADEMIC YEAR
2019/2020

UNIVERSITÀ DEGLI STUDI DI MILANO

DIPARTIMENTO DI SCIENZE FARMACEUTICHE
SCUOLA DI DOTTORATO IN SCIENZE FARMACEUTICHE
XXXIII CICLO

EXTEMPORANEOUS PREPARATIONS IN PERSONALIZED THERAPY: THE DESIGN OF ORODISPERSIBLE DOSAGE FORMS

SETTORE FARMACEUTICO TECNOLOGICO APPLICATIVO
CHIM/09

Tesi di dottorato di:
Garba Mohammed KHALID
Matricola: R11987

Supervisore: Professor Francesca SELMIN
Coordinatore del dottorato: Professor Giancarlo ALDINI

ANNO ACCADEMICO
2019/2020

This Ph.D. thesis is dedicated to Professor Paola Minghetti for her relentless support and inspiration.

Abstract

The advent of printing technologies for the production of orodispersible films (ODF) guides a growing interest in the application of these dosage forms to precision dosing in personalized medicine. Indeed, the tailoring of ODF shape, colour and/or dimension allows end-users to easily identify their own medicinal product, improving both safety and adherence (*Chapter 1*). At the same time, to open real perspectives towards ODF for personalized dosing, the design of such technologies should advance along with the development of easy and non-destructive assays, based on colorimetry and spectroscopy, which can allow to establish the physical and chemical quality of ODF (*Chapter 2*).

This doctoral thesis aimed to demonstrates the feasibility of a novel printing technology to extemporaneously compound ODF on-demand. The basic idea was to propose a novel apparatus that combines a hot-melt ram extruder with the plate of a 3D-printer. As far as the formulation is concerned, maltodextrins plasticized with glycerol were selected since they are excipients accepted for both children and elderly. The preparation method consists of simple operations, involving the mixing of the drug substance with maltodextrins and other excipients, then the loading of the mixture into the ram extruder, heating, and printing of the single ODF directly on the packaging aluminium foil. The versatility of this technology was tested by loading ODF with drugs having different physicochemical characteristics. First, paracetamol was selected as a model to demonstrate the drug payload which resulted in loading up to 74 mg/ 6 cm^2 and, therefore, allowing the preparation of ODF with a drug amount higher than the highest in the market (i.e., 100 mg/ 9cm^2) (*Chapter 3*). Then, diclofenac sodium was loaded as a model of heat-sensitive and bitter drug to prepare ODF intended for the treatment of migraine in paediatric population. The data revealed that, the exposure to relatively low temperature (i.e., ~ 90 °C) during the printing limited the formation of degradation by-products of the drug (< 0.2%).

Furthermore, to improve ODF palatability and patients' handing, a combination of taste-masking agents (TMA), opacifiers, and, when required, an anti-sticking agent are often loaded into ODF. Thus, the effect of these excipients on the physical properties of ODF loaded by diclofenac was also studied. The results revealed that titanium dioxide, selected as an opacifier, improved not only the ODF aesthetic appearance, but also ODF detachment from the primary packaging material, an aspect particularly relevant to prevent breakage during handing (*Chapter 4*).

Olanzapine (OLZ) was finally tested because it can undergo solid-state modifications under different processing conditions. In this case, the comparison on the performance of OLZ ODF prepared by the proposed technology and consolidated solvent casting technique, which requires the use of a large amount of water, revealed that hot-melt ram extrusion prevented the conversion of OLZ from anhydrous Form I to a pseudo-polymorphic form with lower solubility, which could affect the drug bioavailability (*Chapter 5*).

In conclusion, hot-melt ram extrusion printing can be advantageously used to prepare small batches of ODF made of maltodextrins and glycerine, avoiding the use of solvent and harsh temperatures. This basic formula can be exploited to load drugs differing in physicochemical characteristics, and other excipients to provide suitable organoleptic features of the final dosage form.

Riassunto

L'avvento di numerose tecnologie per produzione di film orodispersibili (ODF) ha suscitato un crescente interesse verso l'impiego di questa forma di dosaggio nell'ambito della personalizzazione della terapia. Difatti, la possibilità di ottenere ODF di diverse forme, colori e dimensioni permette a pazienti di identificare facilmente il medicinale, aumentando così la sicurezza e dell'aderenza al trattamento farmacologico (*Capitolo 1*). Tale avanzamento tecnologico deve tuttavia procedere parallelamente allo sviluppo di saggi non distruttivi e di facile esecuzione in farmacia per la determinazione e il controllo della qualità chimica e fisica degli ODF, come requisito imprescindibile alla sicurezza e all'efficacia (*Capitolo 2*).

Scopo della presente tesi di dottorato è quello di dimostrate la possibilità di produrre film orodispersibili su piccola scala mediante l'uso di una una nuova tecnologia di stampa costituita da una siringa termostatata in grado di estrudere a velocità costante la massa fusa di principio attivo ed eccipienti su un piatto mobile. La composizione della miscela comprende una maltodestrina plasticizzata con glicerica in quanto questi eccipienti sono idenei per la produzione di ODF sia per i pazienti pediatrici, sia per gli anziani. Il metodo di preparazione prevede dei semplici passaggi: la miscelazione del principio attivo con il polimero, plasticizzzante ed eventuali altri eccipienti; il caricamento dell'impasto nella siringa e il preriscaldamento dell'impasto fino a completo rammollimento; la conseguente forzatura attraverso l'ago per depositare il film orodispersibile con una forma definita su un foglio di alluminio che costituisce il confezionamento primario. La versatilità di questo approccio è stata verificata preparando ODF contenenti principi attivi con diverse caratteristiche chimico-fisiche. Tra le varie molecule modello, il paracetamolo è stato scelto per dimostrare la fattibilità di caricare una quantità di attivo (74 mg/ 6 cm^2) più elevate rispetto mercato dosaggi di ODF presenti sul mercato (100 mg/9cm^2) (*Capitolo 3*).

Nel caso dei film caricati con diclofenac sodico, utilizzato come esempio di sostanza termosensibile, non si è evidenziata la formazione di prodotti di degradazione dovute alle temperature utilizzate per rammollire la miscela (*Capitolo 4*). Per migliorare la managgevolezza e le proprietà organolettiche dei film, spesso sono aggiunti altri eccipienti quali edulcoranti, aromi e agenti che ne limitano l'appicicosità. In questo ambito, il diossido di titanio, selezionato come opacizzante, non solo ha permesso di migliorare le caratteristiche estetiche dei film, ma ha anche la rimozione del film dal materiale del confezionamento primario, aspetto che risulta particolarmente importante per evitarne la rottura durante la manipolazione da parte del paziente (*Capitolo 4*).

Infine, è stata caricata nei film una quantità pari a 10 mg olanzapine, come modello di sostanza soggetta a polimorfismo. In questo caso il confronto con processi di produzione che richiedono l'utilizzo di una sospensione su base acquosa, ha permesso di evidenziare che la tecnologia proposta elimina la possibilità di conversione dalla forma I alla forma pseudopolimorfica che è caratterizzata da una minore solubilità che potrebbe influire negarivamente sulla biodisponibilità di questa molecola (C*apitolo 5*).

In conclusione, la tecnologia basata su una modifica dell'estrusione a caldo potrebbe essere utilizzata per stampare film costituiti da maltodestrine e glicerina, limitando gli inconvenienti legati all'uso di solventi e altre temperature. Questa formulazione può essere sfruttata per ottenere film contenenti principi attivi con caratteristiche chimico-fisiche diverse, e altri eccipienti richiesti per migliorare le caratteristiche organolettiche di questa forma farmaceutica finita.

Table of Contents

Introduction

Orodispersible films (ODF) consist of a single or multilayer sheet of suitable materials intended to be place in the mouth where they rapidly dispersed upon contact with the saliva without need of water or munching. They provide the opportunity to meet the needs of specific subpopulation of patients suffering from a variety of disorders such as dysphagia due to pathological or psychological issues. In addition, children and elderly, and patients with limited access to water and/or restricted water intake can also benefit from their merits [1,2]. Indeed, the possibility to change size, shape and colour of the ODF have open new scenarios to prepare small batches for personalization of dose in special patient population. Furthermore, ODF can be advantageously used as a carrier for other technologies, such as microparticles, nanocrystals and self-emulsifying systems [1,3–5], which can control the drug release patterns [1]. However, one of the main disadvantage in ODF formulation is related to the limited formulation space [6] which implies a limited drug loading capacity. Secondly, palatability drives the compliance for ODF loaded formulations, but the formulation space often limits the addition of taste masking agents; even if both bitter and/or astringent taste of a drug can be opportunely reduced and/or eliminated [7,8]. Thirdly, the manufacturing process at the industrial scale is mainly based on solvent-casting technologies, which require specialized equipment common only to transdermal patches, and therefore, the number of manufacturers worldwide are limited [1]. Among the critical quality attributes of ODF, satisfactory tensile properties to guarantee packaging and handling during administration without breakage, the disintegration and dissolution in the oral cavity, acceptable taste [1], aesthetic appearance, and stability of the dosage form itself and the loaded drug(s) need to be carefully studied.

More recently, researchers are striving to optimize and/or to develop technologies to exploit ODF peculiarity to produce small batches for individualize therapy. Indeed, the term “customized dosage form” should be related not only to a tailored dose, but also to doses on-demand, shape and colour of a dosage form [1,9] and ODF would also allow end-users to easily identify their own medicine, improving medication safety and adherence [1]. As an example, in the case of children, it has been estimated that the availability of authorized medicinal products for children varies between the range of 48% to 54% of all approved ones and that up to 50% of paediatric patients receive an unlicensed or off-label prescriptions [10]. Indeed, it has been recognized that children are unable to or have difficulties with swallowing tablets or capsules[10,11]. Moreover, crushing tablets, opening capsules, or mixing powders to extemporaneously prepare the required dose with liquids may lead to dose variability, contamination, drug instability, taste and solubility problems, and other consequences for

safety of the patient and the efficacy of the treatment. It is therefore of paramount importance to develop age-appropriate dosage forms, as pointed out by the World Health Organization's (WHO) initiative 'Better medicines for children' [12] and to address some of the European Medicine Agency's (EMA) recommendations [EMA/766040/2015] on age-appropriate dosage forms [13].

Personalized ODF prepared on-demand by printing technologies could potentially fulfil patients' special needs. Furthermore, these processes could make possible the printing of medicines in pandemic outbreak areas to mitigate drug shortages and supply chain disruptions, and potential for making available printing of medicines in war zone, clinical trials in hospital settings [14,15] and preparation of individualized fixed-dose combination products [15–17].

Till now, the proposed printing technologies present some limitations. In particular, the ink-jet printing techniques require the design of formulations which are strictly related to the active pharmaceutical ingredient (API) features; such as the compatibility and solubility of the API with the ink solution, and possible sedimentation of the API from the ink solution which may result in dose variability of the printed ODF [1]. The fused deposition modelling (FDM) printing approach is based on drug loaded filaments which are not commercially available and, therefore, this technique cannot be easily used in a pharmacy setting [18]. Thus, the design of a versatile ODF preparation apparatus and the use of a formulation easy to be prepared is still required.

Aim of the thesis

Based on these considerations, this doctoral thesis aimed to demonstrates the feasibility of a novel printing technology which allows the extemporaneous compounding of ODF in personalized therapy by simple operations.

As far as the formulations is concerned, maltodextrins with DE of 6 (MDX) were selected since they were already used to prepare ODF by casting [3,7,19] and hot-melt extrusion [18, 20, 21].

Regarding the design of the printing equipment, the basic idea was to propose a novel apparatus which combines the ram extrusion with the plate of a FDM in the attempt to manipulate small amount of materials, in the order of few mL or grams.

The work was organized into two steps in order not only to demonstrate the feasibility of the approach, but also to test the versatility of the proposed technology by loading drugs with different physico-chemical peculiarities, such as heat-induced chemical instability and polymorphism. Moreover, the attention was also focused on the effect of excipients generally used to design of ODF, i.e., taste masking agents and opacifiers.

To obtain these purposes, the following objectives were considered:

1. to set-up of printing equipment and the choice of suitable components to prepare ODF. The excipient selection is related to possible safety risks in a subpopulation of patients (i.e., children) and the extrusion process;
2. to load the ODF with drug substances with different requirements, such as dose, thermal sensitiveness, and taste-masking strategy. Regarding the drug substances with a high tendency to polymorphism, the *in vitro* biopharmaceutical properties were compared to those of ODF obtained by a well-established technique (i.e., solvent casting).

Preliminarily, a critical appraisal of the literature on the current trends in the ODF production (*Chapter 1 - Trends in the Production Methods of Orodispersible Films*) and characterization methods from slurries to the finished medicinal products (*Chapter 2 - Trends in the Characterization Methods of Orodispersible Films*) was carried out to individuate which are the unanswered need to meet in terms of ODF preparations and characterizations.

For the proposed printing technique, the first approach was focused on setting up the hot-melt ram extrusion printer and defining the processing variables in terms of material composition (film forming polymers, plasticizers and their ratios); rheological characterization of the polymer blends; printing conditions (printing temperature, angle of deposition, and printing speed); and finally drug loading was tested using paracetamol as a model drug with different amount per ODF to elucidate the application of the technology for personalized dosing (*Chapter 3 - Personalized Orodispersible Films by Hot-melt Ram Extrusion Printing*).

To evaluate the robustness of this novel approach, diclofenac sodium (DNa) was loaded to (i) to determine if the working temperature of 95 ºC is suitable for thermosensitive drug; (ii) to assess the influence of taste-masking agents and an opacifier on the technological properties (i.e. disintegration time, *in vitro* dissolution profiles, tensile properties, and peeling from the packaging material); (iii) to tune the ODF surface area in the attempt to prepare age appropriate DNa ODF for paediatric patients. Finally, a stability test in accelerated conditions was carried out over six-month period (*Chapter 4 - Extemporaneous Printing of Diclofenac Orodispersible Films for Paediatrics*).

Finally, the influence of ODF preparation method on the solid-state of polymorphic drugs was tested using olanzapine (OLZ) as a model drug by comparing hot-melt ram extrusion printing and the conventional solvent casting on the *in vitro* performances of OLZ ODF aiming to evaluate the possible loading of drug with significant physical stability (*Chapter 5- A*

comparison of preparation methods on the in vitro performances of olanzapine orodispersible films).

Refences

[1] Musazzi UM, Khalid GM, Selmin F, et al. Trends in the production methods of orodispersible films. Int. J. Pharm. 2020;576.

[2] Cilurzo F, Musazzi UM, Franzé S, et al. Orodispersible dosage forms: biopharmaceutical improvements and regulatory requirements. Drug Discov. Today [Internet]. 2018;23:251–259. Available from: http://dx.doi.org/10.1016/j.drudis.2017.10.003.

[3] Lai F, Franceschini I, Corrias F, et al. Maltodextrin fast dissolving films for quercetin nanocrystal delivery. A feasibility study. Carbohydr. Polym. [Internet]. 2015;121:217–223. Available from: http://dx.doi.org/10.1016/j.carbpol.2014.11.070.

[4] Musazzi UM, Passerini N, Albertini B, et al. A new melatonin oral delivery platform based on orodispersible films containing solid lipid microparticles. Int. J. Pharm. [Internet]. 2019;559:280–288. Available from: https://doi.org/10.1016/j.ijpharm.2019.01.046.

[5] Talekar SD, Haware R V., Dave RH. Evaluation of self-nanoemulsifying drug delivery systems using multivariate methods to optimize permeability of captopril oral films. Eur. J. Pharm. Sci. [Internet]. 2019;130:215–224. Available from: https://doi.org/10.1016/j.ejps.2019.01.039.

[6] Borges AF, Silva C, Coelho JFJ, et al. Outlining critical quality attributes (CQAs) as guidance for the development of orodispersible films. Pharm. Dev. Technol. 2017;22:237–245.

[7] Cilurzo F, Cupone IE, Minghetti P, et al. Nicotine Fast Dissolving Films Made of Maltodextrins: A Feasibility Study. AAPS PharmSciTech [Internet]. 2010;11:1511–1517. Available from: http://www.springerlink.com/index/10.1208/s12249-010-9525-6.

[8] Cilurzo F, Cupone IE, Minghetti P, et al. Diclofenac fast-dissolving film: Suppression of bitterness by a taste-sensing system. Drug Dev. Ind. Pharm. 2011;37:252–259.

[9] Vakili H, Nyman JO, Genina N, et al. Application of a colorimetric technique in quality control for printed pediatric orodispersible drug delivery systems containing propranolol hydrochloride. Int. J. Pharm. [Internet]. 2016 [cited 2019 Apr 7];511:606–618. Available from: https://linkinghub.elsevier.com/retrieve/pii/S0378517316306627.

[10] Selmin F, Musazzi UM, Cilurzo F, et al. Alternatives when an authorized medicinal product is not available. Med. Access @ Point Care. 2017;1:16–21.

[11] Casiraghi A, Musazzi UM, Franceschini I, et al. Is propranolol compounding from tablet safe for pediatric use? Results from an experimental test. Minerva Pediatr. 2014;66:355–362.

[12] World Health Organization (WHO), 2010. Better Medicines for Children: Country implementation. https://www.who.int/childmedicines/countries/en/ [assessed September 13, 2020].

[13] EMA, 2015. European Medicines Agency: EMA/766040/2015. Report of the expert meeting on paediatric development of fixed-dose combinations (FDCs) for the treatment of human immunodeficiency virus (HIV) infection.

[14] Goyanes A, Madla CM, Umerji A, et al. Automated therapy preparation of isoleucine formulations using 3D printing for the treatment of MSUD: First single-centre, prospective, crossover study in patients. Int. J. Pharm. [Internet]. 2019;567:118497. Available from: https://doi.org/10.1016/j.ijpharm.2019.118497.

[15] Fernández-García R, Prada M, Bolás-Fernández F, et al. Oral Fixed-Dose Combination Pharmaceutical Products: Industrial Manufacturing Versus Personalized 3D Printing. Pharm. Res. 2020;37.

[16] Alomari M, Vuddanda PR, Trenfield SJ, et al. Printing T3and T4oral drug combinations as a novel strategy for hypothyroidism. Int. J. Pharm. 2018;549:363–369.
[17] Alhnan MA, Okwuosa TC, Sadia M, et al. Emergence of 3D Printed Dosage Forms: Opportunities and Challenges. Pharm. Res. [Internet]. 2016;33:1817–1832. Available from: http://dx.doi.org/10.1007/s11095-016-1933-1.
[18] Musazzi UM, Selmin F, Ortenzi MA, et al. Personalized orodispersible films by hot melt ram extrusion 3D printing. Int. J. Pharm. 2018;551:52–59.
[19] Cilurzo F, Cupone IE, Minghetti P, et al. Fast dissolving films made of maltodextrins. Eur. J. Pharm. Biopharm. 2008;70:895–900.
[20] Repka MA, Gutta K, Prodduturi S, et al. Characterization of cellulosic hot-melt extruded films containing lidocaine. Eur. J. Pharm. Biopharm. 2005;59:189–196.
[21] Speer I, Preis M, Breitkreutz J. Prolonged drug release properties for orodispersible films by combining hot-melt extrusion and solvent casting methods. Eur. J. Pharm. Biopharm. [Internet]. 2018;129:66–73. Available from: https://doi.org/10.1016/j.ejpb.2018.05.023.

Chapter 1

Trends in the Production Methods of Orodispersible Films

Chapter 1

1.1 Introduction

Orodispersible films (ODF) are single or multilayer sheets of suitable materials intended to liberate rapidly the loaded active substance in the mouth, forming a fine suspension or solution in the saliva without mastication or water intake. ODF appear attractive for patients affected by functional or psychological dysphagia or, more in general, preferring a liquid dosage form, such as paediatrics [1, 2], geriatrics [3], bedridden and people who cannot have access to water. Indeed, ODF combines the dose accuracy typical of solid dosage forms and the ease of administration characteristic of liquid dosage forms [4]. ODF have the size of a postage stamp and are individually packed so that transportation and consumer handling is friendly. Furthermore, ODF can be advantageously used also as a carrier for other technologies, such as microparticles, nanocrystals and self-emulsifying systems [5, 6,7], which rule the drug release rate and, therefore, its bioavailability.

On the other hands, the main drawbacks are due to the limited formulation space [8] which implies a limited drug loading capacity. As an example, the highest dose available on the market is a 100 mg sildenafil ODF, but potent drugs are generally loaded. Palatability drives the compliance, but the formulation space limits the addition of excipients to taste mask; even if both astringent or bitter taste of drug can be opportunely reduced and/or eliminated [9, 10]. Finally, the manufacturing process at the industrial scale is mainly based on solvent-casting technologies, which require production chains with specialized equipment which are common only to transdermal patches, and therefore, the number of manufacturers worldwide is limited. Nevertheless, similarly to the transdermal patches, the dose loaded in an ODF is defined by their size and, therefore, the same production chain could be used to prepare batches of different drug strengths. Because of this peculiarity, researchers are striving to optimize and/or to develop technologies to exploit this peculiarity in the extemporaneous compounding of small batches of ODF in a pharmacy setting. Since the term “customized dosage form” should be related not only to a tailored dose but also to doses on-demand, shape and colour of a dosage form, this innovation would also allow end-users to easily identify their own medicine, improving the safety and adherence.

This review aims to describe the current trends in the ODF production by continuous manufacturing as well as for the preparation of small batches for an individualize therapy.

The references were extracted from SCOPUS and Web of Science databases using the following keywords: Disintegrant film, Orodispersible film, Fast dissolving film and Oral thin film.

1.2 Solvent casting

Solvent casting is the first and the most widely used method for the preparation of ODF [11, 12, 13]. Since this technique is widely exploited at the industrial level due to the straightforward manufacturing process, it is also the first one investigated in laboratory settings [14]. The solvent casting production process is mainly based on three steps: the preparation of a homogenous slurry mixture of components, obtaining a dried laminate by solvent casting and die cutting of laminate in desired films. For the first step, the active substance and excipients are dissolved and/or dispersed in an appropriate solvent (*e.g.,* water) using the equipment commonly used for the preparation of several liquid or semisolid preparations (*e.g.*, stirring tank at industrial level, beaker in a bain-marie in a laboratory/pharmacy setting). Then, slurries are cast and dried to give a film with a constant thickness which assures the uniformity of drug content. For the industrial continuous manufacturing, these steps require an apparatus able to control both the casting of the viscous slurry on a PET or a siliconized foil (*i.e.*, the carrier) and the solvent evaporation leads to the formation of a dried laminate which is, then, rolled up in jumbo rolls. The jumbo rolls are cut in reels whose length determines one of the two dimensions of the ODF. Afterwards, the reels are loaded in the packaging machine, which unrolls and separates the film from the carrier before the die-cutting in the desired shape. At the same time, the packaging machine seals a bag usually made of three-laminates resistant to moisture material and inserts the dosage form to give the single packed ODF.

To personalize the dose strength according to clinical needs, the patient can cut directly the tape ODF. In this context, the reel can be packaged or loaded in a device able to cut the film in the desired length to define the appropriate dose [15, 16. However, since ODF is handled in a not-controlled environment, the humidity could affect the physical stability of the reel.

Solvent casting can be also adapted to the production of small batches of ODF [16, 17] (**Figure 1.1**) and multi-layer films intended to administer fixed drug combinations [18]. In particular, API with physicochemical

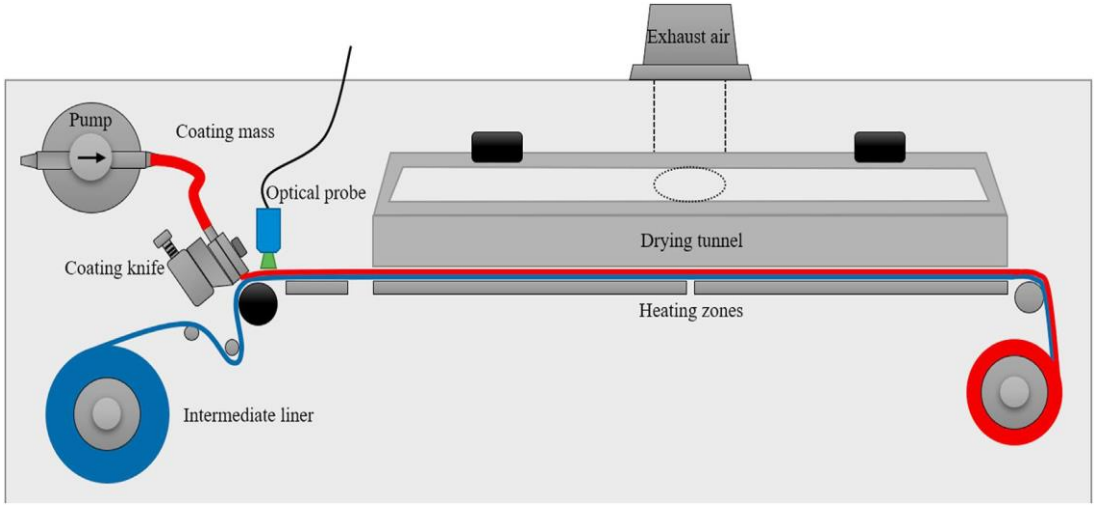

Figure 1.1. Schematic view of the pilot-scale coating bench for continuous oral film manufacturing equipped with the optical probe for wet-film thickness measurement, reprinted from [18], with permission.

incompatibility can be loaded at different strengths in different film layers in the same preparation process.

In case of ODF compounded in a pharmacy setting, machinery described above are generally too expensive and not easy to be adapted at the compounding processes. Alternatively, several methods have been proposed in the literature as summarized in **Table 1.1**. The simplest approach to compound ODF is based on the use of a Petri plate or proper slab, where a known amount of a drug-loaded polymeric slurry is casted and dried at an appropriate temperature [5, 13]. However, the uniformity of content is difficult to assure since the Petri dish/slab has to be maintained perfectly horizontal in the oven to have a film with a constant thickness. To solve this issue, Foo and co-workers proposed a novel unit-dose plate filled by the desired volume of component mixture solution (**Figure 1.2**) [19]. Alternatively, doctor-blade film coaters can be used [14]; the slurry is spread onto a substrate homogeneously by a metering blade which removes the excess of mass and allows to achieve the desired coating thickness; these systems can also be connected with an oven to maximise the solvent evaporation [12, 20]. Nevertheless, the rheological properties and the wettability of the carrier have to be in-depth investigate to assure the film uniform thickness [21]. Thereafter, the obtained dried laminate is die-cut into pieces of the desired size.

Based on of ODF. The dose can be adjusted according to the

Table 1.1– ODF prepared by solvent casting technologies, main components and features.

Apparatus	Film-forming polymer(s)	Plasticizer(s)	Solvent	Other formulative notes	Reference
Automatic film applicator	HPC, HPMC	GLY	Water	Tragacanth, xanthan gum or Arabic gum used as thickening agents	[22]
Automatic film applicator	HPC, HPMC, PEO, SC	GLY, PG, PEG	Water	β-cyclodextrins for taste masking of donepezil	[23]
Automatic film applicator	HPMC	GLY	Water	Loading of prolonged-release diclofenac sodium micro-pellets	[24]
Automatic film applicator	HPMC	GLY	Water	Dissolution of the risperidone nanocrystals are carefully evaluated	[25]
Automatic film applicator	HPMC	GLY, PEG 200	Water	Loading of prednisolone microparticles	[26]
Automatic film applicator	HPMC	GLY, TPGS	Water	Loading of tadalafil nanocrystal	[27]
Automatic film applicator	HPMC	PEG 1500	Water	Films cut using a rotary blade	[28]
Automatic film applicator	PVA	GLY	Water/ethanol	Mesoporous silica nanoparticles as dissolution enhancers	[29]
Automatic film applicator + air-forced oven	MDX	GLY	Water	Loading of melatonin lipid microparticles.	[6]
Automatic film applicator + air-forced oven	MDX	GLY	Water	Improving film tensile strength by PVA nanoparticles	[30]
Automatic film applicator + air-forced oven	MDX	GLY	Water	Loading of quercetin nanocrystals	[31]
Automatic film applicator + air-forced oven	MDX	GLY, amino acids	Water	Used of amino acids as non-traditional plasticizer of maltodextrin	[32]

Automatic film applicator + air-forced oven	Poly-sodium methacrylate, methyl methacrylate	PEG 400	Water	Evaluation of the residual water on film mechanical properties	[33]
Automatic film applicator + air-forced oven	SC	Sorbitol	Water	QbD:	[34]
Continuous manufacturing apparatus	HPC, HPMC	GLY	Water, ethanol or acetone	Comparison with discontinuous process	[35]
Continuous manufacturing apparatus	HPC, PVA	GLY	water/ethanol	Multilayer ODF	[36]
Continuous manufacturing apparatus	HPMC, PVA, HPC	GLY, triethyl citrate, citric acid	Water	Personalization of the dose by a cutter which allows the unroll of the loaded reel	[16]
Plate (acrylic)	Gelatine, SC	Sorbitol	Water	ODF as supplement carrier	[37]
Plate (glass)	Guar gum	Sorbitol	Water	Prolonged release by alginate beads	[38]
Plate (glass)	HPMC	PG	Water	Disintegrants	[39]
Plate (glass)	HPMC, PVA	PEG 400	Water	Lacidipine loaded as nanoparticles	[40]
Plate (non-stick baking tray)	PVA/CMC	GLY	Water	Comparison with printed loaded with clonidine	[41]
Plate (polypropylene)	HPC, Pectin	Not specified	Water	Loading of olmesartan nanocrystal	[42]
Plate (polypropylene)	HPMC E5	PG, GLY	Water/ethanol	poloxamer 407 and hydroxypropyl-β- cyclodextrin to improve the solubility of triclosan	[13]
Plate (polypropylene)	PL/pectin (tamarind)	Sorbitol, GLY, glucose	Water	Taste masking of aprepitant by tamarind pectin	[43]

Plate (Teflon®)	HPMC/chitosan	GLY	Water	Mannitol as drug release modifier (data on animal model)	[44]
Plate (Teflon®)	Kollicoat IR	GLY	Water	Optimization by QbD: orthogonal array Taguchi design	[45]
Plate (unit-dose)	HPMC E5	GLY	Water	Defined unit-dose	[46]
Slab (glass)	HPMC	PEG400	Water	Loading of a self-emulsifying system	[47]
Slab (glass) + polyester liner	MDX	Xylitol, sorbitol	Water	Addition of superdisintegrant in the film base	[48]
Suction film applicator (Erichsen, Hemer, G)	PL/trehalose	GLY	Water	Loading of proteins, Drying by evaporation or sublimation	[49]
Vacuum film applicator (Erichsen, Hemer, G)	HPMC: Carbopol, HPC, sodium CMC	GLY	Water	Loading of poorly water-soluble diazepam	[20]

CMC: carboxymethyl cellulose, GLY: glycerol, HPMC: hydroxypropyl methylcellulose, HPC: hydroxypropyl cellulose, MDX: maltodextrins, QbD: quality by design, PEG: polyethylene glycol, PEO: polyethylene oxide, PG: Propylene glycol, PL: pullulan, PVA: polyvinyl alcohol. SC: pregelatinized starch.

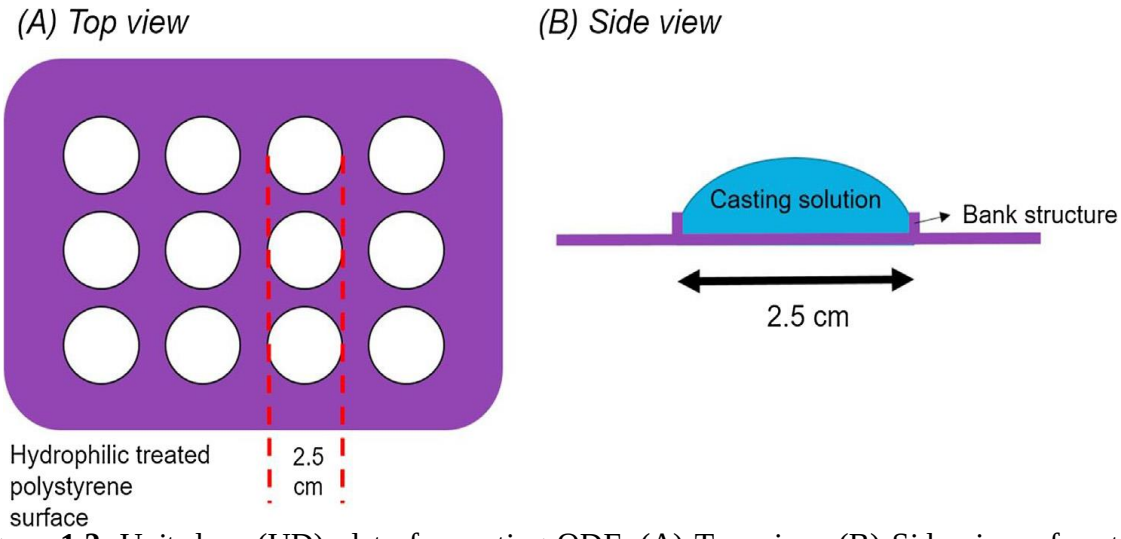

Figure 1.2. Unit-dose (UD) plate for casting ODF. (A) Top view. (B) Side view of casting solution confined in the casting well encircled by bank structures, reprinted from [19], with permission.

patient's needs cutting the reel or laminate at the desired shape. This technology is also suitable to load a particular payload, such as nanocrystals dispersion which can increase the drug dissolution rate [23, 25, 31, 42], or microparticles which permit to obtain a gastroprotection or a prolonged drug release [6, 26, 24]. Obviously, nano- or microsystem might strongly impact on the film mechanical properties.

Generally, the formulation parameters strictly related to the film-forming material have to be monitored to avoid foaming during the mixing or the solvent evaporation, flaking during slitting, cracking during cutting or sticking to the packaging material. In this context, the ratio between the plasticizer and the film-forming material has to be rationalized [9] or particular excipients can be added to maintain suitable film properties. As an example, the tendency of maltodextrin to stick to the primary packaging can be solved by adding a nanofiller [30].

1.3 Electrospinning

Electrospinning is another solvent-based technology explored to produce ODF characterized by a high-porous inner structure [50]. Although differences among electrospinning machineries, the basic set-up consists in a metallic needle, through which the formulation is pumped with a controlled flow and charged under a high-voltage electric current in the 10–35 kV range, above an opposite-charged collector [51]. The active substance can be loaded both before and after the spinning process [52]. In the former case, the main advantage is the improvement of the drug dissolution rate due to the huge surface area of nanofibers. In the

latter case, placebo ODF can be embedded by the drug solution and dried, widening the possible applications of such technology.

Poly(vinyl pyrrolidone), gelatine and poloxamers (**Table 1.2**) are among the most studied materials to obtain electrospun ODF not only because these polymers are suitable to load both API and food supplements [53, 54, 55], but also they enhance the apparent solubility of drug. Indeed, PVP forming hydrogen bonds with the other component(s) [56] allows to stabilize a supersaturated system and, therefore, improve the apparent solubility [57]; poloxamers offer improved wettability in addition to molecular dispersion [58].

Alternatively, to the use of a solvent- and polymeric-based dispersion, the spinning of melted materials was investigated using a complex spironolactone-hydroxypropyl-β-cyclodextrin as model system [59]. Furthermore, aiming to prepare a fixed-dose combination, the combination of electrospinning and inkjet printing was proposed as a valid alternative to the solvent-casting of multi-laminates [36]. Palo and co-authors demonstrated the feasibiliy to deposite lidocaine on the electrospun and cross-linked gelatine substrates by inkjet printing, whereas piroxicam was incorporated within the substrate fibres during electrospinning [60]. The analysis of solid-state of piroxicam, which is a low soluble drug with a monohydrate and three polymorphic forms [61], evidenced that the amorphous state was stabilized by gelatine. Although electrospinning is proposed for large scale-application [62], this technology appears promising for the preparation of small batches due to low operative flow rates from 0.5 to 2.0 mL/h [53, 63]. However, even if the equipment seems simple to use, some drawbacks limit the application for the preparation of ODF in a pharmacy setting. Indeed, the formulation to spin has to be carefully characterized to assure the reproducible formation of nanofibers and the process parameters optimized; the use of solvents can generate hazardous waste and the yield is low electrospinning process requires low viscosity fluid [52, 64].

Table 1.2 – ODF prepared by electrospinning, and HME technologies, main components and features.

Apparatus	Polymer	Solvent	Other notes	Reference
Electrospinning	Eudragit®E	-	Melt electrospinning	[59]
Electrospinning	Gelatin	PG, water	Single and combination of lidocaine HCl and piroxicam loaded by inkjet on electrospun as a substrate	[60]
Electrospinning	PEO	Water	potassium iodate nanocrystals	[54]
Electrospinning	PVA	Water	Riboflavin/caffeine fixed combination	[65]
Electrospinning	PVA, Kollicoat IR, HPMC	Water	Solid dispersion of donepezil with improved dissolution	[62]
Electrospinning	PVP	Ethanol	Amlodipine/valsartan fixed combination	[66]
Electrospinning	PVP K30	Ethanol	Solid dispersions of ketoprofen with improved dissolution	[63]
Electrospinning	PVP K30	Ethanol	Solid dispersions of ibuprofen electrospun with improved dissolution	[67]
Electrospinning	PVP K60	Ethanol	Paracetamol/caffeine fixed combination	[53]
Electrospinning	PVP K90	Water/ethanol	Solid dispersions of irbesartan with improved solubility and dissolution	[68]
Electrospinning	PVP K90, PVP K10	Ethanol	Taste masking of helicid with improved dissolution	[55]
HME	HPC	Triethyl citrate	Effect of Kollidon® VA 64 (KOL) and Soluplus® (SOL) on film dissolution and mechanical properties	[69]
HME	MDX	Glycerol	Cellulose microcrystalline as an anti-sticking agent	[12]

HME	Modified starch	Glycerol	Continuous manufacturing with a degassing port attached to the extruder to avoid air bubbles.	[70]

HPMC: hydroxypropyl methyl cellulose, HPC: hydroxypropyl cellulose, MDX: maltodextrin, PEO: poly(ethylene oxide); PG: Propylene glycol, PVA: poly(vinyl alcohol), PVP: poly(vinyl pyrrolidone

1.4 Hot-melt extrusion

In order to avoid the use of solvent(s) in the ODF production, the feasibility of extrusion technologies has been investigated [71]. In particular, hot-melt extrusion (HME) can be used for both continuous manufacturing and preparation of different dosage forms [72]. In general, HME consists of an apparatus in which a mixture (i.e., API and excipients) is melt and extruded through a die. In the case of film production, their final thickness and wideness is controlled not only by the die dimension but also by the geometry and rotational rate of the calendrer which differently stretches the extrudate during the formation of the reel. The extrusion apparatus can be ram- or screw-based. The first configuration consists of a ram compressing the melt material in a heated barrel and pushing them through a die for the high pressures. The second one consists of one or two rotating screws inside a heated barrel. The twin screw-based design provides a more uniform mixing with respect to the other two configurations. As casting technique, HME can be easily adapted to operate in continuous and to mount process analytical technologies [72].

Despite the possible advantages of such technique, the HME application to ODF preparation is limited to few examples (**Table 1.2**) because polymers used for the preparation of ODF (e.g., polysaccharides) are generally heat sensible and/or exhibit high value of glass transition temperature that cannot easily tuned by adding a plasticizer. Indeed, the addition of large amount of plasticizer can give too sticky or ductile ODF [12]. In 2008, our research group demonstrated the possible application of screw-extrusion technology in the production of maltodextrin ODF [12]. Using the design of experiment, Low and co-workers investigated the effect of drugs and excipients with different physicochemical and technological properties on the performance of ODF made by hydroxypropyl cellulose [69]. They also showed that the disintegration and dissolution profiles can be modulated by the addition of solubilizing polymers. The addition of the API to the basic formulation has not only an impact on the extrudate processability but also on the mechanical properties of the final films. Finally, Pimarande et al. focused the attention on starch matrices plasticized by glycerol, demonstrating that ODF with a very fast disintegration time (6-11 s) can be prepared by single-screw HME (110 °C) [70]. The results also highlighted that a devolatilizing system was needed to remove the vapour created by the melt of the materials and, therefore, to obtain non-sticky, homogeneous extrudates.

With respect to other solvent-based preparation techniques, HME allows preserving better the physicochemical stability of API sensitive to water. However, the higher operating temperatures limited the number of API that can be processed using this technology.

1.5 Printing technologies

Printing of pharmaceuticals refers to two different deposition models both of which can lead to the fabrication of ODF [73, 74]. 2D printing requires the use of an edible carrier ("substrate") that would hold/sorb the deposited ink in a digitally predefined pattern; 3D printing enables also printing in the Z direction by adding material layer-by-layer, resulting in a 3D dosage form. However, despite efforts to move from a discontinuous towards continuous printing process [75], most of the methods described in literature appears more suitable for the preparation of small or very small batches. Furthermore, since the ODF are produced using a preformed film or formed directly with the required surface and shape, the relevance of mechanical properties in the definition of the quality attributes is limited since the dosage form should comply only with the stresses generated by the patient handling and not by those generated by the unrolling of the reels.

1.5.1 Ink-jet printing

Through ink-jet printing (IJP), there are potentially only three main stages of the manufacturing of ODF: (I) the preparation of the ink containing an API as solution or suspension, (II) the jetting of the ink on an edible substrate in a programmed way and (III) the drying (**Figure 1.3**). As exemplified in **Table 1.3**, this technology enables the deposition of several API with high potency [76] and/or a narrow therapeutic index [77].

Based on the mechanism generating the drops, IJP technologies are classified as continuous jetting printing (CJP) and drop-on-demand (DOD) printing [73]. In the first case, there is a consistent ejection of a liquid through a nozzle which produces a continuous stream of ink primary drops "steered" to a landing site to produce the printed pattern. This is obtained by applying an electric charge on some of the drops that deflect the stream from the main axis under an electrostatic field [78]. The jetting of the ink through the nozzle forms a liquid stream, or column, which becomes an elongated tail and ends up in a single primary drop able to impact on the substrate guaranteeing the good quality of printing. In DOD printing, the production of individual drops takes place rapidly under the response of

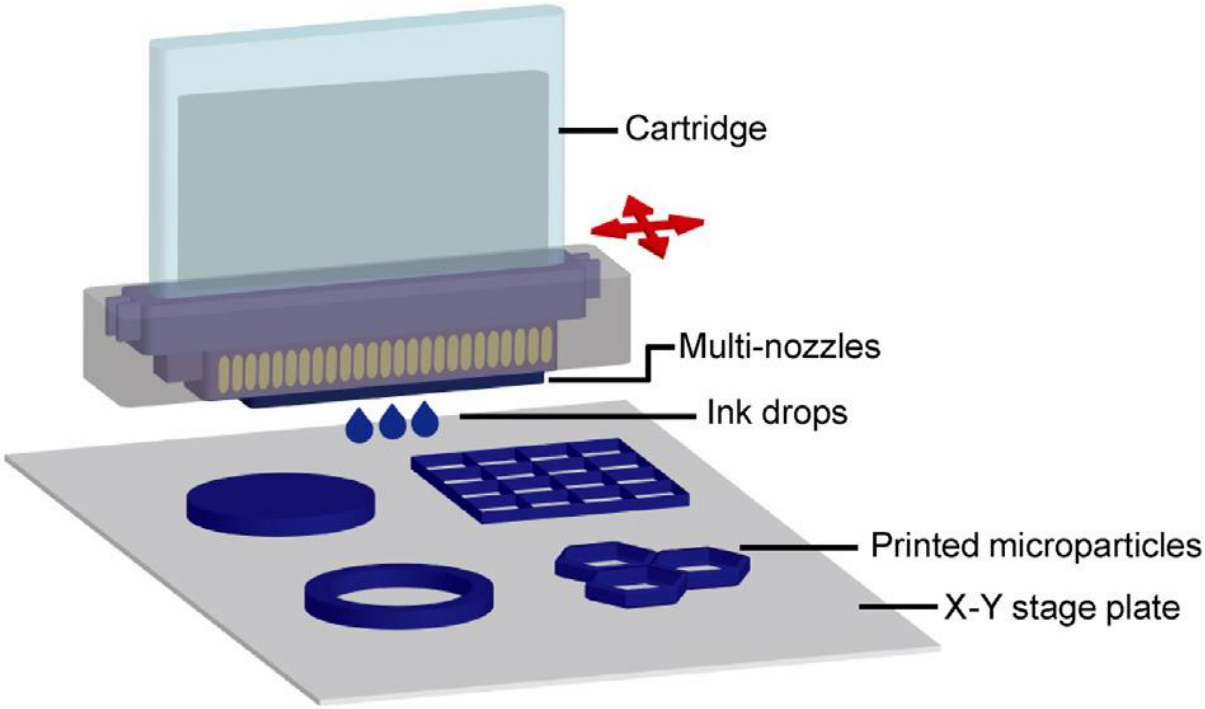

Figure 1.3. Schematic representation of a conventional drop-on-demand piezoelectric inkjet printing system for fabrication of drug-loaded microparticles, reprinted from [79], with permission.

a trigger signal. The drop ejection occurs due to the kinetic energy of drops generated from the source located in the printhead nearby to each nozzle [80] and the two main technologies are piezoelectric and thermal printing. In both cases (i.e., CJP and DOD), the printhead apparatus may be based on a single nozzle or multiple nozzles ranging from 100 to 1000 in number. The thermal IJP uses brief heat pulses generated by a resistive element to the jet fluid. Each print head contains a micro-resistor which heats up rapidly on receipt of electric pulses, forming a superheated vapour bubble. The vapour bubble expands, forcing out the fluid from the nozzle and producing a droplet. Then, the vapour bubble collapses creating a partial vacuum that pulls fluid from the ink reservoir to refill the thermal ink-jet chamber. In piezoelectric IJP, each nozzle is surrounded by a piezoelectric element usually made from lead zirconate titanate. When a voltage is applied to the element, it deforms, creating pressure waves leading to the ejection of the fluid. Once the element returns to its normal shape, the nozzle is filled with ink, ready to be reactivated [73]. Moreover, the droplets can also be dispensed with a high spatial resolution in a given pattern so that IJP can be exploited to print the precise amount of a drug (i.e., haloperidol) in the form of a QR code on an edible substrate [81]. Afterwards, drying can be carried out to reduce the solvent

Table 3 - ODF prepared by printing technologies, main components and features.

Apparatus	ODF				
	Polymer/substrate	**Plasticizer**	**solvent**	**Other notes**	**reference**
Solvent-based methods					
Inkjet	Edible paper	-	3% Tween 20, water	Combination of nanocrystal and inkjet printing technologies	[82]
Inkjet	Edible substrate	-	PG/water (Caffeine ink), PG/ethanol (Loperamide ink).	Recrystallization of printed caffeine was observed on carrier surfaces; loperamide did not recrystallize on any substrates	[83]
Inkjet	HPMC/GLY substrate	-	Ethanol	HPMC/HPC Structured template ODF prepared by casting	[84]
Inkjet	HPMC/GLY substrate	-	Ethanol, DMSO, PG	Combination therapy	[73]
Inkjet	HPMC/GLY substrate	-	PG, water	Impact of contract angle between jetted drop and substrate on printing homogeneity	[85]
Inkjet	HPMC/GLY substrate	-	Polypropylene glycol, propylene carbonate and blue Milliyet dye 28 colourants	Stand-alone and continuous printing of ODF	[86]
Inkjet	HPMC/GLY substrate + mesoporous fumed silica	-	Lactic acid, ethanol, erythrosine	Quick response (QR) code generation	[81]
Inkjet	PVA/CMC/GLY substrate	-	Methanol, water, GLY	Comparison with casting containing the same drug	[41]

Inkjet	Rapidfilm® (Tesa Labtec)	-	Sodium picosulfate ink, polymeric nano-suspension ink, polymeric coating inks	Non-contact printing system that incorporates both piezoelectric and solenoid valve-based inkjet printing	[87]
Inkjet	Sugar-sheet substrate	-	Ethanol, PG	Printing of poorly soluble drugs on a sugar-based substrate	[88]
Thermal Inkjet	commercial potato starch film	-	Water, GLY	Salbutamol sulphate; 40 μg/cm^2 per print pass	[76]
Thermal inkjet	Edible rice paper (Easybake®); sugar paper	-	Yellow edible ink (Deco Enterprises)	Printing on edible substrates and dose differentiation by ink colour intensity	[89]
Thermal Inkjet	HPMC/GLY substrate	-	water	Ink was obtained by dissolving spray-drying microparticles of HPMC and warfarin in water;	[77]
Solvent-free methods					
FDM	PEO; starch or PVA	PG	-	Single and multi-layered films printed with addition of superdisintegrants	[90]
FDM	PVA	-	-	Addition ethanol to moist the PVA/aripiprazole blend	[91]
Semisolid extrusion 3D printing	PVA; HPC	-	-	The polymeric component is wetted with a hydroalcoholic solution to allow the printing, no information on drying	[92]

CMC: microcrystalline cellulose, DMSO: dimethyl sulfoxide, FDM: fused deposition modelling, GLY: Glycerol, HPC: hydroxypropyl cellulose, HPMC: hydroxypropyl methylcellulose, PEG: polyethylene glycol, PEO: polyethylene oxide, PG: Polyethylene glycol, PVA: polyvinyl alcohol.

content. When an organic solvent (e.g., ethanol) is used to solubilize the API, the drying step is essential to fulfil the threshold standards currently in force for the solvent specification; in case of an aqueous solvent, a drying step should reduce the water content to avoid microbial contaminations or improve the ODF stability over time. There are two main mechanisms: absorptive drying at ambient conditions [73] and evaporative drying using hot air convection [93]. In both cases, it is important to investigate the effect of drying on the physical state of the active, if any, and its effect on the therapeutic outcome of the drug.

IJP demands precise control of the process and formulative parameters [93]. The solution volume has to rationalized based on the substrate [79]: varying the volume of solution jetted and/or changing the concentration of the feed determines the amount of drug deposited so that this technology is especially valuable in minimizing wastage of expensive drugs [73]. Moreover, the printing process and the distance between the support and the nozzle should be properly set up in order to avoid any smearing effects, especially when multi-layers are printed on the same support [85].

Hence, the formulation of a printable ink depends the printer system and the mechanism of drop generation [85, 94]. The ink should be optimised at least in terms of viscosity, surface tension, boiling temperature (especially for thermal IJP), solvent evaporation rate [95]. In particular, the surface tension (e.g., $\approx$ 33 mN/m for thermal IJP) should be high enough to enable the formation of spherical droplets and to resist leakage from the print head when the printer is not in operation. The viscosity ($\leq$ 20 mPa s) should be low enough that the fluid can be jetted out, but sufficiently high that the fluid is not ejected too early, which can lead to the formation of a tail, producing satellite droplets [82, 96]. When such parameters are not optimized, the fluid tail (i.e., CJP) can break off on its way toward the substrate causing the formation of different drops and resulting in a bad quality print [97] or the nozzle can clog [98]. It is important that drops land in their designated coordinate on the substrate, because otherwise dose uniformity cannot be assured. Viscosity and surface tension also affect the refilling phase of the drop generator as the solution passes through spouts into the nozzle firing chambers [73]. Therefore, an ink formulation comprises surfactants and viscosity modifiers [80]. Glycols such as polyethylene glycol (PEG) and glycerol are commonly used as viscosity modifiers (**Table 1.3**), but also humectants to avoid the clogging of the nozzle due to the rapid solvent evaporation. Moreover, a colourant can be added to the ink formulation to probe the drug

distribution onto the ODF [18, 87, 90, 99] or to easily differentiate the drugs upon dual deposition of drug fixed combination [99].

The solvent should be selected as a function of drug solubility and the printing technology used. Aqueous solutions are more easily jetted out by thermal IJP since their boiling point generally falls in the optimal temperature range (90-95 °C) for this technology; on the contrary, piezoelectric systems can also be used with organic solvents since the drop formation depends on the mechanical stimuli produced by the piezoelectric sensor [95]. When an aqueous-based solvent system is used, the homogeneity of active substance dosing and deposition on the substrate may be challenging. However, the use of organic solvents has to be carefully evaluated in light of the accepted regulatory threshold specification. Volatile solvents may also induce a rapid API recrystallization after jetting, producing an inhomogeneous deposition and nozzle clogging [85]. On the other side, the use of suspended API or the addition of surfactants can increase the payload of low-soluble active substances. Generally, the particle size of suspended API lower than 1-5 µm is a pre-requisite to avoid clogging [82, 95]. In this context, nanocrystals or nanoparticles, were loaded into inks to improve the drug apparent solubility without affecting the ink printability [82, 87]. For example, 10% nanocrystals of folic acid, a BCS class IV drug, were homogeneously deposited on a common edible paper [82].

In this type of contactless printing, ODF can be obtained on any pharmaceutical grade substrates, such as polymer-based films or placebo ODF [85]. However, the nature of substrate (**Table 1.3** determines the contact angle and the wettability [100], other than the disintegration time and the patient acceptability. The contact angle between the ink and the substrate influences both the payload and API physicochemical stability [94]. In presence of a high contact angle between the jetted drops and the substrate, API cannot be absorbed efficiently before the solvent evaporation and, therefore, it may be crystallized on the film surface with the risk of the API transfer onto the packaging material during storage [83, 85, 101]. Excipients able to improve the substrate porosity (e.g., crospovidone) was added to improve the absorption of API solution into the substrate if the contact angle cannot be further reduced [85].

As an alternative to IJP, flexographic printing technology (FPT) was also proposed. FPT is an offset, rotary printing process in which the ink is metered by an anilox roller onto an unrolled placebo ODF obtained by casting [101]. Subsequently, the solvent is removed by a fan and the film is rolled up again. As an example, Janßen and co-workers successfully printed onto the drug-free ODF using both an API solution (i.e., rasagiline) suspension (i.e., tadalafil) [102]. To

improve the dose accuracy and/or tailor the drug release, Genina and co-workers combined jet-printing of an API solution on paper which was subsequently coated by a polymeric dispersion using FPT release [103]. However, the use of FTP presents two problems regarding the filling of the cells of the anilox roller with ink and the transfer of the ink from the cell to the ODF. Formulation aspects connected to the solution viscosity, contact angles and, in case of suspension, crystal size [83] are the most critical attributes.

Both IJP and FTP allow to maintain the main characteristics of placebo ODF/substrate and obtain ODF differing in terms of mechanical properties and stability compared with films prepared by casting [102]. Moreover, these technologies are more versatile and easier-to-use than other solvent-based ones (i.e., solvent casting, electrospinning). In addition, personalized ODF can be compounded by IJP in a pharmacy setting since the printer is generally adapted from common inkjet printer and is governed by common writing software (e.g., Microsoft Word®) [85]. However, the main IJP drawbacks can be identified in the narrow ink formulative space and API payload, together with the availability of placebo ODF to use as a substrate for the printing.

1.5.2 Fused deposition modelling

The possibility to adapt the fused deposition modelling (FDM) to the production of ODF was also explored. FDM involves the deposition of molten thermoplastic polymer filaments, usually with a diameter of 1.75 mm, through two heated extrusion rollers with a small orifice in a specific 3D laydown pattern which subsequently solidifies on a building plate [104–106]. The technology consists of a software-controlled print head that moves within the x- and y-axes; while the platform, which can be thermostated, moves vertically on the z-axis, creating 3D structures layer-by-layer with a thickness of 100–300 μm by fusing the layers together [106, 107]. The critical parameters are related to the speed of the extruder, the infill density, the height of the layers and the temperature of both the nozzle and the building plate. As summarized in **Table 1.3**, the literature describes only the preparation of polyethylene oxide (PEO) loaded by ibuprofen or paracetamol and poly(vinyl alcohol) and paracetamol [90, 91]. However, its application is limited by the availability of drug loaded-filaments made of a pharma-grade polymer, which are generally preliminarily prepared by hot-melt extrusion [108].

1.6 Conclusions

Different technological solutions, available to prepare ODF, can be potentially chosen according to the physicochemical properties of the API and the batch size. Even if solvent casting is the only consolidate technology at industrial level, HME can be considered as a possible alternative despite the risk of detrimental effects of temperature on API chemical and physical stability.

The advent of printing and electrospinning technologies opens new solutions towards the personalization of the drug dose loaded into ODF: changes in shape and/or dimension would allow have a dose tailored for a specific patient or group; variation of colour would allow end-users to easily identify their own medicine, improving medication safety and adherence. Among printing technologies, IJP is the most investigated technique, even if the ink formulation and availability of edible substrates need to be evaluated case-by-case.

However, which quality controls and how to perform them remain a matter of debate as no clear regulatory requirements are defined in the main Pharmacopoeias, probably because of the novelty of this dosage form. As an example, in the Ph. Eur monograph of orodispersible films, the technological characterization includes only a dissolution test and the evaluation of mechanical strength, to assure ODF handling without any damages, but in both cases specific methods are not reported. It should be also mentioned that the assurance of quality is particularly critical in case of compounded ODF because the safety and quality remain under the responsibilities of pharmacists [109].

The development of non-destructive methods enabling the determination of the uniformity of content in the production of ODF by the continuous manufacturing or by compounding magistral preparations on the basis of prescriptions, is highly desired. Among colorimetry and spectroscopic assays, near-infrared (NIR) spectroscopy appears the most promising since its use is widely adopted as a quality control tool in the pharmaceutical industry and hand-held devices are affordable.

The definition of non-destructive methods for quality control and the availability of printers suitable for the use in a pharmacy setting could open new and real perspective to tailor the dose by ODF. The future of these production technologies depends also on the introduction of a regulatory pathway that permits the development and use of personalized medical products.

References

[1] Orlu, M., Ranmal, S.R., Sheng, Y., Tuleu, C., Seddon, P., 2017. Acceptability of orodispersible films for delivery of medicines to infants and preschool children. Drug Deliv. 24, 1243–1248. https://doi.org/10.1080/10717544.2017.1370512

[2] Visser, J.C., Eugresya, G., Hinrichs, W.L.J., Tjandrawinata, R.R., Avanti, C., Frijlink, H.W., Woerdenbag, H.J., 2017. Development of orodispersible films with selected Indonesian medicinal plant extracts. J. Herb. Med. 7, 37–46. https://doi.org/10.1016/j.hermed.2016.10.002

[3] Slavkova, M., Breitkreutz, J., 2015. Orodispersible drug formulations for children and elderly. Eur. J. Pharm. Sci. 75, 2–9. https://doi.org/10.1016/j.ejps.2015.02.015

[4] Cilurzo, F., Musazzi, U.M., Franzé, S., Selmin, F., Minghetti, P., 2018. Orodispersible dosage forms: biopharmaceutical improvements and regulatory requirements. Drug Discov. Today 23, 251–259. https://doi.org/10.1016/j.drudis.2017.10.003

[5] Lai, F., Franceschini, I., Corrias, F., Sala, M.C., Cilurzo, F., Sinico, C., Pini, E., 2015. Maltodextrin fast dissolving films for quercetin nanocrystal delivery. A feasibility study. Carbohydr. Polym. 121, 217–223. https://doi.org/10.1016/j.carbpol.2014.11.070

[6] Musazzi, U.M., Dolci, L.S., Albertini, B., Passerini, N., Cilurzo, F., 2019. A new melatonin oral delivery platform based on orodispersible films containing solid lipid microparticles. Int. J. Pharm. https://doi.org/10.1016/j.ijpharm.2019.01.046

[7] Talekar, S.D., Haware, R. V., Dave, R.H., 2019. Evaluation of self-nanoemulsifying drug delivery systems using multivariate methods to optimize permeability of captopril oral films. Eur. J. Pharm. Sci. 130, 215–224. https://doi.org/10.1016/j.ejps.2019.01.039

[8] Borges, A.F., Silva, C., Coelho, J.F.J., Simões, S., 2017. Outlining critical quality attributes (CQAs) as guidance for the development of orodispersible films. Pharm. Dev. Technol. 22, 237–245. https://doi.org/10.1080/10837450.2016.1199567

[9] Cilurzo, F., Cupone, I.E., Minghetti, P., Buratti, S., Selmin, F., Gennari, C.G.M., Montanari, L., 2010. Nicotine fast dissolving films made of maltodextrins: A feasibility study. AAPS PharmSciTech 11, 1511–1517. https://doi.org/10.1208/s12249-010-9525-6

[10] Cilurzo, F., Cupone, I.E., Minghetti, P., Buratti, S., Gennari, C.G.M., Montanari, L., 2011. Diclofenac fast-dissolving film: Suppression of bitterness by a taste-sensing system. Drug Dev. Ind. Pharm. 37. https://doi.org/10.3109/03639045.2010.505928

[11] Mashru, R.C., Sutariya, V.B., Sankalia, M.G., Parikh, P.P., 2005. Development and Evaluation of Fast-Dissolving Film of Salbutamol Sulphate. Drug Dev. Ind. Pharm. 31, 25–34. https://doi.org/10.1081/DDC-43947

[12] Cilurzo, F., Cupone, I.E., Minghetti, P., Selmin, F., Montanari, L., 2008a. Fast dissolving films made of maltodextrins. Eur. J. Pharm. Biopharm. 70, 895–900. https://doi.org/10.1016/j.ejpb.2008.06.032

[13] Dinge, A., Nagarsenker, M., 2008. Formulation and evaluation of fast dissolving films for delivery of triclosan to the oral cavity. AAPS PharmSciTech 9, 349–356. https://doi.org/10.1208/s12249-008-9047-7

[14] Allen, L. V., 2016. Compounding Films. Int. J. Pharm. Compd. 20, 298–305.

[15] Allen, J. D., Mungall, D.R., Cobb, M.E., Ostolch, V.E., Hillman, R.S., Stroy, G.H., 1987. Integrated drug dosage form and metering system, EP0224335.

[16] Niese, S., Quodbach, J., 2019. Formulation development of a continuously manufactured orodispersible film containing warfarin sodium for individualized

dosing. Eur. J. Pharm. Biopharm. 136, 93–101. https://doi.org/10.1016/j.ejpb.2019.01.011

[17] Hoffmann, E.M., Breitenbach, A., Breitkreutz, J., 2011. Advances in orodispersible films for drug delivery. Expert Opin. Drug Deliv. 8, 299–316. https://doi.org/10.1517/17425247.2011.553217

[18] Niese, S., Quodbach, J., 2018. Application of a chromatic confocal measurement system as new approach for in-line wet film thickness determination in continuous oral film manufacturing processes. Int. J. Pharm. 551, 203–211. https://doi.org/10.1016/j.ijpharm.2018.09.028

[19] Foo, W.C., Khong, Y.M., Gokhale, R., Chan, S.Y., 2018. A novel unit-dose approach for the pharmaceutical compounding of an orodispersible film. Int. J. Pharm. 539, 165–174. https://doi.org/10.1016/j.ijpharm.2018.01.047

[20] Visser, J.C., Woerdenbag, H.J., Crediet, S., Gerrits, E., Lesschen, M.A., Hinrichs, W.L.J., Breitkreutz, J., Frijlink, H.W., 2015. Orodispersible films in individualized pharmacotherapy: The development of a formulation for pharmacy preparations. Int. J. Pharm. 478, 155–163. https://doi.org/10.1016/j.ijpharm.2014.11.013

[21] Cilurzo, Francesco, Minghetti, P., Pagani, S., Casiraghi, A., Montanari, L., 2008b. Design and characterization of an adhesive matrix based on a poly(ethyl acrylate, methyl methacrylate). AAPS PharmSciTech 9, 748–754. https://doi.org/10.1208/s12249-008-9102-4

[22] Woertz, C., Kleinebudde, P., 2015. Development of orodispersible polymer films with focus on the solid state characterization of crystalline loperamide. Eur. J. Pharm. Biopharm. 94, 52–63. https://doi.org/10.1016/j.ejpb.2015.04.036

[23] Liu, T., Wan, X., Luo, Z., Liu, C., Quan, P., Cun, D., Fang, L., 2018. A donepezil/cyclodextrin complexation orodispersible film: Effect of cyclodextrin on taste-masking based on dynamic process and in vivo drug absorption. Asian J. Pharm. Sci. 14, 183–192. https://doi.org/10.1016/j.ajps.2018.05.001

[24] Speer, I., Lenhart, V., Preis, M., Breitkreutz, J., 2019. Prolonged release from orodispersible films by incorporation of diclofenac-loaded micropellets. Int. J. Pharm. 554, 149–160. https://doi.org/10.1016/j.ijpharm.2018.11.013

[25] Steiner, D., Finke, J.H., Kwade, A., 2017. Redispersion of Nanoparticle-Loaded Orodispersible Films: Preservation of Particle Fineness. Chemie Ing. Tech. 89, 1034–1040. https://doi.org/10.1002/cite.201600139

[26] Brniak, W., Mašlak, E., Jachowicz, R., 2015. Orodispersible films and tablets with prednisolone microparticles. Eur. J. Pharm. Sci. 75, 81–90. https://doi.org/10.1016/j.ejps.2015.04.006

[27] Vuddanda, P.R., Montenegro-Nicolini, M., Morales, J.O., Velaga, S., 2017. Effect of surfactants and drug load on physico-mechanical and dissolution properties of nanocrystalline tadalafil-loaded oral films. Eur. J. Pharm. Sci. 109, 372–380. https://doi.org/10.1016/j.ejps.2017.08.019

[28] Khadra, I., Obeid, M.A., Dunn, C., Watts, S., Halbert, G., Ford, S., Mullen, A., 2019. Characterisation and optimisation of diclofenac sodium orodispersible thin film formulation. Int. J. Pharm. 561, 43–46. https://doi.org/10.1016/j.ijpharm.2019.01.064

[29] Şen Karaman, D., Patrignani, G., Rosqvist, E., Smått, J.H., Orłowska, A., Mustafa, R., Preis, M., Rosenholm, J.M., 2018. Mesoporous silica nanoparticles facilitating the dissolution of poorly soluble drugs in orodispersible films. Eur. J. Pharm. Sci. 122, 152–159.

[30] Franceschini, I., Selmin, F., Pagani, S., Minghetti, P., Cilurzo, F., 2016. Nanofiller for the mechanical reinforcement of maltodextrins orodispersible films. Carbohydr. Polym. 136, 676–681. https://doi.org/10.1016/j.carbpol.2015.09.077

[31] Lai, F., Franceschini, I., Corrias, F., Sala, M.C., Cilurzo, F., Sinico, C., Pini, E., 2015. Maltodextrin fast dissolving films for quercetin nanocrystal delivery. A feasibility study. Carbohydr. Polym. 121, 217–223. https://doi.org/10.1016/j.carbpol.2014.11.070

[32] Selmin, F., Franceschini, I., Cupone, I.E., Minghetti, P., Cilurzo, F., 2015. Aminoacids as non-traditional plasticizers of maltodextrins fast-dissolving films. Carbohydr. Polym. 115, 613–616. https://doi.org/10.1016/j.carbpol.2014.09.023

[33] Musazzi, U.M., Selmin, F., Franzé, S., Gennari, C.G.M., Rocco, P., Minghetti, P., Cilurzo, F., 2018a. Poly(methyl methacrylate) salt as film forming material to design orodispersible films. Eur. J. Pharm. Sci. 115, 37–42. https://doi.org/10.1016/j.ejps.2018.01.019

[34] Mazumder, S., Pavurala, N., Manda, P., Xu, X., Cruz, C.N., Krishnaiah, Y.S.R., 2017. Quality by Design approach for studying the impact of formulation and process variables on product quality of oral disintegrating films. Int. J. Pharm. 527, 151–160. https://doi.org/10.1016/j.ijpharm.2017.05.048

[35] Thabet, Y., Breitkreutz, J., 2018. Orodispersible films: Product transfer from lab-scale to continuous manufacturing. Int. J. Pharm. 535, 285–292. https://doi.org/10.1016/j.ijpharm.2017.11.021

[36] Thabet, Y., Lunter, D., Breitkreutz, J., 2018a. Continuous manufacturing and analytical characterization of fixed-dose, multilayer orodispersible films. Eur. J. Pharm. Sci. 117, 236–244. https://doi.org/10.1016/j.ejps.2018.02.030

[37] Garcia, V.A. dos S., Borges, J.G., Maciel, V.B.V., Mazalli, M.R., Lapa-Guimaraes, J. das G., Vanin, F.M., de Carvalho, R.A., 2018. Gelatin/starch orally disintegrating films as a promising system for vitamin C delivery. Food Hydrocoll. 79, 127–135. https://doi.org/10.1016/j.foodhyd.2017.12.027

[38] Castro, P.M., Sousa, F., Magalhães, R., Ruiz-Henestrosa, V.M.P., Pilosof, A.M.R., Madureira, A.R., Sarmento, B., Pintado, M.E., 2018. Incorporation of beads into oral films for buccal and oral delivery of bioactive molecules. Carbohydr. Polym. 194, 411–421. https://doi.org/10.1016/j.carbpol.2018.04.032

[39] Zhang, H., Han, M.G., Wang, Y., Zhang, J., Han, Z.M., Li, S.J., 2015. Development of oral fast-disintegrating levothyroxine films for management of hypothyroidism in pediatrics. Trop. J. Pharm. Res. 14, 1755–1762. https://doi.org/10.4314/tjpr.v14i10.4

[40] Chandra, A., Chondkar, A.D., Shirodkar, R., Lewis, S.A., 2018. Rapidly dissolving lacidipine nanoparticle strips for transbuccal administration. J. Drug Deliv. Sci. Technol. 47, 259–267. https://doi.org/10.1016/J.JDDST.2018.07.025

[41] Buanz, A.B.M., Belaunde, C.C., Soutari, N., Tuleu, C., Gul, M.O., Gaisford, S., 2015. Ink-jet printing versus solvent casting to prepare oral films: Effect on mechanical properties and physical stability. Int. J. Pharm. 494, 611–618. https://doi.org/10.1016/j.ijpharm.2014.12.032

[42] Alsofany, J.M., Hamza, M.Y., Abdelbary, A.A., 2018. Fabrication of Nanosuspension Directly Loaded Fast-Dissolving Films for Enhanced Oral Bioavailability of Olmesartan Medoxomil: In Vitro Characterization and Pharmacokinetic Evaluation in Healthy Human Volunteers. AAPS PharmSciTech 19, 2118–2132. https://doi.org/10.1208/s12249-018-1015-2

[43] Sharma, R., Kamboj, S., Singh, G., Rana, V., 2016. Development of aprepitant loaded orally disintegrating films for enhanced pharmacokinetic performance. Eur. J. Pharm. Sci. 84, 55–69. https://doi.org/10.1016/j.ejps.2016.01.006

[44] Singh, H., Singla, Y.P., Narang, R.S., Pandita, D., Singh, S., Narang, J.K., 2018. Frovatriptan loaded hydroxy propyl methyl cellulose/treated chitosan based composite fast dissolving sublingual films for management of migraine. J. Drug Deliv. Sci. Technol. 47, 230–239. https://doi.org/10.1016/J.JDDST.2018.06.018

[45] Adeleke, O.A., Tsai, P.-C., Karry, K.M., Monama, N.O., Michniak-Kohn, B.B., 2018. Isoniazid-loaded orodispersible strips: Methodical design, optimization and in vitro-in silico characterization. Int. J. Pharm. 547, 347–359. https://doi.org/10.1016/j.ijpharm.2018.06.004

[46] Foo, W.C., Khong, Y.M., Gokhale, R., Chan, S.Y., 2018. A novel unit-dose approach for the pharmaceutical compounding of an orodispersible film. Int. J. Pharm. 539, 165–174. https://doi.org/10.1016/j.ijpharm.2018.01.047

[47] Talekar, S.D., Haware, R. V., Dave, R.H., 2019. Evaluation of self-nanoemulsifying drug delivery systems using multivariate methods to optimize permeability of captopril oral films. Eur. J. Pharm. Sci. 130, 215–224. https://doi.org/10.1016/j.ejps.2019.01.039

[48] Pechová, V., Gajdziok, J., Muselík, J., Vetchý, D., 2018. Development of Orodispersible Films Containing Benzydamine Hydrochloride Using a Modified Solvent Casting Method. AAPS PharmSciTech 19, 2509–2518. https://doi.org/10.1208/s12249-018-1088-y

[49] Tian, Y., Visser, J.C., Klever, J.S., Woerdenbag, H.J., Frijlink, H.W., Hinrichs, W.L.J., 2018. Orodispersible films based on blends of trehalose and pullulan for protein delivery. Eur. J. Pharm. Biopharm. 133, 104–111. https://doi.org/10.1016/j.ejpb.2018.09.016

[50] Vasvári, G., Kalmár, J., Veres, P., Vecsernyés, M., Bácskay, I., Fehér, P., Ujhelyi, Z., Haimhoffer, Á., Rusznyák, Á., Fenyvesi, F., Váradi, J., 2018. Matrix systems for oral drug delivery: Formulations and drug release. Drug Discov. Today Technol. 27, 71–80. https://doi.org/10.1016/j.ddtec.2018.06.009

[51] Huang, Y., Song, J., Yang, C., Long, Y., Wu, H., 2019. Scalable manufacturing and applications of nanofibers. Mater. Today 28, 98–113. https://doi.org/10.1016/j.mattod.2019.04.018

[52] Thakkar, S., Misra, M., 2017. Electrospun polymeric nanofibers: New horizons in drug delivery. Eur. J. Pharm. Sci. 107, 148–167. https://doi.org/10.1016/j.ejps.2017.07.001

[53] Illangakoon, U.E., Gill, H., Shearman, G.C., Parhizkar, M., Mahalingam, S., Chatterton, N.P., Williams, G.R., 2014. Fast dissolving paracetamol/caffeine nanofibers prepared by electrospinning. Int. J. Pharm. 477, 369–379. https://doi.org/10.1016/j.ijpharm.2014.10.036

[54] Rustemkyzy, C., Belton, P., Qi, S., 2015. Preparation and Characterization of Ultrarapidly Dissolving Orodispersible Films for Treating and Preventing Iodine Deficiency in the Pediatric Population. J. Agric. Food Chem. 63, 9831–9838. https://doi.org/10.1021/acs.jafc.5b03953

[55] Wu, Y.-H., Yu, D.-G., Li, X.-Y., Diao, A.-H., Illangakoon, U.E., Williams, G.R., 2015. Fast-dissolving sweet sedative nanofiber membranes. J. Mater. Sci. 50, 3604–3613. https://doi.org/10.1007/s10853-015-8921-4

[56] Cilurzo, F., Selmin, F., Vistoli, G., Minghetti, P., Montanari L., 2007. Binary

polymeric blends to microencapsulate nitroflurbiprofen: Physicochemical and in silico studies. Eur. J. Pharm. Sci. 31, 202-210. https://doi.org/10.1016/j.ejps.2007.03.010

[57] Cilurzo, F., Minghetti, P., Casiraghi, A., Montanari, L., 2002. Characterization of nifedipine solid dispersions. Int. J. Pharm. 242, 313-317. https://doi.org/10.1016/s0378-5173(02)00173-4

[58] Ali, W., Williams, A.C., Rawlinson, C.F., 2010. Stochiometrically governed molecular interactions in drug: poloxamer solid dispersions. Int. J. Pharm. 391:162-168. https://doi.org/10.1016/j.ijpharm.2010.03.014

[59] Nagy, Z.K., Balogh, A., Drávavölgyi, G., Ferguson, J., Pataki, H., Vajna, B., Marosi, G., 2013. Solvent-Free Melt Electrospinning for Preparation of Fast Dissolving Drug Delivery System and Comparison with Solvent-Based Electrospun and Melt Extruded Systems. J. Pharm. Sci. 102, 508–517. https://doi.org/10.1002/JPS.23374

[60] Palo, M., Kogermann, K., Laidmäe, I., Meos, A., Preis, M., Heinämäki, J., Sandler, N., 2017. Development of Oromucosal Dosage Forms by Combining Electrospinning and Inkjet Printing. Mol. Pharm. 14, 808–820. https://doi.org/10.1021/acs.molpharmaceut.6b01054

[61] Cilurzo, F., Selmin, F., Minghetti, P., Rimoldi, I., Demartin, F., Montanari, L., 2005. Fast-dissolving mucoadhesive microparticulate delivery system containing piroxicam. Eur. J. Pharm. Sci. 24, 355-361. https://doi.org/10.1016/j.ejps.2004.11.010

[62] Nagy, Z.K., Nyúl, K., Wagner, I., Molnár, K., Marosi, G., 2010. Electrospun water soluble polymer mat for ultrafast release of donepezil HCL. Express Polym. Lett. 4, 763–772. https://doi.org/10.3144/expresspolymlett.2010.92

[63] Yu, D.G., Branford-White, C., Shen, X.X., Zhang, X.F., Zhu, L.M., 2010. Solid dispersions of ketoprofen in drug-loaded electrospun nanofibers. J. Dispers. Sci. Technol. 31, 902–908. https://doi.org/10.1080/01932690903223948

[64] Chou, S.F., Carson, D., Woodrow, K.A., 2015. Current strategies for sustaining drug release from electrospun nanofibers. J. Control. Release 220, 584–591. https://doi.org/10.1016/j.jconrel.2015.09.008

[65] Li, X., Kanjwal, M.A., Lin, L., Chronakis, I.S., 2013. Electrospun polyvinyl-alcohol nanofibers as oral fast-dissolving delivery system of caffeine and riboflavin. Colloids Surfaces B Biointerfaces 103, 182–188. https://doi.org/10.1016/J.COLSURFB.2012.10.016

[66] Bukhary, H., Williams, G.R., Orlu, M., 2018. Electrospun fixed dose formulations of amlodipine besylate and valsartan. Int. J. Pharm. 549, 446–455. https://doi.org/10.1016/j.ijpharm.2018.08.008

[67] Yu, D.-G., Shen, X.-X., Branford-White, C., White, K., Zhu, L.-M., Annie Bligh, S.W., 2009. Oral fast-dissolving drug delivery membranes prepared from electrospun polyvinylpyrrolidone ultrafine fibers. Nanotechnology 20, 055104. https://doi.org/10.1088/0957-4484/20/5/055104

[68] Adeli, E., 2015. Irbesartan-loaded electrospun nanofibers-based PVP K90 for the drug dissolution improvement: Fabrication, in vitro performance assessment, and in vivo evaluation. J. Appl. Polym. Sci. 132, 1–10. https://doi.org/10.1002/app.42212

[69] Low, A.Q.J., Parmentier, J., Khong, Y.M., Chai, C.C.E., Tun, T.Y., Berania, J.E., Liu, X., Gokhale, R., Chan, S.Y., 2013. Effect of type and ratio of solubilising polymer on characteristics of hot-melt extruded orodispersible films. Int. J. Pharm. 455, 138–147. https://doi.org/10.1016/j.ijpharm.2013.07.046

[70] Pimparade, M.B., Vo, A., Maurya, A.S., Bae, J., Morott, J.T., Feng, X., Kim, D.W., Kulkarni, V.I., Tiwari, R., Vanaja, K., Murthy, R., Shivakumar, H.N., Neupane,

D., Mishra, S.R., Murthy, S.N., Repka, M.A., 2017. Development and evaluation of an oral fast disintegrating anti-allergic film using hot-melt extrusion technology. Eur. J. Pharm. Biopharm. 119, 81–90. https://doi.org/10.1016/j.ejpb.2017.06.004

[71] Jani, R., Patel, D., 2014. Hot melt extrusion: An industrially feasible approach for casting orodispersible film. Asian J. Pharm. Sci. 10, 292–305. https://doi.org/10.1016/j.ajps.2015.03.002

[72] Wilson, M., Williams, M.A., Jones, D.S., Andrews, G.P., 2012. Hot-melt extrusion technology and pharmaceutical application. Ther. Deliv. 3, 787–797. https://doi.org/10.4155/tde.12.26

[73] Alomari, M., Vuddanda, P.R., Trenfield, S.J., Dodoo, C.C., Velaga, S., Basit, A.W., Gaisford, S., 2018. Printing T3and T4oral drug combinations as a novel strategy for hypothyroidism. Int. J. Pharm. 549, 363–369. https://doi.org/10.1016/j.ijpharm.2018.07.062

[74] Scarpa, M., Stegemann, S., Hsiao, W.-K.K., Pichler, H., Gaisford, S., Bresciani, M., Paudel, A., Orlu, M., 2017. Orodispersible films: Towards drug delivery in special populations. Int. J. Pharm. 523, 327–335. https://doi.org/10.1016/j.ijpharm.2017.03.018

[75] Thabet, Y., Lunter, D., Breitkreutz, J., 2018b. Continuous inkjet printing of enalapril maleate onto orodispersible film formulations. Int. J. Pharm. 546, 180–187. https://doi.org/10.1016/j.ijpharm.2018.04.064

[76] Buanz, A.B.M., Saunders, M.H., Basit, A.W., Gaisford, S., 2011. Preparation of personalized-dose salbutamol sulphate oral films with thermal ink-jet printing. Pharm. Res. 28, 2386–2392. https://doi.org/10.1007/s11095-011-0450-5

[77] Vuddanda, P.R., Alomari, M., Dodoo, C.C., Trenfield, S.J., Velaga, S., Basit, A.W., Gaisford, S., 2018. Personalisation of warfarin therapy using thermal ink-jet printing. Eur. J. Pharm. Sci. 117, 80–87. https://doi.org/10.1016/j.ejps.2018.02.002

[78] Karki, S., Kim, H., Na, S.-J., Shin, D., Jo, K., Lee, J., 2016. Thin films as an emerging platform for drug delivery. Asian J. Pharm. Sci. 11, 559–574. https://doi.org/10.1016/J.AJPS.2016.05.004

[79] Lee, B.K., Yun, Y.H., Choi, J.S., Choi, Y.C., Kim, J.D., Cho, Y.W., 2012. Fabrication of drug-loaded polymer microparticles with arbitrary geometries using a piezoelectric inkjet printing system. Int. J. Pharm. 427, 305–310. https://doi.org/10.1016/j.ijpharm.2012.02.011

[80] Daly, R., Harrington, T.S., Martin, G.D., Hutchings, I.M., 2015. Inkjet printing for pharmaceutics - A review of research and manufacturing. Int. J. Pharm. 494, 554–567. https://doi.org/10.1016/j.ijpharm.2015.03.017

[81] Edinger, M., Bar-Shalom, D., Sandler, N., Rantanen, J., Genina, N., 2018. QR encoded smart oral dosage forms by inkjet printing. Int. J. Pharm. https://doi.org/10.1016/j.ijpharm.2017.11.052

[82] Pardeike, J., Strohmeier, D.M., Schrödl, N., Voura, C., Gruber, M., Khinast, J.G., Zimmer, A., 2011. Nanosuspensions as advanced printing ink for accurate dosing of poorly soluble drugs in personalized medicines. Int. J. Pharm. 420, 93–100. https://doi.org/10.1016/j.ijpharm.2011.08.033

[83] Genina, N., Fors, D., Palo, M., Peltonen, J., Sandler, N., 2013a. Behavior of printable formulations of loperamide and caffeine on different substrates - Effect of print density in inkjet printing. Int. J. Pharm. 453, 488–497. https://doi.org/10.1016/j.ijpharm.2013.06.003

[84] Steiner, D., Finke, J.H., Kwade, A., 2019. SOFTs – Structured orodispersible

film templates. Eur. J. Pharm. Biopharm. 137, 209–217. https://doi.org/10.1016/J.EJPB.2019.03.001

[85] Genina, N., Janßen, E.M., Breitenbach, A., Breitkreutz, J., Sandler, N., 2013b. Evaluation of different substrates for inkjet printing of rasagiline mesylate. Eur. J. Pharm. Biopharm. 85, 1075–1083. https://doi.org/10.1016/j.ejpb.2013.03.017

[86] Thabet, Y., Sibanc, R., Breitkreutz, J., 2018c. Printing pharmaceuticals by inkjet technology: Proof of concept for stand-alone and continuous in-line printing on orodispersible films. J. Manuf. Process. 35, 205–215. https://doi.org/10.1016/j.jmapro.2018.07.018

[87] Planchette, C., Pichler, H., Wimmer-Teubenbacher, M., Gruber, M., Gruber-Woelfler, H., Mohr, S., Tetyczka, C., Hsiao, W.-K.K., Paudel, A., Roblegg, E., Khinast, J., 2016. Printing medicines as orodispersible dosage forms: Effect of substrate on the printed micro-structure. Int. J. Pharm. 509, 518–527. https://doi.org/10.1016/j.ijpharm.2015.10.054

[88] Eleftheriadis, G.K., Monou, P.K., Bouropoulos, N., Fatouros, D.G., 2018. In vitro evaluation of 2D-printed edible films for the buccal delivery of diclofenac sodium. Materials (Basel). 11, 1–14. https://doi.org/10.3390/ma11050864

[89] Wickström, H., Nyman, J.O., Indola, M., Sundelin, H., Kronberg, L., Preis, M., Rantanen, J., Sandler, N., 2017. Colorimetry as Quality Control Tool for Individual Inkjet-Printed Pediatric Formulations. AAPS PharmSciTech 18, 293–302. https://doi.org/10.1208/s12249-016-0620-1

[90] Ehtezazi, T., Algellay, M., Islam, Y., Roberts, M., Dempster, N.M., Sarker, S.D., 2018. The Application of 3D Printing in the Formulation of Multilayered Fast Dissolving Oral Films. J. Pharm. Sci. 107, 1076–1085. https://doi.org/10.1016/j.xphs.2017.11.019

[91] Jamróz, W., Kurek, M., Łyszczarz, E., Szafraniec, J., Knapik-Kowalczuk, J., Syrek, K., Paluch, M., Jachowicz, R., 2017. 3D printed orodispersible films with Aripiprazole. Int. J. Pharm. 533, 413–420. https://doi.org/10.1016/j.ijpharm.2017.05.052

[92] Sjöholm, E., Sandler, N., 2019. Additive manufacturing of personalized orodispersible warfarin films. Int. J. Pharm. 564, 117–123. https://doi.org/10.1016/J.IJPHARM.2019.04.018

[93] Voura, C., Gruber, M.M., Schroedl, N., Strohmeier, D., Eitzinger, B., Bauer, W., Brenn, G., Khinast, J.G., Zimmer, A., 2011. Printable medicines: A microdosing device for producing personalised medicines. Pharm. Technol. Eur. 23, 32–36.

[94] Azizi Machekposhti, S., Mohaved, S., Narayan, R.J., 2019. Inkjet dispensing technologies: recent advances for novel drug discovery. Expert Opin. Drug Discov. 14, 101–113. https://doi.org/10.1080/17460441.2019.1567489

[95] De Gans, B.J., Duineveld, P.C., Schubert, U.S., 2004. Inkjet printing of polymers: State of the art and future developments. Adv. Mater. 16, 203–213. https://doi.org/10.1002/adma.200300385

[96] Içten, E., Giridhar, A., Taylor, L.S., Nagy, Z.K., Reklaitis, G. V., 2015. Dropwise additive manufacturing of pharmaceutical products for melt-based dosage forms. J. Pharm. Sci. 104, 1641–1649. https://doi.org/10.1002/jps.24367

[97] Raijada, D., Genina, N., Fors, D., Wisaeus, E., Peltonen, J., Rantanen, J., Sandler, N., 2013. A Step Toward Development of Printable Dosage Forms for Poorly Soluble Drugs. J. Pharm. Sci. 102, 3694–3704. https://doi.org/10.1002/JPS.23678

[98] Vakili, H., Nyman, J.O., Genina, N., Preis, M., Sandler, N., 2016. Application

of a colorimetric technique in quality control for printed pediatric orodispersible drug delivery systems containing propranolol hydrochloride. Int. J. Pharm. 511, 606–618. https://doi.org/10.1016/j.ijpharm.2016.07.032

[99] Alomari, M., Vuddanda, P.R., Trenfield, S.J., Dodoo, C.C., Velaga, S., Basit, A.W., Gaisford, S., 2018. Printing T3and T4oral drug combinations as a novel strategy for hypothyroidism. Int. J. Pharm. 549, 363–369. https://doi.org/10.1016/j.ijpharm.2018.07.062

[100] Wimmer-Teubenbacher, M., Planchette, C., Pichler, H., Markl, D., Hsiao, W.K.K., Paudel, A., Stegemann, S., 2018. Pharmaceutical-grade oral films as substrates for printed medicine. Int. J. Pharm. 547, 169–180. https://doi.org/10.1016/j.ijpharm.2018.05.041

[101] Buanz, A.B.M., Telford, R., Scowen, I.J., Gaisford, S., 2013. Rapid preparation of pharmaceutical co-crystals with thermal ink-jet printing. CrystEngComm 15, 1031–1035. https://doi.org/10.1039/c2ce26519b

[102] Janßen, E.M., Schliephacke, R., Breitenbach, A., Breitkreutz, J., 2013. Drug-printing by flexographic printing technology - A new manufacturing process for orodispersible films. Int. J. Pharm. 441, 818–825. https://doi.org/10.1016/j.ijpharm.2012.12.023

[103] Genina, N., Fors, D., Vakili, H., Ihalainen, P., Pohjala, L., Ehlers, H., Kassamakov, I., Haeggström, E., Vuorela, P., Peltonen, J., Sandler, N., 2012. Tailoring controlled-release oral dosage forms by combining inkjet and flexographic printing techniques. Eur. J. Pharm. Sci. 47, 615–623. https://doi.org/10.1016/j.ejps.2012.07.020

[104] Chia, H.N., Wu, B.M., 2015. Recent advances in 3D printing of biomaterials. J. Biol. Eng. 9, 1–14. https://doi.org/10.1186/s13036-015-0001-4

[105] Goole, J., Amighi, K., 2016. 3D printing in pharmaceutics: A new tool for designing customized drug delivery systems. Int. J. Pharm. 499, 376–394. https://doi.org/10.1016/j.ijpharm.2015.12.071

[106] Skowyra, J., Pietrzak, K., Alhnan, M.A., 2015. Fabrication of extended-release patient-tailored prednisolone tablets via fused deposition modelling (FDM) 3D printing. Eur. J. Pharm. Sci. 68, 11–17. https://doi.org/10.1016/j.ejps.2014.11.009

[107] Korpela, J., Kokkari, A., Korhonen, H., Malin, M., Narhi, T., Seppalea, J., 2013. Biodegradable and bioactive porous scaffold structures prepared using fused deposition modeling. J. Biomed. Mater. Res. - Part B Appl. Biomater. 101, 610–619. https://doi.org/10.1002/jbm.b.32863

[108] Melocchi, A., Parietti, F., Maroni, A., Foppoli, A., Gazzaniga, A., Zema, L., 2016. Hot-melt extruded filaments based on pharmaceutical grade polymers for 3D printing by fused deposition modeling. Int. J. Pharm. 509, 255–263. https://doi.org/10.1016/j.ijpharm.2016.05.036

[109] Selmin, F., Casiraghi, A., Musazzi, U.M., Fortini, M., Minghetti, P., 2019. An Outlook on the European and Italian Rules to Guarantee Magistral Formulas. Int. J. Pharm. Compd. 23, 6–12.

Chapter 2

Trends in the Characterization Methods of Orodispersible Films

Chapter 2

2.1 Introduction

Orodispersible dosage forms provide the opportunity to meet the special needs of specific subpopulation of patients suffering from a variety of disorders, among which swallowing difficulties (dysphagia), Parkinson's disease, psychosis, thyroid disorder, stroke, and multiple sclerosis are the most relevant [1]. In addition, children and elderly, and patients with limited access to water can also benefit from their advantages [2,3]. Since orodispersible dosage forms came onto the market in the 80s, their development has grown gradually, moving from orodispersible tablets to orodispersible films (ODF) which present the undoubtedly advantages to completely eliminate the fear of choking [3,4]. Moreover, pharmaceutical companies have invested in these dosage forms because they can extend their product portfolio and ODF can be marketed easily as line-extensions. The possibility to change shape and colour of the ODF have open new scenarios to prepare small batches for personalization of the dose in special patient population [5].

ODF are generally made up of plasticized hydrocolloids or blends made thereof that can be laminated by several techniques and sealed in a moisture-protective package [3]. The active pharmaceutical ingredient (API) can be dissolved or dispersed as such or nanocrystals [6] or loaded into microparticles [7] depending on the physicochemical properties of the drug and the desired release pattern. Other components can be surfactants, viscosity modifiers, taste-masking agents and colouring agents, when required [2,5,8].

ODF are prepared by solvent-based or melting-based technique even if, for the purpose of personalized therapy, different types of ODF printing technologies have been proposed [8].

Independently of the batch size, the main critical quality attributes are related to disintegration time, drug dissolution rate, tensile properties and taste evaluation [3,9]. The European Pharmacopeia (Ph. Eur.) states that ODF should disintegrate within 3 min with reference to ODT, even though, the disintegration time of ODF usually ranges from 10 to 60 seconds [3], but most of the other ODF quality attributes are yet to be categorically defined and most quality controls are related to [10]. The development of small batches has also pointed out that not-destructive and versatile analytical methods are also required [8].

In this work, we appraised the current literature on the ODF characterization methods from slurries to the finished medicinal products, referred both to industrial mass production and small-scale on demand ODF for personalized therapy. In this context, the description of compendial and not-compendial methods required to demonstrate the quality and the

acceptance criteria of an ODF produced industrially or prepared in a pharmacy setting is pointed-out.

To fulfil this aim, the references were extracted from SCOPUS and Web of Science databases by matching the following keywords: Orodispersible film, Fast dissolving film, Oral thin film, Quality assessment, Quality control, Characterization, Assay, None-destructive, Disintegration, *In vitro* dissolution, and Mechanical properties.

2.2 Characterization of the slurries used for film preparation

Regardless of the preparation methods, the rheological characterization of slurries containing all the formulation components is of high significance to rationalize the design space of ODF formulation.

Highly viscous slurries for casting can entrap air bubbles which can create defects in the dried film and affect the uniformity of drug contents [11,12]. However, the presence of air bubbles could be minimized by stirring the slurry under vacuum, centrifugation, using degassed water [13], sonication, or storing the slurry in a refrigerator [11]. Moreover, to limit the entrapment of air bubbles, the film-forming material can be preliminarily dispersed in a medium and then mixed with the solution/slurry containing other excipients including surfactant(s) [12]. Low viscous slurries can limit the content uniformity because the mass may lead to running of the slurry in a direction opposite to the coating process directly after coating the liner [11] or, in case of suspended API, sedimentation may occur before casting [14]. It is worthy of note that also the fraction of suspended API can increase the slurry viscosity. As an example, Woertz and Kleinebudde demonstrated that relative viscosity of the suspension is independent of the type of cellulose derivative used, but dependent on the fraction of loperamide and ibuprofen [12]. Another requirement of slurries to be cast is the wettability onto the backing layer to avoid its shrinkage and, therefore, the uniformity of content and ODF appearance. To modify the contact angle between slurry and the backing layer, surfactants and/or thickening agents are generally added [2,15]. Moreover, the backing layer should be carefully selected on a case-by-case basis depending on the composition of the drug-polymer mixture bearing in mind the role of surface-active agent and thickening agents. As an example, a surfactant with low HLB (i.e. sorbitan oleate) was necessary to uniformly spread slurries made of maltodextrins and glycerine onto the silicone release liner [14].

Also, in case of HME, the viscosity of the melt affects the consistency and printability of the ODF. Again, in the case of maltodextrins, the shear viscosity data indicated that the plasticizer amount was more relevant then the polymer molecular weight [5]. In case of the ink-jet printing, the critical aspects to be optimized are viscosity and surface tension [8]. First, the viscosity should be low enough that the fluid can be jetted out, but sufficiently high that the fluid is not ejected too early, which can lead to the formation of satellite droplets [16]. Similarly, the surface tension is expected to be high enough to enable the formation of spherical droplets and to resist leakage from the print head when the printer is in stand-by. Poorly optimized and inconsistent viscosity and/or surface tension of the ink solution can clog nozzles decreasing the uniformity of printing viz a viz reducing the drug content uniformity [8,17]. Additionally, viscosity and surface tension also affect the refilling phase of the drop generator as the solution passes through spouts into the nozzle firing chambers. Depending on the requirements of the print head manufacturer, the dynamic viscosity and the surface tension range 8–20 mPa*s and 24–36 mN/m, respectively [17].

Data on the viscosity of polymer solutions are also reported in the case of continuously working pilot-scale coating bench to avoid unintentionally flows of solution at the wrong side of the coating knife without forming a film on the intermediate liner. In this case the value of 1 Pa*s was optimal [18]. Consequently, adjustment can be done in terms of polymer concentration, or adding viscosity modifiers, such as glycerol and polyethylene glycol (PEG) [18].

2.3 ODF physical, organoleptic and mechanical characterizations

*2.3.1 **Thickness and weight variation***

In general, ODF exhibits a thickness between 50 and 1000 μm depending on the loaded API [19], polymer [20] and plasticizer [21]. Even if it is not a golden rule, too thick ODF have a prolonged disintegration time and too thin exhibit poor mechanical properties.

The measurement of ODF thickness uniformity is directly related to the film weight and, therefore, to the uniformity of dose [19]. The thickness is usually measured offline using a well-calibrated electronic digital micrometre, scanning electron photomicrography, screw gauge, or by vernier calliper. There are some online detection systems, such as backscatter sensors, that employs an in-line chromatic confocal measurement system to determine the wet film thickness in continuous manufacturing processes [22].

2.3.2 Organoleptic evaluation

Since these dosage forms disintegrate directly onto the oral cavity, suitable palatability is required. The taste masking strategy is selected considering that, compared to liquid formulations, the API is not diluted, and the formulation space is limited due to the low weight of the film. The effectiveness of taste-masking technique can be evaluated by *in vitro* and *in vivo* tests. The former uses taste sensors with an array of multichannel to mimic the conditions of taste buds in human tongues. These sensors are commonly called electronic tongues (e-Tongues, or ET). The popularity of these systems has been increasing in pharmaceutical fields due to rapidity, simplicity, relatively low cost, and lack of risks compared to human models [23]. ET is broadly divided into two categories. First, in the insent taste-sensing system, where the taste sensor output exhibits different patterns for chemical substances that have different taste qualities, mainly sweetness, bitterness, saltiness, sourness, and umami [24-26]. The second system consists of a quantitative taste sensor, such as the α-ASTREE electronic tongue able to evaluate the overall taste of a product by using the output value from different electrodes. This taste sensor consists of an array of seven liquid cross-sensitive electrodes or sensors based on the ChemFET technology, an auto-sampler, and an associated interface electronic module. In the presence of dissolved compounds, a potentiometric difference is measured between each of the seven sensors and the Ag/AgCl reference electrode [27,28].

Despite these advantages, e-tongues cannot discriminate between one chemical flavour and another particularly for complex mixtures. Therefore, The palatability evaluation is generally carried out by trained taste panels of 4-15 people [29] in the age group of 18 to 30 years of both sexes to produce sensory profiles [23]. However, this procedure is complex due to ethical and toxicological considerations, especially when new drug substances are under investigation, and adult preferences are significantly different from children's taste. On the other hand, taste panels in children are nearly impossible because of ethical reasons and their inability to describe taste attributes and their preferences [24].

2.3.3 Moisture content determination

The residual water content needs particular attention because a certain amount of water can be desired to ensure the flexibility of the ODF and to circumvent brittleness [24]; but at the same time, a high amount can alter the mechanical properties and promote stickiness and microbiological bioburden or instability of the loaded API [5,30]. Even though the residual water content depends on the characteristics of film-forming material and the highest values

reported in the literature for loss on drying (i.e. LOD ~20%) concerns the poly(methyl methacrylate)s where water acts as plasticizer [31].

The determination of water sorption and desorption profiles allows to estimate the ODF hygroscopicity and identify the role of APIs and/or excipients on the total water contents in the final product. High water sorption might be correlated to disintegration behaviour, but also predicts the need of special packaging and storage conditions [24]. Usually, ODF are subjected to an initial drying stage from ambient to 0% relative humidity to ensure that percent changes in weight during the sorption-desorption cycle are on a dry weight basis. The dried sample is then subjected to a stepwise increase and decrease in relative humidity from 0 to 95% and 95 to 0%, respectively at 25 ºC. The total weight of water absorbed (sorption phase) and lost (desorption phase) are recorded [32-34].

However, the control of the environmental conditions (i.e. temperature and relative humidity) during preparation and/or production and the selection of an appropriate primary packaging material should be selected to avoid water exchange with the surrounding environments [33]. It is worth noting that, preservatives are sometimes included in ODF formulations to deter the microbial activities [24].

The quantification of residual water is generally obtained using thermogravimetry, infrared light balances, or Karl Fischer titration [32]. In some situations, thermogravimetric analysis (TGA) helps to define the type of water associated to the matrix. Moreover, the weight loss can be easily quantified and related dehydration, evaporation of low-boiling compounds or thermal degradation by-product [10].

2.3.4 **Mechanical properties**

Tensile properties

The mechanical strength of ODF is considered of particular importance in up-scaled pharmaceutical manufacturing. Automated processes working on machines, such as rolls to transfer films from drying to storage or coiling up of ODF before cutting, requires sufficient robustness of the produced ODF without damage or breakage [24]. The European Pharmacopeia [35] specifies that ODF should *'possess suitable mechanical strength to resist handling without being damaged*', but there is no further explanation on how to define a suitable mechanical strength of ODF, or what specific parameters should be measured with upper or lower limits. Since a standard method is yet to be established, mechanical properties are determined according to guidelines referred to the tensile properties of thin plastic sheeting

and foil materials, namely ASTM D882 01 and DIN EN ISO 527, respectively. For instance, the ASTM D882 01 method consists of fixing an ODF specimen with a defined dimension between two clamps and pulling the upper clamp at a specific speed and applied force until it breaks [36]. For instance, a typical stress-strain curve for ODF **Figure 2.1** consists of 3 main regions namely; an initial linear elastic deformation of the film (left) as a result of the application of the stress, the second is the film necking due to stretching (centre), and finally the film break or plastic deformation (right).

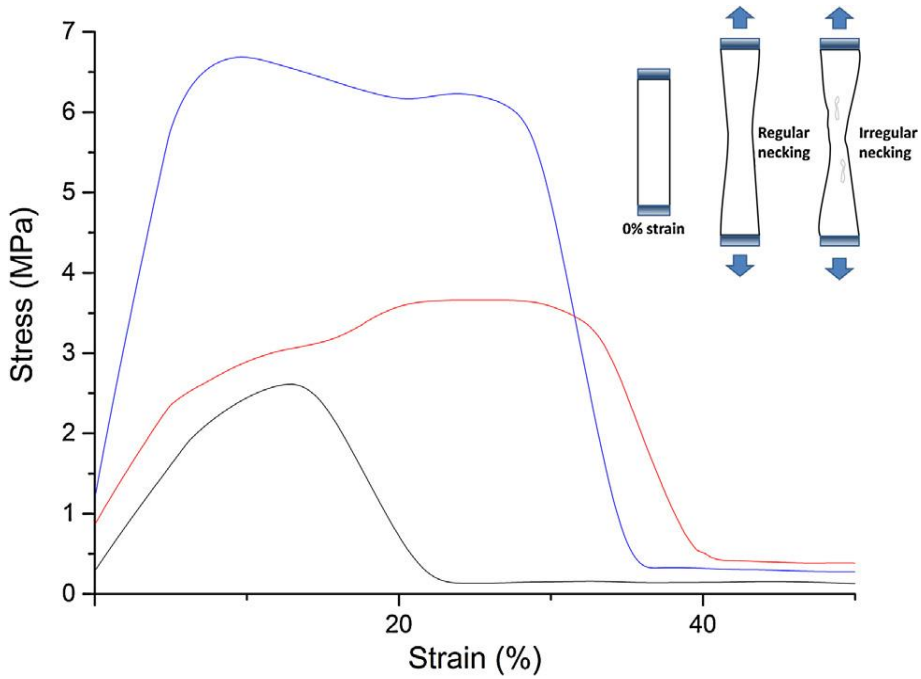

Figure 2.1. Typical stress-strain curve for ODF, adopted from [37].

From the stress–strain curve, the following parameters can be extrapolated and used to define the mechanical properties of an ODF:

Tensile strength (TS): is the resistance of the ODF to an applied force/stress prior to its break, or the maximum stress applied to a point at which the ODF specimen breaks. It is calculated by the maximum force at rupture divided by the cross-sectional area of the ODF as given in the equation 1:

$$TS = \frac{\text{maximum load (Force max)}}{\text{ODF initial cross} - \text{sectional area of the film (Area initial)}} \quad (1)$$

Young's modulus (*E'*) or elastic modulus: is the measure of ODF stiffness. It is calculated as the slope of the linear portion of the stress-strain curve. Hard and brittle ODF generally possess higher tensile strength and higher Young's modulus values [2,19].

Percent elongation at break (ε): application of stress on ODF specimen stretches its dimension and this is referred to as a strain. Percent elongation at break is determined by dividing the extension at the moment of rupture of the specimen (L) by the initial gauge length of the specimen (L_0) and multiplying by 100 according to the following equation:

$$\varepsilon = \frac{L - L0}{L0} \text{ x } 100. \qquad (2)$$

Tensile energy to break (TEB): TEB is defined by the area under the stress-strain curve per unit volume of the ODF specimen between the clamps. TBE values reflect the toughness of the ODF. The value is in units of energy, and it is calculated as follows:

$$TBE = \frac{AUC}{V0} \qquad (3)$$

Where AUC is the area under the stress vs displacement (strain) curve; V_0 is the volume of the specimen between the clamps and is equal to the rectangular cross-sectional area of the specimen x the original length of the sample between the clamps [31,38].

Tear resistance (TR) and puncture test

Tear resistance (TR) measures of the ability of a sheet or film materials to resist tearing. This parameter is related to ODF ultimate resistance to rupture. Usually, a very low load speed of the texture analyser (51 mm/min) is employed and is designed to measure the force to initiate tearing of the ODF. The maximum stress, or force, required to tear the specimen is recorded as the tear resistance value in Newton [2].

On the other hand, puncture test measures the force needed to displace and, finally, to puncture the film [24]. As illustrated in **Figure 2.2**, the ODF specimen is clamped in between two test plates with a cylindrical hole in the middle and the puncturing probe is moving down onto the film surface at a defined velocity. Results obtained from these measurements can be used to calculate the following values [24]:

Elongation to puncture: $\varepsilon p\ (\%) = \frac{\sqrt{r^2+D^2}-r}{r} \text{ x } 100 \qquad (4)$

Puncture strength: $PS = \frac{\text{load required to puncture the ODF (Fload)}}{\text{cross−sectional area of the edge of ODF (A)}} \qquad (5)$

Energy to puncture per unit volume: $\Delta Ep = \frac{\text{area under the load vs.displacement curve (AUC)}}{\text{volume of the film located in the cavity of the film holder (V)}}$ (6)

where:

r is the radius of the ODF located in the cavity of the film holder,

D is the displacement of the probe from point of contact to point of puncture,

A is the cross-sectional area of the edge of the ODF located in the path of the cylindrical hole of the ODF holder [24].

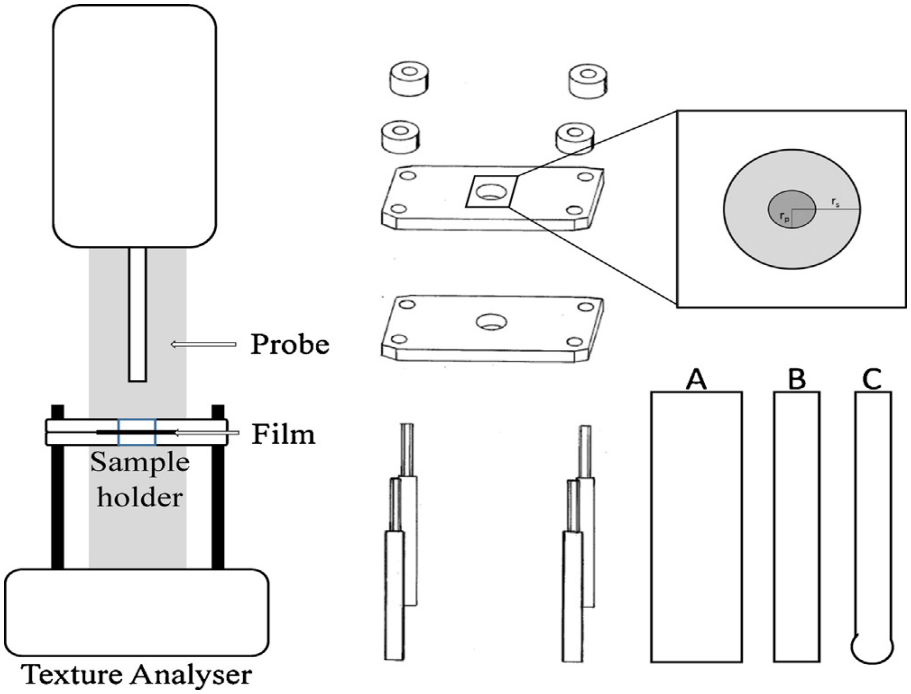

Figure 2.2. Experimental setup for ODF puncture test (left) and sample holder for film preparations (right): rs: radius of samples, rp: radius of the probe. The geometry of cylindrical probes A and B and spherical probe C, adapted from [36]

Flexibility (or folding endurance)

ODF flexibility test measures the ability of the ODF to withstand handling without fracture during the formation of the jumbo roll or during the unrolling operation, as well as during the consumption by the patient. It can also be relevant for the characterization of extemporaneously prepared ODF where access to heavy-duty equipment for tensile properties measurement is difficult. To assess flexibility, ODF are folded in the central area until breakage or up to a

predefined maximum folding time [31,39]. Also in this case, there are no references on standard procedures or the minimum folding time acceptable to assume damage-free handling [24]. In general, the film is folded until the formation of cracks [39] or bended over a mandrel for a predetermined number of times and the ODF is considered flexible if no cracks were visible at a 5× magnification using optical microscopy [40].

Stickiness

The stickiness, or tackiness, is related to the immediacy of the bond under low contact pressure between a compact specimen and the surface of another material. Stickiness can affect ODF handling because too sticky ODF can present difficulty detachment from the packaging material and stick to the patient's fingers during administration. It could be defined as quick stick, initial adhesion, or stickiness [41].

ODF stickiness can be evaluated qualitatively and quantitatively by thumb tack test and probe tack test, respectively. First, the thumb can be pressed lightly on a film sample for a short period and, then, quickly withdrawn. By varying the pressure and time of contact and noting the difficulty of pulling the thumb from the film, it is possible to perceive how easily, quickly, and/or strongly the film can form a bond with the thumb [31].

The probe tack test measures the force required to separate the test probe tip from ODF with predefined dimension. The test can be performed using texture analyser testing machine which measure the maximum detachment stress calculated by dividing the maximum detachment force by the probe surface area [30].

Most of the methods reported in this section are thought and developed mainly for industrial purposes and often require specialized expertise and relatively expensive equipment. Nevertheless, folding endurance and thumb tack can be adapted to the requirements of small-scale setting, easily performed by trained pharmacist.

2.4 Solid-state characterization

Methods used for characterization of the drug physical state are generally used also in the field of ODF. Differential scanning calorimetry (DSC) enables to analyse both the melting point and glass transition temperature [42,43]. As DSC analysis can be complicated by the residual water content or the presence of excipients with low decomposition temperature, such as glycerol, these data are often confirmed and/or integrated by X-ray diffraction patterns [44] and attenuated total reflection Fourier transform infrared (ATR-FTIR) [42]. The latter can be also

used to assess the homogeneity in composition [31] and possible drug-polymer interactions in ODF [19].

Surface morphological analysis by imaging techniques are useful to support solid state data [24]. As an example, in the case of solvent casting , self-aggregation of the drug-polymer matrix may occur during drying because of the convective and intermolecular forces [42]. The resulting 'waved' surface of ODF can be an index of homogeneity, aggregated/scattered drug distribution [19,42]. Additionally, the asymmetrical distribution of crystal seeds, which can be detected by polarized light microscopy, might facilitate uneven drug distribution within the ODF. Also SEM could be used to depict drug crystals or changes during storage on the ODF surface [43,44]. Moreover, this microscopy technique can reveal surface characteristics in the physical microstructure due to different manufacturing process of ODF, surface features and hence can be used to support dissolution and disintegration results [45]; scanning cross-sectional areas of an ODF, it is also possible to visualize the inner inter-connections between multilayer composites.

2.5 Drug content uniformity

The drug content in ODF is generally quantified by standard drug assay methods. Limits of content uniformity range between 85 and 115% according to European Pharmacopoeias [2]. However, the test for uniformity of dosage units [46] is considered to be among the most appropriate for validating dose uniformity of a manufactured batch of ODF (24) on 10 individual ODF with a single dose. The uniformity of dosage units is assessed by calculating the acceptance value (AV):

$$AV = |M\text{-}\bar{x}| + ks$$

Where M is the reference value, which depends on the target drug content, $\bar{x}$ is the mean of individual determined contents in percent of the label claim, k is the acceptability constant that varies depending on dosage units (2.4 for n = 10; 2.0 for n = 30) and s is the standard deviation [47].

In most cases, high-performance liquid chromatography (HPLC) is used for the determination of drug content in the final dosage form. Nevertheless, the need to implement such assay also to control the process during the continuous manufacturing has been driving the development of none-destructive techniques. As summarized in **Table 2.1,** portable handheld near infrared (NIR) spectrometer, calorimeter, and Raman spectrophotometer can allow to identify and

quantify API, limiting the use of elaborate and time-consuming analytical techniques. This would also complement and consolidate the using ODF in personalized pharmacotherapy [8].

Table 2.1. Innovations in none-destructive analytical techniques for identification and quantification of drugs in ODF and other related solid dosage forms

Method	Description	Drug(s) tested and strength	Excipients	Application	Comments	Reference
Handheld NIR spectroscopy (MicroNIRTMPro 1700 ES Spectrometer)	The Mini NIR is a portable compact and lightweight with an overtone NIR spectral region of 950–1650 nm. A transflectance measuring geometry was used by applying black surface. The model was first validated using chemometrics.	Ondansetron Chlorpheniramine maleate, Indomethacin, Nitrofurantoin, Dexamethasone each at doses of 1, 2, 3, 4,5, 6, 8, and 10 mg.	HPMC and glycerol	Extemporaneous ODF made by combined solvent casting and unit-dose plate	Small size, portability, simple user interface, rapid measurement, and real-time prediction results. Applicable to individual ODF to enhance patient safety.	[48]
Handheld NIR spectroscopy (BOMEM MB-160 spectrometer), Raman spectroscopy in a backscattering setup (Kaiser RXN1 Microprobe)	Multivariate data analysis was performed using MatLab R2015a and PLS Toolbox 8.0.1 for the NIR and Raman respectively to identify and quantify the active ingredient.	Haloperidol, propranolol hydrochloride and montelukast sodium at dose ranges between 0.6 – 12.6 mg	HPMC, macrogol 4000, glycerol, polysorbate 20, and poloxamer 188.	Inject printed ODF on HPMC substrate	Valuable, non-destructive, fast and complementary tool for quantification inkjet-printed drug(s).	[48]
Calorimetry (CLM-194 digital handheld colorimeter)	Samples were studied on reflective measurement mode under the same condition for all measurements (n = 3).	propranolol hydrochloride at a dose of 0.1 – 3.2 mg	Water, glycerol, red edible ink	Inkjet-printed ODF on 3 substrates, namely: edible rice paper, edible icing sheet, and coated edible rice paper	reliable method to distinguish the small colour differences between formulations containing an escalating dose of	[50]

	Each colour is described by three numerical values of luminance and two chromatic components representing the shift from green to red and from blue to yellow, respectively. The colour difference parameters were subsequently calculated by the CLM-194 Interface software in Cartesian coordinates.				propranolol hydrochloride.	
Handheld Raman spectrophotometer (TruScan™ RM and IDRaman Mini)	For each formulation, the influence of the sampling is evaluated by acquiring 3 spots at different locations of the solid dosage form. The 3 spots were averaged to get a unique spectrum. Data processing and validation were performed using Matlab R2018b, and multivariate analysis.	Paracetamol, Ibuprofen, Tramadol, Pseudoephedrine chlorhydrate, Caffeine, triprolidine at dose range of 37.5 – 1000 mg	MCC, mannitol, magnesium stearate, lactose.	Compressed Tablets. Application can be extended to continuous manufacturing or compounded ODF.	Enhanced the representativeness of the sampling. Useful for single or fixed-dose combination of drugs in solid dosage forms.	[51]

HPMC: Hydroxy propyl methyl cellulose, MCC: Microcrystalline cellulose, NIR: Near-infrared

2.6 Disintegration test

To date, the European Pharmacopoeia only requires that ODF 'disperse rapidly', but detailed information is not available on the acceptable maximum time both in vitro and in vivo [52]. To fill this gap, reference on the ODF disintegration time is being made with respect to orodispersible tablets using disintegration medium in water or pH 6.8 phosphate buffer as disintegration medium [3]. Literature data also suggest the use of "simulated-saliva fluids", but again media differing in quali-quantitative composition are reported. As no compendial methods is specified, several set-up have been emerging to take into consideration some peculiarities of ODF with respect to ODT such as variation in the ODF dimensions, simulating the physiological condition in the mouth, mechanical stress of the tongue and most importantly to improve precision in the endpoint detection. From the list reported in **Table 2.2**, it is clear the main limitation of the proposed methods is the clear determination of endpoints.

Table 2.2. Summary of modified methods to test ODF disintegration. All tests were carried out at 37 °C.

Method	Medium and test condition	Endpoint detection	Comment	Reference
Petri dish	10 mL distilled water	Time for ODF break	Visual observation may not be accurate, and breaking only may not justify disintegration	[53]
Modified disintegration apparatus with a vertical ODF clip	Purified water with ODF moving vertically at 30 stroke/ min	Time require for the ODF to disintegrate	The method can eliminate the tendency of ODF sticking to the vessel wall	[54]
Thermomechanical analysis	Purified water 250 µL drop after annealing ODF coated in a crucible dis with 900 µm width. Measuring sensor is attached with a constant force of 0.02 N	The swelling of the film is measure using thermo-mechanically as reference for ODF disintegration.	It may not be suitable for non-swellable film-form forming materials.	[55]
Disintegration test system with electronic end-point detection	Water, pH 6.0 phosphate buffer, and simulated salivary fluid. Top and bottom ODF clamp with a 3 g weight attached to the bottom clamp connected to a brass conductor which when released with ODF piece during disintegration sends a signal to the analyser	Disintegration time recorded electronically from the analyser	The method mimics the human tongue when licking coupled with automatic electronic end-point detection could improve extrapolation to humans in real life.	[52]
Slide frame	700 mL Purified water. ODF are clamp in an arm that moves up and down with a frequency of 30 cycles/min over a distance of 55 mm horizontally into the medium.	The time at which complete disintegration occurs is considered as the disintegration time assessed by visual inspection	The method prevents sticking of ODF on the mesh wall in the conventional tablets and capsule disintegration testing unit	[56]
Disintegration test unit (DTU) with a clear endpoint	ODF holder comprises two L-shaped pieces: a base piece and a top piece held together by magnets that are built into each of their vertical plates. The ODF holders are dip into a disintegration	The disintegration endpoint is defined as the breaking of the ODF from the viewing area. The disintegration time of each sample is automatically	Suitable for quality control of ODF at the early stage of development and for industrial manufacturing with improved end-point detection and automatic recording.	[57]

	basket from the top with vessels containing 700 mL of the media. The DTU moves together with the disintegration basket during the stroke movements of the test inside the vessel. The DTU holds the ODFs in a horizontal position	recorded on the built-in timer on the disintegration apparatus		
Slide frame and ball (SFaB)	A stainless-steel ball (diameter 10 mm, and weight 4 g) is place on top of the ODF which simulates the mechanical stress of the tongue to break through the wetted ODF with 900 µL physiological media and dropped on the bottom of the disintegration unit. The total area of the ODF to be exposed for the test is 2x3 cm.	Endpoint indicates the time needed for the stainless-steel ball to break through the wetted ODF and fall down the unit.	the clear endpoint enables the simulation of physiological conditions in the oral cavity and mimic the mechanical force of the tongue. Suitable for research and development of ODF. However, it does not take into consideration the disintegration of the whole ODF.	[58,59]
PharmaTest® film disintegration tester	It is a modified form of pharmacopeial disintegration test set up for tablets and capsules equipped with six sample holders for ODF with an integrated clamping device. Mass (3 g) are fixed to the lower end of each ODF along with the lower clamp which simulates the applied mechanical stress of the tongue. Each ODF is housed in its transparent glass tube. The whole unit is immersed in the testing vessel filled with 900 mL media. Each clamp moves 30 strokes per minute within a distance of 55 mm.	The time taken for the 3 g weight to drop down and close the contact between two sieve halves of the gridded floor is measured as the disintegration endpoint.	Able to mimic the mechanical forces in the tongue, use of physiological media and the automatic endpoint detection. Applicable for industrial manufacturing quality control of ODF.	[58]

2.7 *In-vitro* dissolution

Ph. Eur. states that a suitable test should be carried out to demonstrate the appropriate release of the active substance(s) and reference is given to the dissolution test for the conventional solid dosage forms [60]. Also, in this case, methods adapted for solid dosage forms cannot be appropriate for ODF because placing ODF in the vessel, without any sample holding accessory, might lead to poor reproducibility of results: ODF can easily float, stick on the paddle or vessel. Similar issues might arise using basket set-up, flow-through system, or sinkers [24]. Regarding apparatus, the paddle apparatus (USP type II) is more used than the basket apparatus (USP type I) even if modifications, e.g. reduced volume of the dissolution medium or vessel shape, have been introduced. [33], as summarized in **Table 2.3**.

Generally speaking, operative conditions should be reproducible, representative, and, possibly, well suited to predict the *in vivo* performance. To pursue these aims, the physiological condition and mechanical forces in the oral cavity need to be taken into consideration, particularly the *in-vivo* small volume of the saliva and the short residence time of ODF in the mouth.

As ODF usually exhibit a rapid dissolution, online UV-spectrometry fibre optic sensor systems [3] are gaining increasing interest to provide a reliable dissolution profiles overcoming the difficulties related to conventional sampling procedures (**Table 2.3**).

Table 2.3. Modified *in vitro* dissolution methods for ODF. All experiments were carried out at 37±0.5 °C.

Dissolution method	**Media volume and composition**	**Stirring rate**	**Sampling**	**Analytical method**	**Special features**	**Reference**
JP15 paddle apparatus	900 mL of pH 1.2 phosphate buffer	50 rpm	10 mL 2 min for 120 min	HPLC		[61]
Ph.Eur. basket dissolution apparatus	500 mL freshly deionized water	25 rpm	3 min	UV–Vis spectroscopy		[23]
Ph. Eur. paddle dissolution apparatus	500 mL vessel filled with 400 g of degassed pH 7.4 sodium phosphate buffer	50 rpm	Automated	UV-fibre optical probe	▪ Inline detecting points each second by UV-fibre optical probe immersed into the dissolution medium. ▪ 'One Chamber Method' used enabling the dissolution of the drug and the concentration detection in the same chamber, using the complete 400 g fluid as dissolution medium. ▪ 'Punch & Filter Method' which mimic the conditions in the oral cavity was also incorporated.	[62]
Beaker Stirring Method	150 mL pH 6.8 simulated saliva and pH 1.3, artificial gastric media	200 rpm	1 mL every 30 seconds in the first 5 min, then at 15, 30, 60 and 120 min	UV spectroscopy	▪ Two different media were employed to simulate the conditions in the oral cavity and in the stomach. ▪ Beaker was used as the dissolution vessel under magnetic stirrer.	[63,64]

USP dissolution apparatus-I	900 mL pH 6.8 phosphate buffer	100 rpm	5, 10, and 30 min	HPLC-UV system		[4]
USP type II apparatus	50 mL pH 6 phosphate buffer	50 rpm	1 mL	HPLC	▪ The withdrawn samples were centrifuged at 15.000 rpm at 20 °C for 10 min, to remove residual particles.	[65]
Modified petri dish approach (closed cylindrical glass vial housed in a thermostat shaking water bath)	5 mL of pH 6.8 simulated saliva pre-heated	10 rpm	5 mL (as a whole in triplicates)	UV–Vis spectroscopy	▪ The modified petri dish was coupled with a digital stopwatch. ▪ Changes in test sample physical forms were viewed under a white fluorescent light to enhance visibility ▪ Dissolution time represented the period required for each strip to undergo complete solvation/dissolution into a homogenous solution. ▪ The pH of the final solution was also tested.	[66,67]
Ph. Eur. paddle dissolution apparatus	900 mL freshly deionized water and pH 5.7 artificial saliva	50 rpm		UV–Vis spectroscopy	▪ Two different media were used.	[31]
Ph. Eur. basket dissolution apparatus	900 mL freshly deionized water, maintained	50 rpm	2 min intervals	UV–Vis spectroscopy		[5]

USP type-IV (flow-through cell) combined with paddle apparatus (USP type II).	Artificial saliva, artificial gastric fluid, artificial intestine fluid, pH 6.6 phosphate buffer 16.2 ± 0.06 mL	50 rpm	60 s for 1000 min (online automated)	UV–Vis spectroscopy	▪ The system was operated in closed-loop by means of a peristaltic pump. ▪ In-house sample holder FH3D (22.6 mm) held the ODF with adhesive tape which prevent floating, sticking together, and adherence of the ODF to the chamber wall. ▪ Four different media were used	[68]

2.8 Evaluation of shelf-life

The stability of ODF must be evaluated according to the International Conference on Harmonization (ICH) guidelines for oral dosage forms. In long term, intermediate or accelerated stability conditions. ODF properties evaluated over time are related to their critical quality attributes usually mechanical properties, disintegration and dissolution. All these aspects can be affected by ageing but also by variation of humidity.

Thus, the packaging of the films plays an important role to ensure that ODF maintain their quality attributes over time, e.g. drug content and dissolution rate [69]. Furthermore, as ODF are highly sensitive to humid conditions, moisture uptake should be also monitored [70].

Air-tight primary packaging materials, such as aluminium sachets, are often necessary to preserve ODF feature over time [71] despite the high costs. Foil, paper or plastic pouches can be considered as secondary packaging material. Though, their suitability needs to be carefully evaluated for a specific formulation including aspects of ODF stability and packaging materials suitability for pharmaceuticals [11].

2.9 *In vitro* biopharmaceutical evaluation

ODF are designed to cause the release drug substances therein for either systemic or a local effect. For local treatment, absorption of the API is not desired, as side effects may occur. When a systemic effect is required, the API can either be swallowed and absorbed via the gastrointestinal tract or be absorbed via the oromucosal membrane. Absorption through the oromucosal membrane may increase the bioavailability compared to conventional oral solid dosage forms when the API is affected by significant first-pass metabolism [2]. Such an improvement of the bioavailability may be advantageous for new ODF products but may also cause problems related to toxicity if not carefully studied prior to clinical application. Controlled absorption of API from ODF through the oral mucosa can be also achieved by incorporating excipients, e.g., ion exchange resins, or complementary process, e.g. particle coating techniques [11,72,73]. Therefore, regardless the approach followed, absorption through the oral mucosa should also be investigated using both *in vitro* or *in vivo* permeation studies. As an example, *ex vivo* permeation study of iloperidone loaded in ODF was carried out using porcine tissue on Franz diffusion cell in pH 6.8 phosphate buffer [74]. Similarly, Santi et al., investigated the permeation of lidocaine using oesophageal isolated epithelium in pH 7.4 phosphate buffer [75]. Pharmacokinetics studies comparing the plasma concentration curves of API loaded in ODF and other conventional solid dosage forms available in the market

can permit to assess when a dose adjustment is required in ODF formulations. These studies can as well be achieved using human volunteers [70,76], and/or animal models [61,74].

2.10 Conclusions

ODF have been attracting more and more attention among researchers and pharmaceutical industries as innovative dosage forms able to solve some of the peculiar problems of convention solid and liquid dosage forms. In recent years, ODF are a fastest growing part of personalized medicine. Therefore, advancement in the characterization technologies needs to evolve to evaluate their specific attributes. What is left is for the regulatory authorities to step out and harmonize means of quality standards for ODF evaluation as currently, they are very scanty and not well explicit where they exist.

Moreover, for ODF extemporaneously prepared in small batches for personalized therapy, less complex, easy to use and none-destructive assays need to be optimized. Along with methods to quantify the drug contents and uniformity, mechanical properties are of vital importance. Tackiness (thumb tack test), and folding endurance could be easily evaluated to guarantee the mechanical quality of ODF prepared on demand. These tests do not need any intensive equipment and they can be easily conducted by a well-trained pharmacist.

References

[1] Badgujar, B.P.; Mundada, A.S. The technologies used for developing orally disintegrating tablets: A review. *Acta Pharm.* **2011**, 61(2), 117–39.

[2] Dixit, R.P.; Puthli, S.P. Oral strip technology: Overview and future potential. *J Control Release*. **2009**, 139(2), 94–107.

[3] Cilurzo, F.; Musazzi, U.M.; Franzé, S.; Selmin, F.; Minghetti, P. Orodispersible dosage forms: biopharmaceutical improvements and regulatory requirements. *Drug Discov Today*. **2018**, 23(2), 251–9. Available from: http://dx.doi.org/10.1016/j.drudis.2017.10.003

[4] Pimparade, M.B.; Vo, A.; Maurya, A.S.; Bae, J.; Morott, J.T.; Feng, X.; Kim, D.W.; Kulkarni, V.I.; Tiwari, R.; Vanaja, K.; Murthy, R.; Shivakumar, H.N.; Neupane, D.; Mishra, S.R.; Murthy, S.N. Repka, M.A. Development and Evaluation of an Oral Fast Disintegrating Anti-allergic Film Using Hot-melt Extrusion Technology. *Eur J Pharm Biopharm*. **2017**, 119, 81–90. Available from: http://dx.doi.org/10.1016/j.ejpb.2017.06.004

[5] Musazzi, U.M.; Selmin, F.; Ortenzi. M.A.; Mohammed, G.K.; Franzé, S.; Minghetti, P.; Cilurzo, F. Personalized orodispersible films by hot melt ram extrusion 3D printing. *Int J Pharm*. **2018**, 551(1–2), 52–9.

[6] Lai, F.; Franceschini, I.; Corrias, F.; Sala, M.C.; Cilurzo, F.; Sinico, C.; Pini, E. Maltodextrin fast dissolving films for quercetin nanocrystal delivery. A feasibility study. *Carbohydr. Polym*. **2015**, 121, 217–223. https://doi.org/10.1016/j.carbpol.2014.11.070

[7] Musazzi, U.M.; Passerini, N.; Albertini, B.; Dolci, L.S.; Cilurzo, F. A new melatonin oral delivery platform based on orodispersible films containing solid lipid microparticles. *Int. J. Pharm*. **2019**, 559, 280–288. https://doi.org/10.1016/j.ijpharm.2019.01.046

[8] Musazzi, U.M.; Khalid, G.M.; Selmin, F.; Minghetti, P.; Cilurzo, F. Trends in the production methods of orodispersible films. *Int J Pharm*. **2020**, 576.

[9] Amelian, A.; Wasilewska, K.; Wesoły, M.; Ciosek-Skibińska, P.; Winnicka, K. Taste-masking assessment of orally disintegrating tablets and lyophilisates with cetirizine dihydrochloride microparticles. *Saudi Pharm J*. **2017**, 25(8),1144–50.

[10] Borges, A.F.; Silva, C.; Coelho, J.F.J.; Simões, S. Outlining critical quality attributes (CQAs) as guidance for the development of orodispersible films. *Pharm Dev Technol*. **2017**, 22(2), 237–45.

[11] Krampe, R.; Visser, J.C.; Frijlink, H.W.; Breitkreutz, J.; Woerdenbag, H.J.; Preis, M. Oromucosal film preparations: points to consider for patient centricity and manufacturing processes. *Expert Opin Drug Deliv*. **2016**,13(4), 493–506. Available from: http://www.tandfonline.com/doi/full/10.1517/17425247.2016.1118048

[12] Kianfar, F.; Chowdhry, B.Z.; Antonijevic, M.D.; Boateng, J.S. Novel films for drug delivery via the buccal mucosa using model soluble and insoluble drugs. *Drug Dev Ind Pharm*. **2012**, 38(10), 1207–20.

[13] Das N.G.; Das, S.K. Development of Mucoadhesive Dosage Forms of Buprenorphine for Sublingual Drug Delivery. *Drug Deliv J Deliv Target Ther Agents*. **2004**, 11(2), 89–95.

[14] Woertz, C.; Kleinebudde, P. Development of orodispersible polymer films with focus on the solid state characterization of crystalline loperamide. *Eur J Pharm Biopharm*. **2015**, 94, 52–63. Available from: http://dx.doi.org/10.1016/j.ejpb.2015.04.036

[15] Vuddanda, P.R.; Montenegro-Nicolini, M.; Morales, J.O.; Velaga, S. Effect of surfactants and drug load on physico-mechanical and dissolution properties of nanocrystalline tadalafil-loaded oral films. *Eur J Pharm Sci*. **2017**,109, 372–80.

Available from: https://doi.org/10.1016/j.ejps.2017.08.019
[16] Içten, E.; Giridhar, A.; Taylor, L.S.; Nagy, Z.K.; Reklaitis, G.V. Dropwise additive manufacturing of pharmaceutical products for melt-based dosage forms. *J Pharm Sci*. **2015**, 104(5), 1641–9.
[17] Azizi, M.S.; Mohaved, S.; Narayan, R.J. Inkjet dispensing technologies: recent advances for novel drug discovery. *Expert Opin Drug Discov*. **2019**, 14(2), 101–13. Available from: https://doi.org/10.1080/17460441.2019.1567489
[18] Alomari, M.; Mohamed, F.H.; Basit, A.W.; Gaisford, S. Personalised dosing: Printing a dose of one's own medicine. *Int J Pharm*. **2015**, 494(2), 568–77. Available from: http://dx.doi.org/10.1016/j.ijpharm.2014.12.006
[19] Nair, A.B.; Kumria, R.; Harsha, S.; Attimarad, M.; Al-Dhubiab, B.E.; Alhaider, I.A. In vitro techniques to evaluate buccal films. *J Control Release*. **2013**, 166(1),10–21.
[20] Patel, V.M.; Prajapati, B.G.; Patel, M.M. Effect of Hydrophobic Polymers on Buccoadhesive Eudragit Patches of Propanolol Hydrochloride Using Factorial Design. *AAPS PharmSciTech*. **2007**, 8(2), E1-8.
[21] Cao, N.; Yang, X.; Fu, Y. Effects of various plasticizers on mechanical and water vapor barrier properties of gelatin films. *Food Hydrocoll*. **2009**, 23(3), 729–35. Available from: http://dx.doi.org/10.1016/j.foodhyd.2008.07.017
[22] Niese, S.; Quodbach, J. Application of a chromatic confocal measurement system as new approach for in-line wet film thickness determination in continuous oral film manufacturing processes. *Int J Pharm*. **2018**, 551(1–2), 203–11.
[23] Cilurzo, F.; Cupone, I.E.; Minghetti, P.; Buratti, S.; Gennari, C.G.M.; Montanari, L. Diclofenac fast-dissolving film: Suppression of bitterness by a taste-sensing system. *Drug Dev Ind Pharm*. **2011**, 37(3), 252–9.
[24] Preis, M.; Woertz, C.; Kleinebudde, P.; Breitkreutz, J. Oromucosal film preparations: classification and characterization methods. *Expert Opin Drug Deliv*. **2013**, 10(9), 1303–17. Available from: http://www.tandfonline.com/doi/full/10.1517/17425247.2013.804058
[25] Miyanaga, Y.; Tanigake, A.; Nakamura, T.; Kobayashi, Y.; Ikezaki, H.; Taniguchi, A.; Matsuyama, K.; Uchida T. Prediction of the bitterness of single, binary- and multiple-component amino acid solutions using a taste sensor. *Int J Pharm.* **2002**, 248(1–2), 207–18.
[26] Haraguchi, T.; Yoshida, M.; Kojima, H.; Uchida, T. Usefulness and limitations of taste sensors in the evaluation of palatability and taste-masking in oral dosage forms. *Asian J Pharm Sci*. **2016,** 11(4), 479–85. Available from: http://dx.doi.org/10.1016/j.ajps.2016.03.001
[27] Haraguchi, T.; Yoshida, M.; Uchida, T. Evaluation of ebastine-loaded orally disintegrating tablets using new apparatus of detecting disintegration time and e-tongue system. *J Drug Deliv Sci Technol*. **2014**, 24(6), 684–8. Available from: http://dx.doi.org/10.1016/S1773-2247(14)50137-2
[28] Nakamura, H.; Uchida, S.; Sugiura, T.; Namiki, N. The prediction of the palatability of orally disintegrating tablets by an electronic gustatory system. *Int J Pharm*. **2015**, 493(1–2), 305–12. Available from: http://dx.doi.org/10.1016/j.ijpharm.2015.07.056
[29] Al-Kasmi, B.; Al-Rahal, O.; El-Zein, H.; Nattouf, A.H. Structural and in vitro in vivo evaluation for taste masking. *Expert Opin. Drug Deliv.* **2018**, 15(11), 1105–1116.
[30] Khadra, I.; Obeid, M.A.; Dunn, C.; Watts, S.; Halbert, G.; Ford, S.; Mullen A. Characterisation and optimisation of diclofenac sodium orodispersible thin film formulation. *Int J Pharm*. **2019**, 561:43–6. Available from: https://linkinghub.elsevier.com/retrieve/pii/S037851731930105X

[31] Musazzi, U.M.; Selmin, F.; Franzé, S.; Gennari, C.G.M.; Rocco, P.; Minghetti, P.; Cilurzo F. Poly(methyl methacrylate) salt as film forming material to design orodispersible films. *Eur J Pharm Sci*. **2018**, 115, 37–42. Available from: https://doi.org/10.1016/j.ejps.2018.01.019

[32] Lal, M.; Lai, M.; Estrada, M.; Zhu, C.; Developing a Flexible Pediatric Dosage Form for Antiretroviral Therapy: A Fast-Dissolving Tablet. *J Pharm Sci*. **2017**, 106(8), 2173–7. Available from: http://dx.doi.org/10.1016/j.xphs.2017.05.004

[33] Borges, A.F.; Silva, C.; Coelho,; J.F.J.; Simões, S. Oral films: Current status and future perspectives: I-Galenical development and quality attributes. *J Control Release*. **2015**, 206, 1–19. Available from: http://dx.doi.org/10.1016/j.jconrel.2015.03.006

[34] Boateng, J.S.; Auffret, A.D.; Matthews, K.H.; Humphrey, M.J.; Stevens, H.N.E.; Eccleston, G.M. Characterisation of freeze-dried wafers and solvent evaporated films as potential drug delivery systems to mucosal surfaces. *Int J Pharm*. **2010**, 389(1–2), 24–31. Available from: http://dx.doi.org/10.1016/j.ijpharm.2010.01.008

[35] European Pharmacopoeia Commission. Oromucosal Preparations. In: European Pharmacopoeia. 8th ed. Strasbourg: European Directorate for the Quality of Medicines (EDQM); **2014**.

[36] Preis, M.; Knop, K.; Breitkreut, J. Mechanical strength test for orodispersible and buccal films. *Int J Pharm*. **2014**, 461(1–2), 22–9. Available from: http://dx.doi.org/10.1016/j.ijpharm.2013.11.033

[37] Franceschini, I.; Selmin, F.; Pagani, S.; Minghetti, P.; Cilurzo, F. Nanofiller for the mechanical reinforcement of maltodextrins orodispersible films. *Carbohydr. Polym.*, **2016**, 136, 676–681.

[38] Radebaugh, G.W.; Murtha, J.L.; Julian, T.N.; Bondi, J.N. Methods for evaluating the puncture and shear properties of pharmaceutical polymeric films. *Int J Pharm*. **1988**, 45(1–2), 39–46.

[39] Puratchikody, A.; Prasanth, V.V.; Mathew, S.T.; Kumar, B.A. Development and characterization of mucoadhesive patches of salbutamol sulfate for unidirectional buccal drug delivery. *Acta Pharm*. **2011**, 61(2), 157–70.

[40] Cilurzo, F.; Cupone, I.E.; Minghetti, P.; Selmin, F.; Montanari, L. Fast dissolving films made of maltodextrins. *Eur. J. Pharm. Biopharm.* **2008**, 70(3), 895–900.

[41] Minghetti, P.; Cilurzo, F.; Casiraghi, A. Measuring adhesive performance in transdermal delivery systems. *Am J Drug Deliv*. **2004**, 2(3), 193–206. Available from: http://www.embase.com/search/results?subaction=viewrecord&from=export&id=L39272805

[42] Karki, S.; Kim.; H, Na, S.J.; Shin, D.; Jo, K.; Lee, J. Thin films as an emerging platform for drug delivery. *Asian J Pharm Sci*. **2016**, 11(5), 559–74. Available from: http://dx.doi.org/10.1016/j.ajps.2016.05.004

[43] Coates, J. Interpretation of Infrared Spectra, A Practical Approach. *Encycl Anal Chem*. **2006**, 1–23. Available from: http://doi.wiley.com/10.1002/9780470027318.a5606

[44] Pongjanyakul, T.; Suksri, H. Alginate-magnesium aluminum silicate films for buccal delivery of nicotine. *Colloids Surfaces B Biointerfaces*. **2009**, 74(1), 103–13.

[45] Preis, M.; Pein, M.; Breitkreutz, J. Development of a taste-masked orodispersible film containing dimenhydrinate. *Pharmaceutics*. **2012**, 4(4), 551–62.

[46] European Pharmacopoeia Commission. 2.9.40 uniformity of dosage units. In: European Pharmacopoeia. edition 7.0. European Directorate for the Quality of Medicines (EDQM); Strasbourg, France: **2008**.

[47] European Pharmacopoeia Commission. Oromucosal Preparations. In European Pharmacopoeia. 7.4 edition. European Directorate for the Quality of Medicines

(EDQM); Strasbourg, France; **2012**. p. 4257-Updated monograph on 'oromucosal preparations' by the European Pharmacopoeia.

[48] Foo, W.C.; Widjaja, E.; Khong, Y.M.; Gokhale, R. Chan, S.Y. Application of miniaturized near-infrared spectroscopy for quality control of extemporaneous orodispersible films. *J Pharm Biomed Anal*. **2018**;150:191–8. Available from: http://dx.doi.org/10.1016/j.jpba.2017.11.068

[49] Edinger, M.; Iftimi, L.D.; Markl, D.; Al-Sharabi, M.; Bar-Shalom, D.; Rantanen, J.; Genina, N. Quantification of Inkjet-Printed Pharmaceuticals on Porous Substrates Using Raman Spectroscopy and Near-Infrared Spectroscopy. *AAPS PharmSciTech*. **2019**, 20(5).

[50] Vakili, H.; Nyman, J.O.; Genina, N.; Preis, M.; Sandler, N. Application of a colorimetric technique in quality control for printed pediatric orodispersible drug delivery systems containing propranolol hydrochloride. *Int J Pharm*. **2016**, 511(1), 606–18. Available from: https://linkinghub.elsevier.com/retrieve/pii/S0378517316306627

[51] Coic, L.; Sacré, P.Y.; Dispas, A.; Dumont, E.; Horne, J.; De Bleye, C.; Fillet, M.; Hubert P.; Ziemons. E. Evaluation of the analytical performances of two Raman handheld spectrophotometers for pharmaceutical solid dosage form quantitation. *Talanta*. **2020**, 214, 120888. Available from: https://doi.org/10.1016/j.talanta.2020.120888

[52] Preis, M.; Gronkowsky, D.; Grytzan, D.; Breitkreutz, J. Comparative study on novel test systems to determine disintegration time of orodispersible films. *J Pharm Pharmacol*. **2014**, 66(8), 1102–11.

[53] El-Setouhy, D.A.; El-Malak, N.S.A. Formulation of a Novel Tianeptine Sodium Orodispersible Film. *AAPS PharmSciTech*. **2010**, 11(3), 1018–25. Available from: http://www.springerlink.com/index/10.1208/s12249-010-9464-2

[54] Sakuda, Y.; Ito, A.; Sasatsu, M.; Machida, Y. Preparation and evaluation of medicinal carbon oral films. *Chem Pharm Bull*. **2010**, 58(4), 454–7.

[55] Garsuch, V.; Breitkreutz, J. Novel analytical methods for the characterization of oral wafers. *Eur J Pharm Biopharm*. **2009**, 73(1), 195–201. Available from: http://dx.doi.org/10.1016/j.ejpb.2009.05.010

[56] Visser, J.C.; Woerdenbag, H.J.; Crediet, S.; Gerrits, E.; Lesschen, M.A.; Hinrichs, W.L.J.; Breitkreutz, J.; Frijlink H.W. Orodispersible films in individualized pharmacotherapy: The development of a formulation for pharmacy preparations. *Int J Pharm*. **2015**, 478(1), 155–63. Available from: http://dx.doi.org/10.1016/j.ijpharm.2014.11.013

[57] Low, A.; Kok, S.L.; Khong, Y.M.; Chan, S.Y.; Gokhale, R. A New Test Unit for Disintegration End-Point Determination of Orodispersible Films. *J Pharm Sci*. **2015**, 104(11), 3893–903.

[58] Speer, I.; Steiner, D.; Thabet, Y.; Breitkreutz, J.; Kwade, A. Comparative study on disintegration methods for oral film preparations. *Eur J Pharm Biopharm*. **2018**, 132, 50–61.

[59] Steiner, D.; Finke, J.H.; Kwade, A. Efficient production of nanoparticle-loaded orodispersible films by process integration in a stirred media mill. *Int J Pharm*. **2016**, 511(2), 804–13. Available from: http://dx.doi.org/10.1016/j.ijpharm.2016.07.058

[60] Anon, Mucoadhesive preparations monograph. In European Pharmacopoeia. (9.5 edn), Council of Europe Suppl. 9.5. **2018**

[61] Nishimura, M.; Matsuura, K.; Tsukioka, T.; Yamashita, H.; Inagaki, N.; Sugiyama, T.; Itoh, Y.. In vitro and in vivo characteristics of prochlorperazine oral disintegrating film. *Int J Pharm*. **2009**, 368(1–2), 98–102.

[62] Krampe, R.; Sieber, D.; Pein-Hackelbusch, M.; Breitkreutz, J. A new biorelevant

dissolution method for orodispersible films. *Eur J Pharm Biopharm*. **2016**, 98, 20–5. Available from: http://dx.doi.org/10.1016/j.ejpb.2015.10.012

[63] Nalluri, B.N.; Sravani, B.; Anusha, V.S.; Sribramhini, R.; Maheswari, K.M. Development and Evaluation of Mouth Dissolving Films of Sumatriptan Succinate for Better Therapeutic Efficacy. *J Appl Pharm Sci*. **2013**, 3(8), 161–6.

[64] Senta-Loys, Z.; Bourgeois, S.; Pailler-Mattei, C.; Agusti, G.; Briançon, S.; Fessi, H. Formulation of orodispersible films for paediatric therapy: investigation of feasibility and stability for tetrabenazine as drug model. *J Pharm Pharmacol*. **2017**, 69(5), 582–92.

[65] Wimmer-Teubenbacher, M.; Planchette, C.; Pichler, H.; Markl, D.; Hsiao, W.K.; Paudel, A.; Stegemann, S. Pharmaceutical-grade oral films as substrates for printed medicine. *Int J Pharm*. **2018**, 547(1–2), 169–80. Available from: https://doi.org/10.1016/j.ijpharm.2018.05.041

[66] Adeleke, O.A.; Tsai, P.C.; Karry, K.M.; Monama, N.O.; Michniak-Kohn, B.B. Isoniazid-loaded orodispersible strips: Methodical design, optimization and in vitro-in silico characterization. *Int J Pharm*. **2018**, 547(1–2), 347–59. Available from: https://doi.org/10.1016/j.ijpharm.2018.06.004

[67] Garsuch, V.; Breitkreutz, J. Comparative investigations on different polymers for the preparation of fast-dissolving oral films. *J Pharm Pharmacol*. **2010**, 62(4), 539–45. Available from: http://doi.wiley.com/10.1211/jpp.62.04.0018

[68] Speer, I.; Preis, M.; Breitkreutz, J. Novel Dissolution Method for Oral Film Preparations with Modified Release Properties. *AAPS PharmSciTech*. **2019**, 20(1), 7. Available from: http://link.springer.com/10.1208/s12249-018-1255-1

[69] Fahmy, R.H.; Badr-Eldin, S.M. Novel delivery approach for ketotifen fumarate: Dissofilms formulation using 32 experimental design: In vitro/in vivo evaluation. *Pharm Dev Technol*. 2**014**, 19(5), 521–30.

[70] ElMeshad, A.N.; El-Hagrasy, A.S. Characterization and Optimization of Orodispersible Mosapride Film Formulations. *AAPS PharmSciTech*. **2011**, 12(4), 1384–92.

[71] Hoffmann, E.M.; Breitenbach, A.; Breitkreutz, J. Advances in orodispersible films for drug delivery. *Expert Opin Drug Deliv*. **2011**, 8(3), 299–316. Available from: http://www.tandfonline.com/doi/full/10.1517/17425247.2011.553217

[72] Shang, R.; Liu, C.; Quan, P.; Zhao, H.; Fang, L. Effect of drug-ion exchange resin complex in betahistine hydrochloride orodispersible film on sustained release, taste masking and hygroscopicity reduction. *Int. J. Pharm.* **2018**, 545(1–2), 163–169.

[73] Speer, I.; Lenhart, V.; Preis, M.; Breitkreutz, J. Prolonged release from orodispersible films by incorporation of diclofenac-loaded micropellets. *Int. J. Pharm.* **2019**, 554, 149–160.

[74] Londhe, V.; Shirsat, R. Formulation and Characterization of Fast-Dissolving Sublingual Film of Iloperidone Using Box–Behnken Design for Enhancement of Oral Bioavailability. *AAPS PharmSciTech*. **2018**, 19(3), 1392–400.

[75] Santi, P.; Traversone, V.; Padula, C.; Pozzetti, L.; Nicoli, S. In Vitro Evaluation of Mucoadhesive Films for Gingival Administration of Lidocaine. *AAPS PharmSciTech*. **2013**, 14(4), 1279–83.

[76] Reiner, V.; Giarratana, N.; Monti, N.C.; Breitenbach, A.; Klaffenbach, P. Rapidfilm®: An innovative pharmaceutical form designed to improve patient compliance. *Int J Pharm*. **2010**, 393(1–2), 55–60. Available from: http://dx.doi.org/10.1016/j.ijpharm.2010.03.055

Chapter 3

Personalized Orodispersible Films by Hot-Melt Ram Extrusion Printing

3.1 Introduction

Commercially available oral medicinal products do not satisfy all needs of special populations, such as dysphagics [1] paediatrics [2], geriatrics [3] and patients with allergies or dietary restriction [4]. In these cases, the drug has to be re-formulated or made from different inactive ingredients to comply the specific medical needs.

When the required dose is not available, the most common solution, which implies to split a solid dosage form, often occurs in dose inaccurancy [5, 6]. The possible alternative is to compound a personalized drug product, e.g., solutions, syrups, capsules and tablets, in pharmacy settings. Despite this approach allows personalizing the dose, issues related to possible inaccuracy are only partially solved. As an example, the use of spoons or syringes would not allow the precise withdraw of the exact volume of liquids. On the other hands, the administration of tablets and capsules, which overcomes this drawback, can be associated with swallowing problems or fear of chocking and, in these cases, the patient compliance and the therapeutic adherence remain quite low [1].

In the recent years, orodispersible dosage forms have been proposed in the personalization of the therapy [7], especially for children [8] and elderly [9] due to the possibility of combining the advantages of solid dosage forms and liquid formulations. Despite both orodispersible tablets and films (ODF) can be currently compounded in pharmacy settings [10, 11], the latter results are particular attractive since the dose is defined not only by the drug strength, but also by the dimensions of the ODF itself. In the selection of the appropriated manufacturing and/or compounding process, several technical and economic aspects have to be considered, e.g. the small batch production due limited number of dosage forms required for an individual patient, the cleaning procedure of the equipment to avoid the cross-contaminations, the number of critical process parameters to control during the preparation and, last but not least, the necessity of a moisture proof packaging to protect ODF over the shelf-life.

In literature, both solvent casting and printing technologies have been proposed to prepare ODF. The former consists in a lab-coater apparatus that combines a doctor knife unit to assure the uniformity of thickness, and therefore of the drug content, to an oven to dry the slurry. Nevertheless, the residual moisture content in ODF is one of the main critical limitation of this strategy due to the impact on the film mechanical properties and stability [12]. As an alternative, the simplest approach consists of depositing a known amount of a drug loaded polymeric slurry on a support, e.g., petri dish, flat moulds or unit-dose plate, drying in an oven and cutting the obtained film [13, 14, 15]. In this case, the possible risks of dose inaccuracy are

related to the lack of perfect alignment of the support base or the oven shelf that can cause the movement of the slurry and, therefore, a not-uniform film thickness. Ink-jet printing, which is based on the drug loading onto an edible film, is probably the widest explored printing technology to produce ODF. The feasibility of this approach was demonstrated with several drugs [3] also in fixed combinations [16]. Moreover, inkjet printing can enable the simultaneous and independent dosing of drug combinations, as demonstrated using triiodothyronine and thyroxine, easily recognized by adding two different colouring agents [17]. The addition of a colouring agent to the ink can also permit the simple visualization of the uniformity of printed structures and, therefore, drug content [18]. Despite these advantages, this technology cannot be easily applied to load poorly soluble drugs, since inks need to be formulated case-by-case to avoid the drug sedimentation, which is the main source of dose inaccuracy. Hence some Scarpa and co-workers opts to formulate not-aqueous solutions, nanosuspensions or lipidic inks [3]. Alternatively, the melt ink-jet printing allows a good control of the drug solid state and film morphology [19, 20] and the flexographic printing was also tested to impregnate placebo ODF with a precise dose of a drug [21].

More recently, fused deposition modelling (FDM) 3D printing, which is usually explored to design solid oral dosage forms [22] with different geometries [23] and release characteristics [24] was also studied in the attempt to avoids the need of preformed films [25]. Nevertheless, the application of such technology to the extemporaneous preparation of ODF could be very complicated because drug-loaded filaments have to be preliminarily produced by hot-melt extrusion [26] or obtained by impregnation of commercial filament [24] with all the limitation described by Fuenmayor and co-workers [27].

This work describes a novel approach to print ODF intended for personalized therapy. The basic idea of the proposed technology arose from the combination of a hot melt ram extruder, able to extrude a drug/polymer/plasticizer blend, and the typical aligned plate of 3D printers whose movements allow the deposition material of the desired dimensions and shape. Maltodextrins were tested as the main component of the formulation since the possibility to obtain ODF by hot-melt extrusion is documented [28] as well as the feasibility to tune the ODF mechanical properties by varying the maltodextrins molecular weight and/or the plasticizer ratio [29, 30].

3.2 Materials

Maltodextrins with a dextrose equivalent (D.E.) equal to 6 (Glucidex® IT6, MDX6) and 12 (Glucidex® IT12, MDX12) were kindly obtained by Roquette (France). Paracetamol (PAR), glycerine and titanium dioxide (TiO_2) were purchased from Farmalabor (Italy). Span® 80 was supplied from Croda (Spain). Glycine (GLY) was purchased from ACEF. (Italy). All solvents were of analytical grade unless specified.

3.3 Methods

3.3.1 Rheological characterization of maltodextrin/plasticizer blends

Compression tests – Tests were performed on 0.4 mm thick laminates made of MDX6 and glycerine in the 80/20 and 84/16 ratios in order to assess their softening temperature. Laminates were prepared by solvent casting technique by using a laboratory-coating unit Mathis LTE-S(M) (Switzerland). MDX6 (75% w/w) and glycerine in water at 80 °C under stirring. After a rest period of at least 24 h to remove air bubbles, the aqueous dispersion was cast onto a silicone release liner with a 650 μm thickness. The coating rate was fixed at 1 m/min, and the cast dispersion was dried in the oven at 80 °C for 30 min with a horizontal air circulation speed of 1200 rpm.

Laminates were placed in the rheometer (Physica MCR 300 rheometer, Anton Paar GmbH, Austria) at 50 °C, compressed with a normal force of 10 N using a 25 mm upper plate and heated at the heating rate of 5 °C/min. The softening temperature was expressed as the onset of the curve resulting from the analysis.

Frequency sweep experiments - Tests were performed on selected ODF, among those reported in **Table 3.1**, from 100 to 0.1 Hz (angular frequency – ω of 620-0.628 s^{-1}) in the strain-controlled mode using a plate-plate geometry, 25 mm diameter at the temperature of 80, 90, 100 and 110 °C (Physica MCR 300 rheometer, Anton Paar GmbH, Austria). The strain was set at 5% to be in the linear viscoelastic regime of the blends. In order to estimate a possible relationship between the rheological data and the feasibility to print the designed formulations, the shear viscosity at 1.1 s^{-1}shear rate was calculated according to Cox-Merz rule. The shear rate value was also determined since it corresponds to the extrusion rate during the printing of the ODF.

Table 3.1 – Composition of placebo and paracetamol (PAR) loaded ODF obtained by printing. The main components were maltodextrins with a dextrose equivalent of 6 (MDX6) and 12 (MDX12), glycerine (GLN), glycine (GLY) and titanium dioxide (TiO_2). Loss of drying (LOD) and disintegration time (Disgr) are enlisted. The ODF stickiness is expressed by the following score system: A (no sticky), B (sticky), and C (very sticky).

Form	ODF composition (%, w/w)						LOD (%, w/w)	Stickiness (A, B, C)	Disgr. (s)
	MDX6	MDX12	GLN	GLY	PAR	TiO_2			
1	84.00	-	16.00	-	-	-	-*	-*	-*
2	82.75	-	16.00	1.25	-	-	-*	-*	-*
3	81.50	-	16.00	2.50	-	-	7.8±2.6	A	86±33
4	81.40	-	16.00	2.50	-	0.10	10.9±2.8	A	73±15
5	-	84.00	16.00	-	-	-	-*	-*	-*
6	-	83.90	16.00	1.25	-	0.10	-*	B	90±10
7	-	81.40	16.00	2.50	-	0.10	-*	C	103±7
8	61.60	-	11.60	1.80	25.00	-	8.1±1.4	A	75±5
9	80.00	-	20.00	-	-	-	7.1±2.2	A	53±35
10	79.90	-	20.00	-	-	0.10	5.6±1.4	A	65±28
11	78.75	-	20.00	1.25	-	-	5.7±0.9	B	111±29
12	77.50	-	20.00	2.50	-	-	8.9±1.5	C	96±46
13	70.00	-	17.50	-	12.50	-	7.5±1.7	A	75±29
14	60.00	-	15.00	-	25.00	-	7.3±1.7	A	34±14
15	50.00	-	12.50	-	37.50	-	4.8±1.2	A	42±2

*: not determinable

3.3.2 Preparation of ODF by printing

Design of the printer - The printer was designed modifying a Cartesian FDM 3D printer (Futura Group Srl, Italy), as depicted in **Figure 3.1**. In particular, the apparatus used for the filament extrusion was replaced by in-house vertical ram extruder. The 60 mL extruding chamber was thermostated in the range from 30 to 200 °C and ended with a Luer-lock system fitting 1.8 cm length needles with a gauge ranging from 18 to 20 G. The melted materials extruded through the die was deposited on a 20×20 cm aluminium packaging foil. This foil also consisted in the primary packaging of ODF. The ram speed and the chamber temperature were controlled by Repetier-Host 2.0.1 software (Hotword GMBH, Germany); the film dimension and number per each print were designed by 3D builder (Microsoft, USA) and converted in G-code. Finally, ODF were sealed with another packaging foil without further manipulations.

Preparation of the mixture for printed ODF - The mixtures were obtained by mixing the exactly weighted amount of each component in a mortar according to the composition reported in **Table 3.1**. The final weight of each mixture was about 10 g.

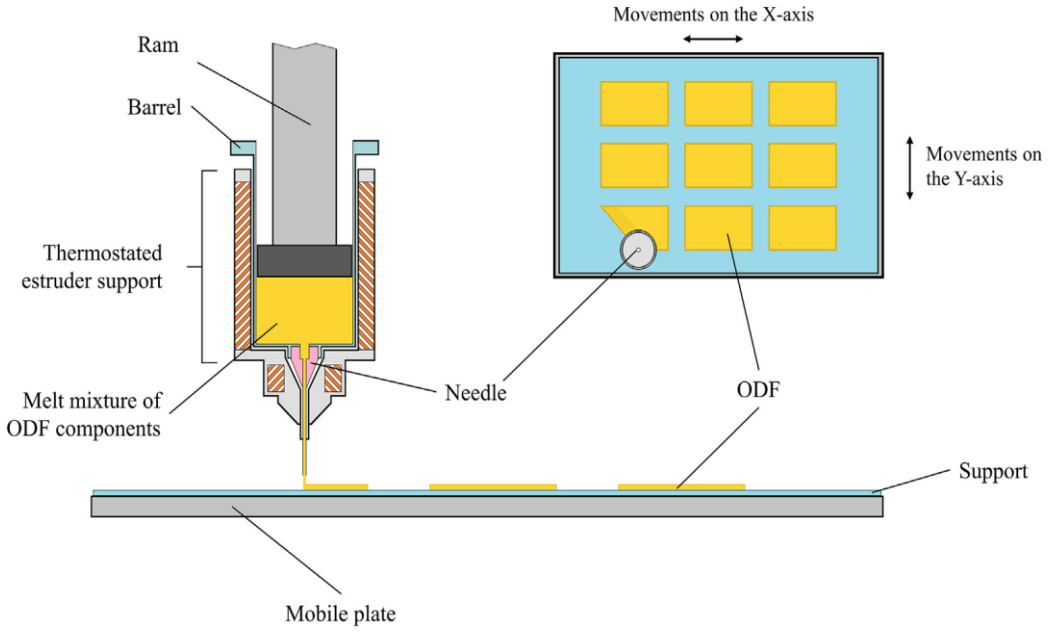

Figure 3.1. The main features of hot melt ram extrusion printer.

3.3.3 Preparation of cast ODF - ODF containing 25% w/w paracetamol was also prepared by solvent casting technique and used as reference for dissolution studies. Briefly, an aqueous dispersion was prepared by mixing MDX6, glycerine, Span® 80 in distilled water at 80 °C

under stirring. After at least 24 h of rest to remove air bubbles, the aqueous dispersion was cast onto a silicone release liner with a 150 µm thickness. The coating rate was fixed at 1 m/min, and the cast dispersion was dried in the oven at 80 °C for 30 min with a horizontal air circulation speed of 1200 rpm. The obtained cast ODF (formulation C1) had the following composition: 57 % w/w MDX6, 16 % w/w glycerine, 2 % w/w Span® 80, and 25% w/w paracetamol.

3.3.4 Physical and technological characterizations

Film thickness – The film thickness was measured by using a micrometer MI 1000 µm (ChemInstruments, USA).

Film stickiness – The ODF stickiness at different plasticizer contents was evaluated by the thumb tack test. Briefly, the thumb was pressed lightly on a film sample for a short time and, then, quickly withdrawn. By varying the pressure and time of contact and noting the difficulty of pulling the thumb from the adhesive, it is possible to perceive how easily, quickly and strongly the adhesive can form a bond with the thumb. All the tests were simultaneously performed and blind. The stickiness of the ODF was expressed by the following score system: A (no sticky), B (sticky), and C (very sticky) [12].

Tensile properties – Tests were conducted according to ASTM International Test Method for Thin Plastic Sheeting (D 882-02) using an Instron 5965 texture analyser (Instron, UK), equipped with a 50 N load cell. The film was cut into 80×15 mm strips and equilibrated at 25±1 °C for 1 week.

Each test strip was longitudinal by placed in the tensile grips on the texture analyser. Initial grip separation and the crosshead speed were 20 mm and 12.5 mm/min, respectively. The test was considered concluded at the film break. The following parameters were determined:

Tensile strength (TS) was calculated by dividing the maximum load by the original cross-sectional area of the specimen.

Percent elongation at break (E%) was calculated according to the following equation:

$$E\% = \frac{L - L_0}{L_0} \times 100$$

where L_0 is the initial gage length of the specimen and L is the length at the rupture.

Elastic modulus or Young's modulus (Y) was calculated as the slope of the linear portion of the stress-strain curve.

Tensile energy to break (TBE) was defined by the area under the stress-strain curve. The results were expressed in MPa.

Loss of drying

The loss on drying (LOD) in films was determined gravimetrically by using a thermobalance (Gilbertini, Italy). Film samples were kept at 105 °C until constant weight.

Disintegration test

The disintegration test was carried out in water according to specifications of the monograph on "Disintegration of tablets and capsules" reported in the Ph. Eur. The results complied the Ph. Eur. requirement for orodispersible tablets if the disintegration time was lower than 3 min.

Drug content

A 3×2 cm loaded ODF was dissolved in 100 mL purified water, sonicated for 10 min and diluted 1:10. Paracetamol content was determined spectrophotometrically at 243 nm (UV-Vis spectrometer, Lambda 25, Perkin Elmer, Italy). The calibration curves ranged from 10 to 100 µg/mL ($R^2 < 0.999$).

In vitro dissolution test

The in vitro dissolution test was carried out in a Ph. Eur. basket dissolution apparatus using 3×2 cm samples of paracetamol loaded ODF. The dissolution medium was 900 mL freshly deionized water, maintained at 37±1 °C and stirred at 50 rpm. Paracetamol concentrations were assayed spectrophotometrically at 243 nm (UV-Vis spectrometer, Lambda 25, Perkin Elmer, Italy) every 2 min and the calibration curve was in the range of 10-100 µg/mL ($R^2 < 0.999$). A loaded ODF prepared by solvent casting technique (25% w/w) was used as control. The results were expressed as the mean and standard deviation values of four replicas for each tested formulation.

3.4 Results and discussion

3.4.1 Rheological characterizations

In order to determine the temperature range suitable for frequency sweep experiments, preliminary compression tests were performed on laminates made of MDX6. This material was

supposed to present the highest softening temperature, having the highest M_w. The softening temperatures of laminates containing 20% w/w or 16% w/w glycerine were at about 79.5 °C and 99.7 °C, respectively. Therefore, the temperature range of frequency sweep experiments was set in the range 80-110 °C. The results evidenced that all tested samples did not present a pseudo-plastic behaviour, i.e. no plateau viscosity was reached at low angular frequency, probably due to the high number of interactions arising among –OH groups. As an example, the rheological pattern of formulation 1 (MDX6/glycerine ratio: 80/20) is exemplified in **Figure 3.2.**

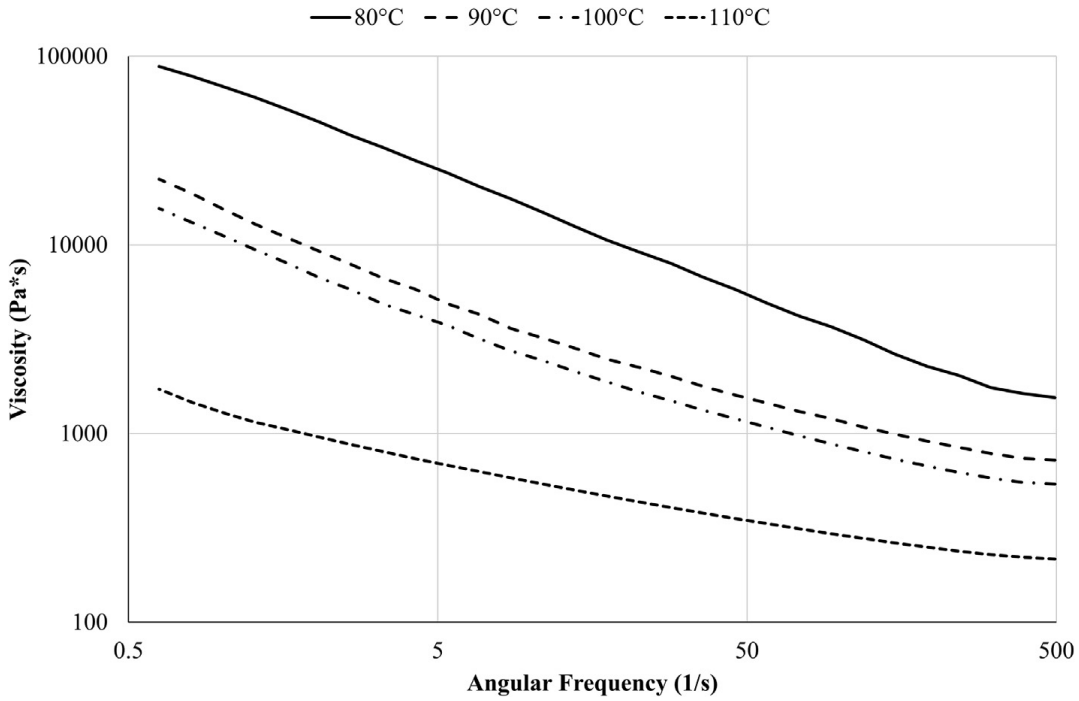

Figure 3.2. Frequency sweeps curves of Formulation 9 performed at 80 °C, 90 °C, and 110 °C.

To estimate the possible behaviour of formulations upon printing, the shear viscosity was also measured. The amount of the plasticizer was more relevant than the MDX molecular weight in determining the viscosity of the blend (**Table 3.2**). Furthermore, in agreement with the previous DSC data [31], glycine significantly ameliorated the fluidity of the melted blends **(Table 3.2**).

3.4.2 Set-up of printing operative conditions

On the bases of the frequency sweep data the temperature for the hot-melt ram extrusion of formulations containing the 20% and 16% w/w glycerine was set at 85 °C and 95 °C,

respectively. Moreover, based on the results of compression tests, a time lapse of 10 min between the mixture loading and the beginning of the ram movement was established to permit the complete melting of the formulation. The set-up of the operative conditions, the needle inner diameter, the relative distance between the extruder needle and the mobile plate, the speed of the mobile plate and the filling angle, was defined by using Formulation 4 and Formulation 9 (**Table 3.1**). In particular. Formulation 9, having the highest glycerine content, was selected to

Table 3.2. Shear viscosity values (η) of selected formulations calculated at the 1.1 s−1 shear rate and different temperatures. Tests were carried out on films made of maltodextrins with a dextrose equivalent of 6 (MDX6) or 12 (MDX12) and plasticized by glycerine (GLN) or glycine (GLY).

Form.	Composition (%, w/w)				T (°C)	η (Pa*s)
	MDX6	MDX12	GLN	GLY		
1	84.00		16.00		100	21000
					110	11600
2	82.75		16.00	1.25	90	7270
					100	7140
					110	6260
3	81.50		16.00	2.50	80	36370
					90	14480
					100	4030
					110	665
5		84.00	16.00		80	39960
					90	19680
					100	3470
					110	2860
9	80.00		20.00		80	14800
					90	3200
					100	2430
					110	540
11	78.75		20.00	1.25	80	5980
					90	4015
					100	1445
					110	513
12	77.50		20.00	2.50	80	8350
					90	5450
					100	1850
					110	800

check the impact of fluidity of the melt on printability. Conversely, Formulation 4 was tested as a worst case since it contained the lowest amount of glycerine, glycine as non-traditional plasticizer and TiO_2 a very fine inert powder usually used to mask possible visual defects of ODF.

First, the extrusion of formulation 4 at the extrusion 1.1 s^{-1} shear rate was possible only using the 18 gauge-needle (inner diameter 0.838 mm). Secondly, the suitable deposition of the melted blend on packaging foil was possible only setting the distance from the needle tip to the surface of the packaging material foil in the range of 0.5-0.8 mm. Indeed, at distances lower than 0.5 mm, the needle tip scratched the film causing irregularity and roughness on the surface, whilst

at distances higher than 0.8 mm, the extruded material could not deposit in a consistent and uniform way. Thirdly, the impact of print rate on the film formation was investigated in the 10-50 mm/s range increasing the extrusion shear rate, accordingly. The maximum rate which allowed the deposition of a filament with a uniform diameter, resulted 12 mm/s and 50 mm/s for formulations 4 and 9, respectively.

Finally, the effect of the filling angle on the homogeneity and tensile properties of films was studied by printing at 90°, 120° 135°, 150° and 180° with respect to the X-axis of the packaging material foil (**Figure 3.3**).

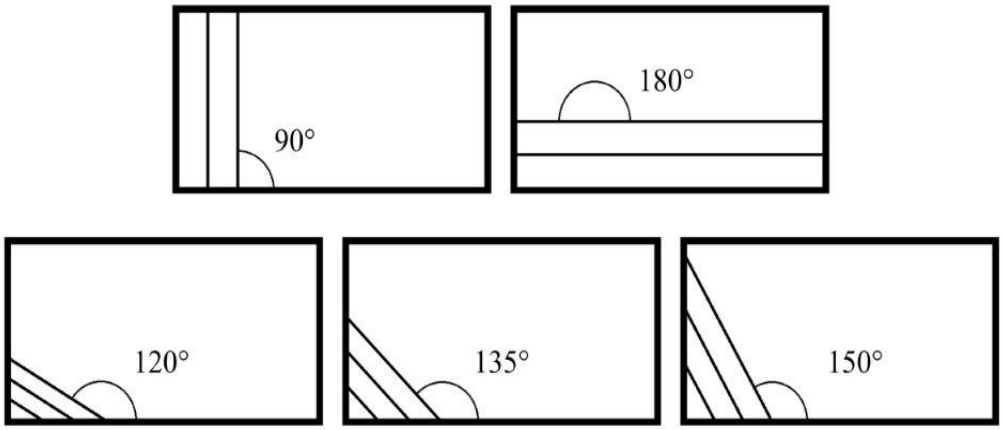

Figure 3.3. Schemes of filling angles of printed films.

The results indicated that the filling angle did not affect the film appearance. In the case of formulation 4, some small differences were noticed in the main descriptors of the tensile property (**Table 3.3**), suggesting an influence of the filling angle on the film inner organization. Indeed, due to the peculiar preparation process, it was possible to speculate that the printed

Table 3.3 – Tensile properties of formulation 4 (16% w/w glycerine) and 9 (20% w/w glycerine) printed at different filling angles (mean ± St.Dev., n = 5).

Form.	Filling Angle (°)	TS (MPa)	Y (MPa)	E% (%)	TBE (MPa)
4	90	0.07±0.01	1.29±0.26	441±166	0.17±0.09
	120	0.06±0.01	0.82±0.30	992±83	0.35±0.05
	135	0.06±0.01	0.84±0.20	705±118	0.25±0.03
	150	0.07±0.01	1.17±0.14	602±145	0.29±0.04
	180	0.11±0.01	1.90±0.09	591±65	0.47±0.06
9	90	0.37±0.15	8.07±4.69	127±56	0.38±0.14
	120	0.19±0.05	2.76±1.69	431±155	0.66±0.12
	135	0.48±0.19	7.62±2.59	139±74	0.41±0.07
	150	0.45±0.10	10.19±2.91	180±53	0.51±0.09
	180	0.38±0.20	7.53±2.73	184±88	0.44±0.15

films had some high-dense zones at the deposition lines of extruded materials and some low-dense zones between the previous ones due to the reorganization of the melted materials after deposition. Therefore, toughness (e.g., TS and TBE) reached the highest values when the highly dense zones of the films were parallel to the tensile force applied (i.e., 180°). On the contrary, the lowest TBE values were determined when the dense material zones were perpendicular (i.e., 90°) since the film resistance to deformation was mainly limited by thin and low-dense zones, which were expected to be mechanically weak. Interestingly, ODF printed at the filling angle of 120° showed the highest field of elasticity (i.e., the lowest *Y* values) and a satisfactory toughness probably due to a cooperation between high-dense and low-dense zones during the elongation phase. A similar trend was observed in the case of formulation 9 printed at 120° confirming that the orientation of the high-dense and low-dense zones influenced the tensile properties (**Table 3.3**).

The comparison of the tensile data on these two formulations evidenced an anomalous result considering the plasticizer content. Indeed, the higher glycerine concentration, the lower the ductility (E% values) and the tenacity of the film (TS). This feature can be attributed to glycine and TiO_2, which act as non-traditional plasticizers [31] and nanofiller of maltodextrins [32], respectively.

On the bases of the obtained data, the following process parameters were set and used for further studies:

- needle gauge: 18;

- needle-to-packaging material foil distance: 0.6 mm;
- print rate: 12 mm/s;
- ram rate: 10 mm/s (corresponding to a calculated shear rate of the melted mixture of 1.1 s^{-1});
- filling angle: 120°.

3.4.3 ODF characterization

All printed films presented relatively low LOD values (**Table 3.1**) if compared to other formulations [12] and the thickness in the 150-250 μm range was considered suitable for patient's handling. Moreover, ODF dissolved within 3 min complying with Ph. Eur. specifications for orodispersible dosage forms [33].

Although the tensile properties and stickiness of printed ODF are not as critical as for those industrially produced by solvent casting technique, which are rolled up on reels and cut, their investigation is worthy of interest to avoid problems during the patient's handling.

The data obtained during the definition of the process parameters evidenced an impact of mixture composition on the printability. The formulations containing 16% w/w glycerine were not consistently extruded through an 18 gauge-needle unless glycine was also added at the concentration of 2.5% or 1.25% w/w glycine for MDX6 (formulations 3 and 4) and MDX12 (formulation 6), respectively. These results suggested that the shear viscosity, calculated at 1.1 s^{-1} of shear rate, might be lower than 7 kPa*s. Nevertheless, formulations made of MDX12 (formulations 6 and 7) were stickier than those based on MDX6 (formulations 3 and 4) (**Table 3.1**), confirming the relevance of the maltodextrin molecular weight. Moreover, in ODF prepared with MDX6 and the highest glycerine concentration, the concomitant presence of glycine increased the elasticity in a concentration-dependent way and had a negative impact on toughness. Indeed TS, TBE and *Y* values (**Table 3.4**) decreased in the following order: formulation 9 > formulation 11 > formulation 12 ($p < 0.05$).

As expected, the addition of TiO_2 (see formulation 3 vs. formulation 4; formulation 10 vs. formulation 9, **Table 3.4**) decreased the *Y* values suggesting that the peeling of film from the packaging foil should be easier.

Based on these results, some generic considerations on preparation methods and the ODF characteristics can be drawn. First, the disintegration time of printed ODF is more similar to that of films with similar composition, but prepared by hot-melt extrusion (≥ 45 s), rather than

Table 3.4 – Tensile properties of printed ODF (mean ± St.Dev., n = 5).

Form.	TS (MPa)	Y (MPa)	E% (%)	TBE (MPa)
1	-*	-*	-*	-*
2	-*	-*	-*	-*
3	0.09±0.05	2.44±0.1.87	> 1000	0.38±0.17
4	0.06±0.01	0.82±0.30	992±83	0.35±0.05
5	-*	-*	-*	-*
6	-*	-*	-*	-*
7	-*	-*	-*	-*
8	0.75±0.12	23.13±1.72	71±15	0.30±0.07
9	0.19±0.05	2.76±1.69	431±155	0.66±0.12
10	0.05±0.03	0.81±0.47	312±146	0.05±0.01
11	0.09±0.01	1.37±0.68	423±60	0.32±0.29
12	0.01±0.01	0.13±0.01	414±76	0.02±0.01
13	0.53±0.15	10.91±6.36	142±34	0.56±0.12
14	0.43±0.04	8.83±2.06	160±55	0.51±0.16
15	0.43±0.10	8.68±4.07	86±24	0.28±0.06

*: not determinable

by solvent casting (≈ 10 s) [28]. Furthermore, the disintegration times (**Table 3.1**) were closed to the results reported for film prepared by FDM 3D printing [25, 34]. Secondly, the printed ODF showed weaker tensile properties than the parent casted and hot-melt extruded ODF probably because the peculiar deposition of melted material did not allow obtaining a uniform film in comparison to extrusion. As a consequence, the TS values of extruded ODF composed by MDX12, glycerine and cellulose microcrystalline in the 66:22:11 ratio [28] resulted 5-fold higher than formulation 9. Moreover, the solvent casting technique allowed to obtain higher cohesion of the ODF matrix, since the maltodextrin chains and glycerine could rearrange in a dense structure during the solvent evaporation phase, resulting in a film with suitable mechanical properties even at thinner thickness.

It is noteworthy that the proposed maltodextrin ODF showed a higher elasticity and a lower toughness than that of PVA-based ones [34], while the overall tensile properties were similar to those of films made of PEO and starch [25].

When paracetamol was loaded as model drug, ODF appeared whitish without significant differences in thickness and weight (**Table 3.5**) or in the disintegration time with respect to the corresponding placebo formulations (**Table 3.1**). Paracetamol could be loaded in ODF up to

35% w/w (**Table 3.5**) and in all cases the uniformity of dosage units was within the limit (L_1 ± 15%) set by the European Pharmacopoeia [35].

Table 3.5 – Weight and paracetamol (PAR) content of ODF prepared by printing (mean ± St.Dev., n = 3).

Formulation	ODF weight (mg)	Drug content	
		(mg)	(%, w/w)
8	233±45	73.56±3.90	23.49±0.23
13	175±57	22.06±6.87	11.83±0.36
14	215±4	48.94±8.96	25.10±1.31
15	159±15	48.91±5.76	35.76±0.29

In agreement with the literature data [12], the paracetamol loaded into ODF altered the tensile properties (**Table 3.4**) increasing the ODF toughness (e.g., TS; $p < 0.01$) and, consequently, decreasing its ductility (i.e., E%; $p < 0.02$) with respect to placebo formulations (i.e., formulations 4 and 9). However, this effect was not related to the paracetamol content since no significant differences in terms of TS, Y and E% values (formulations 13-15) were observed. However, a slight decrease of TBE values observed in 35% w/w drug loaded ODF ($p < 0.01$) suggested that a high payload can create inhomogeneous spot in the inner structure of an ODF causing the alterations of its mechanical properties [12].

As shown in the dissolution profiles reported in **Figure 3.4**, about 80% of paracetamol was dissolved within 6 min so that the proposed printed ODF can be classified as very rapidly dissolving dosage forms according to the FDA [36]. However, slight differences were observed depending on plasticizer content since ODF containing 20% w/w glycerine dissolved faster ($t_{80\%} \leq 2$ min) than those with 16% ($t_{80\%} \approx 6$ min). The dissolution profiles resulted superimposable in comparison to Formulation C1 produced by casting technique. These results confirmed the ability of maltodextrins to improve the dissolution rate of several active ingredients such as piroxicam [28], diclofenac [30] and in some cases to enhance the mucosae permeation also in comparison with other film forming materials used to prepare ODF as demonstrated in the case of sumatriptan [37].

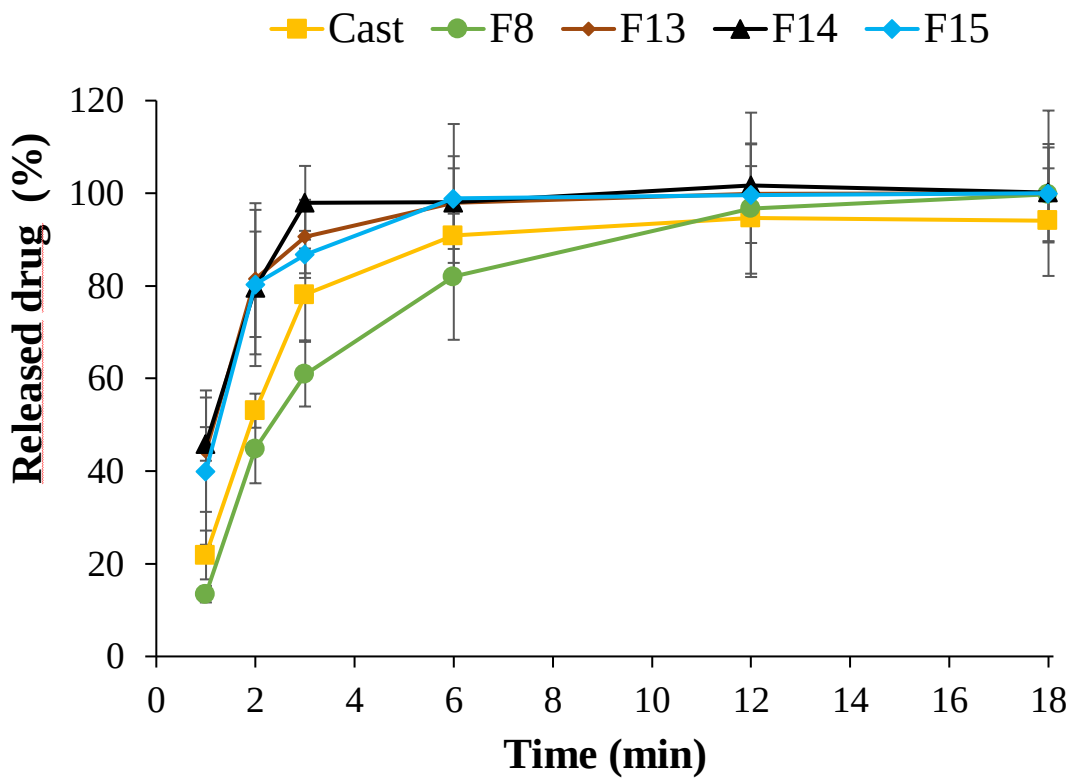

Figure 3.4. Dissolution profiles of paracetamol from ODF obtained by printing (Formulations 8, 13-15) and casting solvent technology (Formulation C1) (mean ± St.Dev., n=4).

3.5 Conclusions

The feasibility to prepare MDX-ODF by hot melt ram extrusion printing was demonstrated. The proposed preparation method consists of a simple procedure involving the mixing of the active ingredient with MDX and other excipients, the wetting of the mixed powders by glycerine, the loading into the ram extruder and the printing of the single dosage form directly on the packaging foil. This aspect is relevant since the printed ODF can be sealed with another packaging foil avoiding handling of the dosage form. The drug strength can be easily defined designing the size of ODF. The uniformity of drug amount per unit of these medicinal products should be guarantee aiming to serve the interest of patients.

Conversely to the industrial products, the drug strength cannot be quantified due to the limitation of pharmacy equipment, time and costs (Resolution CM/Res) [38]. As proposed for ink-jet printing, the drug homogeneity in the wet mixture could be indirectly checked by adding small amounts of colourant during the mixing, which is the most critical operation. Indeed, variation in ODF thickness and dimensions, can be indirectly determined gravimetrically.

The proposed method also appears to be more versatile than FDM 3D printing, where it is necessary to produce drug loaded filaments, to obtain the final object. With respect to the ink-jet printing technologies, the proposed approach presents the advantage to not require the preliminary preparation of placebo ODF. Moreover, avoiding the use of solvents, this method also reduces the risks of drug polymorphism. Based on this evaluation, we consider this method as a good opportunity to extemporaneously prepare tailored solid dosage forms in hospital and community pharmacies.

References

[1] Cilurzo F., Musazzi U.M., Franzé S., Selmin F., Minghetti P. Orodispersible dosage forms: biopharmaceutical improvements and regulatory requirements. Drug Discov. Today. 2018; 23(2), 251-259.

[2] Visser J.C., Woerdenbag H.J., Hanff L.M., Frijlink H.W. Personalized medicine in pediatrics: the clinical potential of orodispersible films. AAPS PharmSciTech. 2017;18, 267-272.

[3] Scarpa M., Stegemann S., Hsiao W.-K., Pichler H., Gaisford S., Bresciani M., Paudel A., Orlu M. Orodispersible films: towards drug delivery in special populations. Int. J. Pharm. 2017; 523(1), 327-335.

[4] Minghetti P., Pantano D., Gennari C.G.M., Casiraghi A. Regulatory framework of pharmaceutical compounding and actual developments of legislation in Europe. Health Policy. 2014; 117(3), 328-333.

[5] Casiraghi A., Musazzi U.M., Franceschini I., Berti I., Paragò V., Cardosi L., Minghetti, P. Is propranolol compounding from tablet safe for pediatric use? Results from an experimental test. Minerva Pediatrica. 2014; 66(5), 355-362.

[6] Somogyi O., Meskó A., Csorba L., Szabó P., Zelkó R. Pharmaceutical counselling about different types of tablet-splitting methods based on the results of weighing tests and mechanical development of splitting devices. Eur. J. Pharm. Sci. 2017; 106, 262-273.

[7] Visser J.C., Woerdenbag H.J., Crediet, S., Gerrits, E., Lesschen, M.A., Hinrichs, W.L.J., Breitkreutz, J., Frijink H.W. Orodispersible films in individualized pharmacotherapy: the development of a formulation for pharmacy preparations. Int. J. Pharm. 2015; 478, 155-163.

[8] Orlu M., Ranmal S.R., Sheng Y., Tuleu C., Seddon P. Acceptability of orodispersible films for delivery of medicines to infants and preschool children. Drug Delivery. 2017; 24(1), 1243-1248.

[9] Slavkova M., Breitkreutz J. Orodispersible drug formulations for children and elderly. Eur. J. Pharm. Sci. 2015; 75, 2-9.

[10] Jha A.K., Chetia D. Development and statistical analysis of glipizide loaded fast-dissolving tablets using Plantago ovata husk as a superdisintegrant. Int. J. Pharm. Compd. 2011; 15(6), 521-525.

[11] Allen L.V. Basics of compounding: compounding films. Int. J. Pharm. Compd. 2016; 20 (4), 298-305.

[12] Musazzi U.M. Selmin F., Franzé S., Gennari C.G.M., Rocco P., Minghetti P., Cilurzo F. Poly(methyl methacrylate) salt as film forming material to design orodispersible films. Eur. J. Pharm. Sci. 2018;115, 37-42.

[13] Dinge A., Nagarsenker M. Formulation and evaluation of fast dissolving films for delivery of triclosan to the oral cavity. AAPS PharmSciTech. 2008 9(2), 349-356.

[14] Liu C., Chang D., Zhang X., Sui H., Kong Y., Zhu R., Wang W. Oral fast-dissolving films containing lutein nanocrystals for improved bioavailability: formulation development, in vitro and in vivo evaluation. AAPS PharmSciTech. 2017; 18, 2957-2964.

[15] Foo W.C., Khong Y.M., Gokhale R., Chan S.Y. A novel unit-dose approach for the pharmaceutical compounding of an orodispersible film. Int. J. Pharm. 2018; 539, 165-174.

[16] Thabet Y., Lunter D., Breitkreutz J. Continuous inkjet printing of enalapril maleate onto orodispersible film formulations. Int. J. Pharm. 2018; 546, 180–187.
[17] Alomari M., Vuddanda P. R., Trenfield S. J., Dodoo C. C., Velaga S., Basit A. W., Gaisford S. Printing T_3 and T_4 oral drug combinations as a novel strategy for hypothyroidism, Int. J. Pharm. 2018; 549(1-2), 363-369.
[18] Goyanes A., Vakili H., Nyman J.O., Genina N., Preis M., Sandler N. Application of a colorimetric technique in quality control for printed pediatric orodispersible drug delivery systems containing propranolol hydrochloride. Int. J. Pharm. 2016; 511, 606–618.
[19] Içten E., Giridhar A., Taylor L.S., Nagy Z.K., Reklaitis G.V. Dropwise additive manufacturing of pharmaceutical products for melt-based dosage forms. J. Pharm. Sci. 2015; 104(5), 1641–1649.
[20] Içten E., Giridhar A., Nagy Z.K., Reklaitis G.V. Drop-on-demand system for manufacturing of melt-based solid oral dosage: effect of critical process parameters on product quality. AAPS PharmSciTech. 2016; 17(2), 284-293.
[21] Janßen E.M., Schliephacke R., Breitenbach A., Breitkreutz J. Drug-printing by flexographic printing technology—A new manufacturing process for orodispersible films. Int. J. Pharm. 2013; 441(1–2), 818-825.
[22] Awad, A., Trenfield, S.J., Goyanes, A., Gaisford, S., Basit, A.W. Reshaping drug development using 3D printing. Drug Discov. Today. 2018; 23, 1547-1555.
[23] Sadia M., Arafat B., Ahmed W., Forbes R.T., Alhnan M.A. Channelled tablets: An innovative approach to accelerating drug release from 3D printed tablets. J. Control. Rel. 2018; 269, 355-363.
[24] Kadry H., Al-Hilal T.A, Keshavarz A., Alam F., Xu C., Joy A., Ahsan F. Multi-purposable filaments of HPMC for 3D printing of medications with tailored drug release and timed-absorption, Int J Pharm. 2018; 544(1), 285-296.
[25] Ehtezazi T., Algellay M., Islam Y., Roberts M., Dempster N.M., Sarker S.D. The application of 3D printing in the formulation of multi-layered fast dissolving films. J. Pharm. Sci. 2018; 107, 1076 1085.
[26] Cunha-Filho M., Araújo M.R., Gelfuso G.M., Gratieri T. FDM 3D printing of modified drug-delivery systems using hot melt extrusion: a new approach for individualized therapy. Ther. Deliv. 2017; 8(11), 957-966.
[27] Fuenmayor E., Forde M., Healy V.A., Devine M.D., Lyons G.J., McConville C., Major I. Material considerations for fused-filament fabrication of solid dosage forms. Pharmaceutics. 2018; 10(2), 44
[28] Cilurzo F., Cupone I.E., Minghetti P., Selmin F., Montanari L. Fast dissolving films made of maltodextrins. Eur. J. Pharm. Biopharm. 2008; 70 (3), 895-900.
[29] Cilurzo F., Cupone I.E., Minghetti P., Buratti S., Selmin F., Gennari C.G.M., Montanari L. Nicotine fast dissolving film made of maltodextrins: a feasibility study. AAPS PharmSciTech. 2010; 11(4), 1511-1517.
[30] Cilurzo F., Cupone I.E., Minghetti P., Buratti S., Gennari C.G.M., Montanari L. Diclofenac fast-dissolving film: suppression of bitterness by a taste-sensing system. Drug Dev. Ind. Pharm. 2011; 37(3), 252-259.
[31] Selmin F., Franceschini I, Cupone IE, Minghetti P, Cilurzo F. Aminoacids as non-traditional plasticizers of maltodextrins fast-dissolving films. Carbohyd. Pol. 2015; 115, 613-616.

[32] Franceschini I., Selmin F., Pagani S., Minghetti P., Cilurzo F. Nanofiller for the mechanical reinforcement of maltodextrins orodispersible films. Carbohydrate Polymers. 2016; 136, 676-681.
[33] European Pharmacopeia (Ph. Eur.). Monograph on Tablets (01/2018:0478). In European Pharmacopeia, 9th Edition Supplement 9.5. 2018a
[34] Jamroz W., Kurek M., Lyszczarz E., Szafrenic J., Knapik-Kowalczuk J., Syrek K., Paluch M., Jachowich R. 3D printed orodispersible films with Aripiprazole. Int. J. Pharm. 2017; 533, 413-420.
[35] European Pharmacopeia (Ph. Eur.). Monograph on Uniformity of Dosage Units (04/2017:20940). In European Pharmacopeia, 9th Edition Supplement 9.5. 2018b.
[36] Food and Drug Administration (FDA). Waiver of in vivo bioavailability and bioequivalence studies for immediate-release solid oral dosage forms based on a biopharmaceutics classification system (Guidance for industry), 2017.
[37] Soni, G., Yadav, K.S. Fast-dissolving films of sumatriptan succinate: factorial design to optimize in vitro dispersion time. J. Pharm. Innov. 2015; 10, 166-174.
[38] Resolution CM/Res(2016)1 on quality and safety assurance requirements for medicinal products prepared in pharmacies for the special needs of patients.

Chapter 4

Extemporaneous Printing of Diclofenac Orodispersible Films for Paediatrics

4.1 Introduction

Orodispersible films (ODF) are unique unit dosage forms intended to be placed onto the tongue where they rapidly dissolve or disintegrate in contact with saliva to form a suspension or solution of the loaded drug easily to be swallowed. ODF exhibit several merits over the conventional oral dosage forms. For instance, their administration does not require water or chewing. These features make them relevant for groups of patients, such as uncooperative, those with swallowing deficits, patients with restricted water/fluid intake, or travellers with limited or no access to water [1]. ODF have been recently also proposed as an alternative technological platform for customizing small batches [2] to address the unmet needs of a patient, and therefore, to improve therapeutic adherence [3, 4], or to overcome a limitation in dose or dosage forms of medicinal products available on the market [5].

Among the critical quality attributes of ODF, satisfactory tensile properties to guarantee packaging and handling during administration without breakage, the disintegration and dissolution in the oral cavity, acceptable taste [6, 7, 8], aesthetic appearance, and stability of the dosage form itself and the loaded drug(s) are of paramount importance. In particular, the selection of taste-masking agents (TMA; i.e., sweeteners and/or flavouring agents) depends not only on the improvement of palatability [8, 9], but also on their compatibility with other formulation components, the possible impact on the drug dissolution rate [10] and mechanical properties [6].

The preparation of ODF can occur by traditional solvent casting technique or printing technologies which have received extensive attention to develop ODF especially for personalized dosing [11, 12]. Recently, we proposed a novel hot-melt extrusion printing technique for the extemporaneous preparation of small batches of ODF made of maltodextrins plasticized with glycerol [12]. This technology is solvent-free and, therefore, can be advantageously used to load drugs which are chemically or physically unstable in aqueous or solvent systems and to eliminate the use of organic solvents. On the other hand, the relatively high working temperature (~95 °C) could cause degradation of thermosensitive components.

The present study investigated the feasibility to print ODF loaded with diclofenac sodium (DNa) which is a well-known thermosensitive and bitter drug. The possibility to tune the ODF surface in the attempt to prepare age-appropriate dosage form for paediatric patients was also studied. Indeed, diclofenac is frequently prescribed for paediatrics in special medical needs [13], but no liquid formulations (i.e. syrup or suspension) are commercially available due to its instability. Based on previous work, taste-masking agents (i.e., mint, liquorice-mint and

sucralose or a combination thereof) [7], and an opacifier (titanium dioxide, TiO_2), were also added to the formulation and their effects on ODF properties were assessed in terms of disintegration time, *in vitro* dissolution profile, tensile properties, and peel test. Moreover, to evaluate the robustness of this approached, a stability study in accelerated conditions was carried out over six months.

4.2 Materials

Maltodextrin, with a dextrose equivalent equal to 6 (MDX, Glucidex® IT6), was obtained from Roquette (France). Diclofenac sodium (DNa), glycerol, and titanium dioxide (TiO_2) were purchased from Farmalabor (Italy). Sucralose was obtained from Sigma Aldrich (Italy). Mint and liquorice mint flavours were kindly donated by Kerry Ingredients and Flavours Italia (Italy). All solvents were of analytical grade unless otherwise specified. For the dissolution studies, the following Simulated Salivary Fluid (SSF) was prepared: 1 L contained 0.844 g NaCl, 1.2 g KCl, 0.193 g $CaCl_2.2H_2O$, 0.111 g $MgCl_2.6H_2O$ and 0.342 g K_2HPO_4, the pH was adjusted at 5.7±0.1 using 1M hydrochloric acid (HCl).

4.3 Methods

4.3.1 ODF preparation

ODF were prepared by hot-melt printing as already described by Musazzi et al., [12], according to the composition reported in **Table 4.1**. Briefly, a paste of the various excipients was prepared in a mortar and transferred into the extruding chamber heated at 95±1 °C for 10 min. The melt was extruded to print the ODF of the desired dimensions (1×1 cm, 1×2 cm 2×3 cm or 2×10 cm) on a 20×20 cm aluminium primary packaging foil kindly provided by IBSA Spa (Italy). The printed ODF were sealed with another packaging aluminium foil without further manipulations. The ram speed (12 mm/s) and the chamber temperature were controlled by Repetier-Host 2.0.1 software (Hotword GmbH, Germany); the film dimension and number per each print were designed by 3D Builder® (Microsoft, USA) and converted in G-code.

Table 4.1. Compositions (% w/w) of the placebo and diclofenac sodium (DNa) loaded ODF by printing made up of maltodextrin (MDX6), glycerol (GLY), water (H_2O), taste-masking agents TMA) (mint, liquorice-mint and sucralose) and titanium dioxide (TiO_2). ODF thickness, weight, loss on drying (LOD), moisture content (MC), disintegration time (Dist. Time), and drug content (DC) are presented as mean ± standard deviation (SD). n.d.: not determined.

Form.	ODF compositions (% w/w)								Thickness (µm)	Weight (mg)	LOD (%)	MC (%)	Dist. Time (s)	DC (%)
	MDX6	GLY	H_2O	DNa	Mint	Liquorice-mint	Sucralose	TiO_2						
F1	78.00	20.00	2.00	-	-	-	-	-	220 ±27	333 ± 26	3.3 ± 1.1	9.6 ± 0.1	38 ± 2	-
F2	68.64	17.60	1.76	12.00	-	-	-	-	252 ± 14	246 ± 5	3.7 ± 1.3	8.0 ± 0.1	46 ± 1	10.95±0.14
F3	64.40	16.50	1.70	12.00	5.40	-	-	-	254 ± 13	251 ± 8	4.3 ± 0.8	n.d.	62 ± 3	12.19±0.14
F4	66.50	17.10	1.70	12.00	-	2.70	-	-	259 ± 16	219 ± 6	3.7 ± 0.4	n.d.	72 ± 1	12.01±0.47
F5	67.90	17.40	1.70	12.00	-	-	1.00	-	345 ± 11	295 ± 28	5.0 ± 0.3	n.d.	65 ± 4	14.75±0.36
F6	61.50	15.80	1.60	12.00	5.40	2.70	1.00	-	292 ± 9	216 ± 3	4.2 ± 1.7	8.3 ± 0.0	56 ± 1	12.48±0.21
F7	73.80	18.90	1.90	-	5.40	-	-	-	298 ± 9	258 ± 9	4.4 ± 0.4	n.d.	64 ± 5	-
F8	75.90	19.50	1.90	-	-	2.70	-	-	287 ± 9	238 ± 19	5.6 ± 0.4	n.d.	78 ± 2	-
F9	77.20	19.80	2.00	-	-	-	1.00	-	323 ± 18	246 ± 2	4.7 ± 1.2	n.d.	61 ± 1	-
F10	70.90	18.20	1.80	-	5.40	2.70	1.00	-	318 ± 17	200 ± 7	3.3 ± 0.5	8.1 ± 0.0	50 ± 1	-
F11	77.9	20	2.00	-	-	-	-	0.10	223 ± 4	190 ± 4	4.9 ± 0.1	8.4 ± 0.2	45 ± 8	-
F12	68.6	17.6	1.70	12.00	-	-	-	0.10	289 ± 9	249 ± 9	4.0 ± 0.4	8.8 ± 0.1	35 ± 6	12.45±0.09
F13	61.40	15.80	1.60	12.00	5.40	2.70	1.00	0.10	271 ± 9	225 ± 1	3.8 ± 0.3	15.1 ± 0.4	72 ± 2	11.73±0.71

4.3.2 Physical and technological characterizations

Film thickness

The film thickness was measured by using a micrometre MI 1000 μm (ChemInstruments, USA). The accuracy of the instrument was 2.5 μm ± 0.5%.

ODF water content

Loss on drying (LOD): the LOD of the ODF was determined gravimetrically by using a thermobalance (Gilbertini, Italy). Film samples were kept at 100 °C until constant weight, and the percentage of moisture loss was calculated.

Karl-Fisher titration water content determination: The apparatus (Mettler Toledo, Switzerland) was initially calibrated with anhydrous methanol. ODF sample was accurately weighed and transferred into an empty glass vial; then, 1.5 mL anhydrous methanol was added and sealed with a rubber closure. The vial was sonicated for 30 min; afterward, 0.5 mL of the prepared sample suspension was injected into the titration chamber. The water content was calculated according to Equation (1)

$$\text{water content (\%)} = \frac{Ms - Mm}{Mo} \times 100 \quad (1)$$

where:
M_s is the mass of water in the sample introduced into the titration chamber,
M_m is the mass of water in the anhydrous methanol
M_0 is the initial mass of the ODF.

Drug content

A specimen of 2×3 cm was dissolved in 10 mL purified water, sonicated for 15 min and filtered by a 0.45 μm polypropylene membrane filter (VWR®, Italy). The filtered solution was then diluted 1:1. The drug concentrations were quantified by HPLC analysis (Agilent HP 1100, Chemstation, Hewlett Packard, Santa Monica, USA). The following chromatographic conditions were used: column: InterClone™ (5 μm ODS, 100 Å, 150×4.6 mm, Phenomenex®, USA); mobile phase: methanol/phosphate buffer pH 2.5 (66/34, % v/v); flow rate: 1.2 mL/min;

wavelengths: 254 nm and 275 nm; temperature: 45 °C; injection volume: 10 µL. The drug concentrations were determined from a known standard curve in the 4–300 µg/mL range (R^2 = 0.999). The retention times of DNa and impurity A were 7.7 min and 4.7 min, respectively.

Tensile properties

Tensile tests were done using an Instron 5965 texture analyser (Instron, UK) as previously described (11). Briefly, 2×3 cm strips were equilibrated at 25±1 °C for one week, and the test was performed with a 2 cm initial grip separation and at 50 mm/min crosshead speed until sample breaks. The following parameters were calculated:

- tensile strength (σ) was calculated by dividing the maximum load by the original cross-sectional area of the film specimen, and it was expressed in force per unit area (MPa);
- Young's modulus or elastic modulus (*Y*) was calculated as the slope of the linear portion of the stress-strain curve. The result was expressed in force per unit area (MPa);
- tensile energy to break (*TEB*) was defined by the area under the stress-strain curve. The value is in units of energy per unit volume of the specimen's initial gage region;
- percent elongation at break (ε) was calculated by dividing the extension at the moment of rupture of the specimen by the initial gauge length of the specimen and multiplying by 100 according to Equation (2)

$$\varepsilon(\%) = \frac{L - Lo}{Lo} \times 100 \quad (2)$$

where L_0 is the initial gauge length of the specimen, and L is the length at the rupture.

An average of five measurements was taken for each formulation.

Peeling from the packaging materials

The test was conducted on 2×10 cm printed ODF using an Instron 5965 texture analyzer (Instron, UK). Two experimental setups were employed to mimic the in-use conditions (i.e., the peeling of the ODF from the primary packaging material by the patient or the caregiver, protocol A) or to discriminate the impact of the excipients on the ODF adhesion to the primary packaging material, protocol B.

Protocol A: about 0.5 cm of the film was carefully separated from the primary packaging material, and an adhesive tape leader (0.3 cm) was attached to the film and the packaging material separately. The prepared specimens were stored at 25±0.1 °C for 15 min and then positioned horizontally to the instrument's clamps with the free ends of the tape leaders of the film and packaging material inserted into the upper and lower grips respectively. Five specimens each were freely pulled at a peel speed of 300 mm/min. F1 and F11 were tested with this setup.

Protocol B: Double-faced adhesive tape was used to fix the backside of the primary packing material of the film onto a stainless-steel standard plate. Each film was folded about 0.5 cm from the primary packaging, and a tape leader was placed on about 0.3 cm of the exposed film with the adhesive side of the tape attached to one end of the film (bottom). The film was smoothed with a 2 Kg roller to and pro twice. The remaining part of the tape leader was folded on itself to form a double thickness leader, and the tip of the tape was then attached to the film (top). Each specimen was placed on the instrument with the stainless-steel plate fixed to the lower grip at 180° angle and the free end of the tape leader being placed into the upper grip. Five specimens each were pulled from the plate at a peel speed of 300 mm/min. Formulations; F1, F2, F6, F11, F12, and F13 were tested.

The static peel force was calculated as the arithmetic mean of all values of the linear portion of the curve. The dynamic peel values were calculated by dividing the registered forces by the width of the film and are expressed in newton per millimetre (N/mm). The results are expressed as the mean ± standard deviation of five specimens.

Disintegration test

The disintegration test was carried out according to specifications of the monograph on the "Disintegration of tablets and capsules" reported in the Ph. Eur. The results complied with the Ph. Eur. requirements for orodispersible tablets if the disintegration time was lower than 3 min.

In vitro dissolution test

The in vitro dissolution test was conducted using Ph. Eur. basket dissolution apparatus SR8 PLUS dissolution test station (Hanson Research, Chatsworth, USA). The dissolution media were 500 mL freshly deionized water and simulated saliva fluid (SSF) at pH = 5.7 ± 0.1, maintained at 37 ± 1 °C and stirred at 25 ± 1 rpm [10]. DNa loaded ODF samples (2×3 cm) were used. DNa concentrations were assayed spectrophotometrically at 275 nm (UV–Vis

spectrometer, Lambda 25, Perkin Elmer, Italy) after 1, 2, 3, 6, 9, 12, 18 and 24 min, and the calibration curves were in the range of 10–100 μg/mL (R^2 = 0.999). The results were expressed as the mean and standard deviation values of three replicas for each tested formulation. The dissolution results were expressed as the time required for releasing 80% of the DNa (t_{80}).

4.3.3 ODF Accelerated Stability study

Accelerated stability study was performed on formulations F2, and F13 (**Table 4.1**). Samples were stored at 40±2 °C and 75±5% relative humidity (Memmert Climate Chamber ICH110, GmbH, Germany). At each sampling point (i.e., 0, 1, 3 and 6 month), ODF were visually inspected, and the *in vitro* dissolution in pH 5.7±0.1 SSF performed, and drug content and possible impurities assayed as previously described.

4.3.4 Statistical analysis

The performances of the ODF were compared by paired t-test and analysis of the variance (one-way ANOVA) followed by Bonferroni post-hoc analyses (IMB SPSS V25). The level of significance was taken as $p < 0.05$. Outliers were rejected, according to Dixon's t-test.

4.4 Results and discussion

4.4.1 ODF characterization

The adopted experimental condition permitted to obtain DNa loaded ODF without significant visual defects; the further addition of TiO_2 made their appearance completely homogenous and whitish. The range of ODF thickness was suitable for the patient's handling (**Table 4.1**). The residual water content observed was acceptable for this type of formulation [12], despite the differences related to the measurement method (**Table 4.1**). Indeed, LOD was determined by a thermobalance that measures the evaporation of adsorbed water on the surface, while the Karl-Fisher titration measures both the surface unbound and bound water. All formulations disintegrated within 80 s complying the Ph. Eur. specifications.

The formulation components influenced the tensile properties of ODF. As an example, **Figure 4.1** shows the stress-strain curves for the placebo films (F1 and F10) and the DNa loaded ODF (F2), DNa ODF with all TMA (F6), and DNa, TMA and TiO_2 loaded ODF (F13). At low strain values, the tensile profile of all ODF appeared linear, indicating elastic deformation. Afterward, the behaviour was mainly dominated by the type of loaded excipients. Indeed, the tensile

strength (σ), which is an index of the maximum force reached by each film before plastic deformation, markedly increased in drug loaded ODF independently of the presence of TMA. The deformation became plastic with the strain increase; the neck formation was also observed in all formulations, even though it was more prominent in the placebo ODF. Hence, it was evident that the σ and elasticity were predominantly influenced by the loading of DNa and partly by TiO_2, rather than TMA. **Table 4.2** summarizes the quantitative results of the tensile measurements.

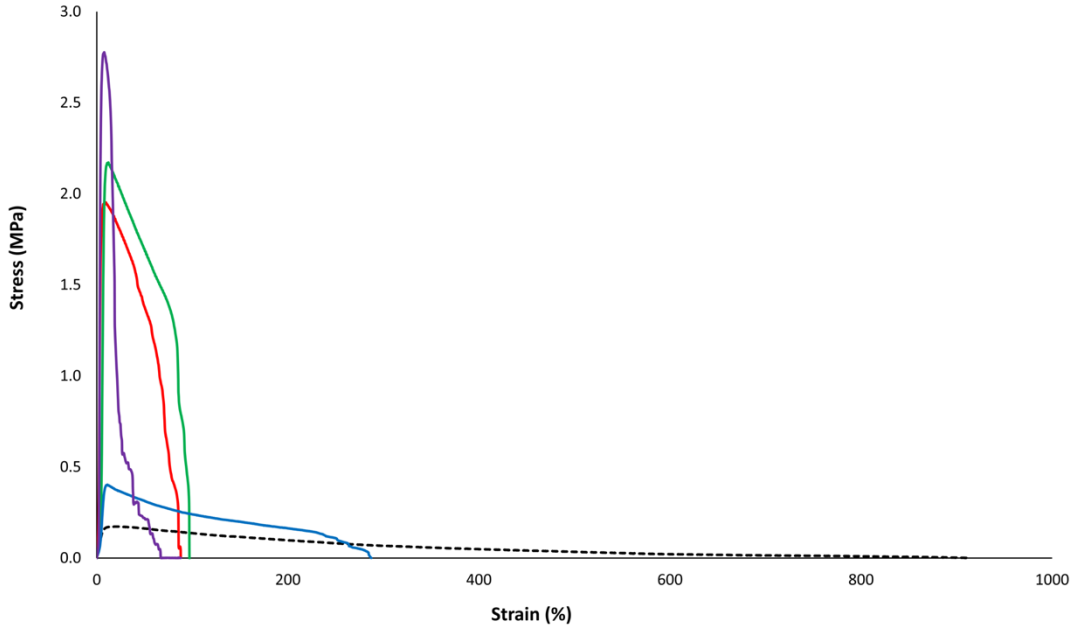

Figure 4.1. Stress-strain curves of the placebo ODF F1 (black dotted line), DNa only loaded ODF F2 (green solid-line), DNa plus TMA loaded ODF F6 (red solid-line), TMA only loaded ODF F10 (blue solid-line), and), DNa plus TMA and TiO_2 (F13) ODF F13 (purple solid-line).

As already mentioned, the loading of DNa into ODF increased the σ values (F1 versus F2) ($p \leq 0.03$). This trend was also maintained in the DNa loaded ODF containing TMA, as a single component or in combination (F1 versus F3, F4, F5, and F6) ($p \leq 0.01$). However, the overall contribution of TMA on the tensile properties was limited since the σ values measured for F2 and F6 did not significantly change, even when the nano-sized TiO_2 was added in F13. This finding markedly differs from those reported for ODF with the same composition obtained by solvent-casting, where the addition of TMA increased the plasticity compared to the placebo formulation [10].

Adding only DNa (F2) or a combination with all TMA (F6) (**Table 4.2**), the ε values decreased with respect to placebo ODF (F1) about 9- and 14-folds, respectively ($p<0.0001$). In parallel,

a decrease in the film elasticity (*Y*) in both F2 and F6 was observed in comparison to F1 ($p<0.01$). The increase of the *Y*-value was also measured comparing F1 to formulations containing DNa and a specific TMA (i.e., F3, F4, and F5). Moreover, lower *Y* was measured when TMA were added individually to the placebo ODF (F2 versus F7, F8, and F9). This trend shows that the observed increase in *Y* was predominantly due to the presence of DNa.

Finally, the ODF toughness, measured as the tensile energy to break (TBE), increased by loading DNa (F1 versus F2, $p<0.01$) and decreased after also adding TMA (F2 versus F6, $p<0.0001$). A similar result was also observed comparing the TBE valued of F2 with those of placebo ODF loaded by a specific TMA or combination thereof (F2 versus F7, F8, F9, and F10, $p\leq0.02$). Moreover, no significant differences in TBE were evident comparing the value registered for F6 to those obtained by F7, F8, and F9 (Table 4.2). These results demonstrated that the decrease in the film toughness could be mainly attributed to the TMA.

As expected, TiO_2 decreased DNa loaded film's elasticity, as evidenced by an increase in the *Y* value (F2 versus F12, $p<0.05$; and F2 versus F13, $p=0.004$). This data agrees with previous data concerning not only TiO_2 [12] but also other nanosized materials such as poly-(vinyl acetate) nanoparticles [14, 15] and quercetin nanocrystals [16]. In all these cases, such materials increased the stiffness of maltodextrin made ODF, suggesting that the size of particulate can be used to tune the tensile properties of ODF. In order to deeply understand the influences of TiO_2 on the film mechanical properties, the force required to peel-off the ODF from the primary packaging material, on which the ODF was printed, was studied.

When the real condition for the ODF peeling was simulated (method A, **Table 4.2**), F1 was characterized by high static and dynamic peel forces required to detach the ODF from the packaging material compared to F11. Moreover, F1 shows an erratic detachment

Table 4.2. Tensile properties (mean ± SD, n=5) and static and dynamic peel forces of ODF from the primary packaging material (mean ± SD, n=5) of prepared ODF. n.d.: not determined.

Form.	**σ (MPa)**	***Y* (MPa)**	**ε (%)**	***TBE* (MJ/m^3)**	**Static peel force (N/mm)**		**Dynamic peel force (N/mm)**	
					Method A	*Method B*	*Method A*	*Method B*
F1	0.17 ± 0.03	2.06 ± 0.65	850 ± 56	0.48 ± 0.08	0.038±0.011	0.19 ± 0.05	0.015±0.003	0.13 ± 0.03
F2	2.21 ± 0.54	47.38 ± 24.97	91 ± 12	1.45 ± 0.27	n.d.	0.07 ± 0.01	n.d.	0.05 ± 0.01
F3	2.29 ± 0.60	71.22 ± 27.90	103 ± 15	1.52 ± 0.33	n.d.	n.d.	n.d.	n.d.
F4	1.62 ± 0.59	44.24 ± 19.10	114 ± 33	0.97 ± 0.19	n.d.	n.d.	n.d.	n.d.
F5	1.39 ± 0.17	49.02 ± 12.33	103 ± 28	1.14 ± 022	n.d.	n.d.	n.d.	n.d.
F6	1.82 ± 0.76	77.80 ± 48.21	53 ± 18	0.57 ± 0.37	n.d.	0.05 ± 0.00	n.d.	0.02 ± 0.01
F7	0.38 ± 0.05	7.80 ± 1.64	256 ±47	0.67 ± 0.18	n.d.	n.d.	n.d.	n.d.
F8	0.43 ± 0.08	7.30 ± 2.84	272 ± 53	0.68 ± 0.13	n.d.	n.d.	n.d.	n.d.
F9	0.28 ± 0.04	4.26 ± 1.04	375 ± 75	0.45 ± 0.08	n.d.	n.d.	n.d.	n.d.
F10	0.96 ± 0.10	25.04 ± 5.79	105 ± 7	0.69 ± 0.09	n.d.	n.d.	n.d.	n.d.
F11	1.33 ± 0.28	33.70 ± 11.70	144 ± 35	1.27 ± 0.11	0.020±0.001	0.13 ± 0.03	0.009±0.003	0.08 ± 0.01
F12	2.06 ± 0.31	87.16 ± 17.50	103 ± 1	1.52 ± 0.33	n.d.	0.04 ± 0.01	n.d.	0.02 ± 0.00
F13	2.25 ± 0.40	101.71 ± 15.52	49 ± 7	0.64 ± 0.10	n.d.	0.03 ± 0.00	n.d.	0.02 ± 0.00

pattern indicating high intimate contact between the ODF and the packaging material so that more energy was required to separate them. In contrast, a linear curve was obtained with low static and dynamic peel forces and a steady detachment pattern when TiO_2 was added in F11 (**Figure 4.2**).

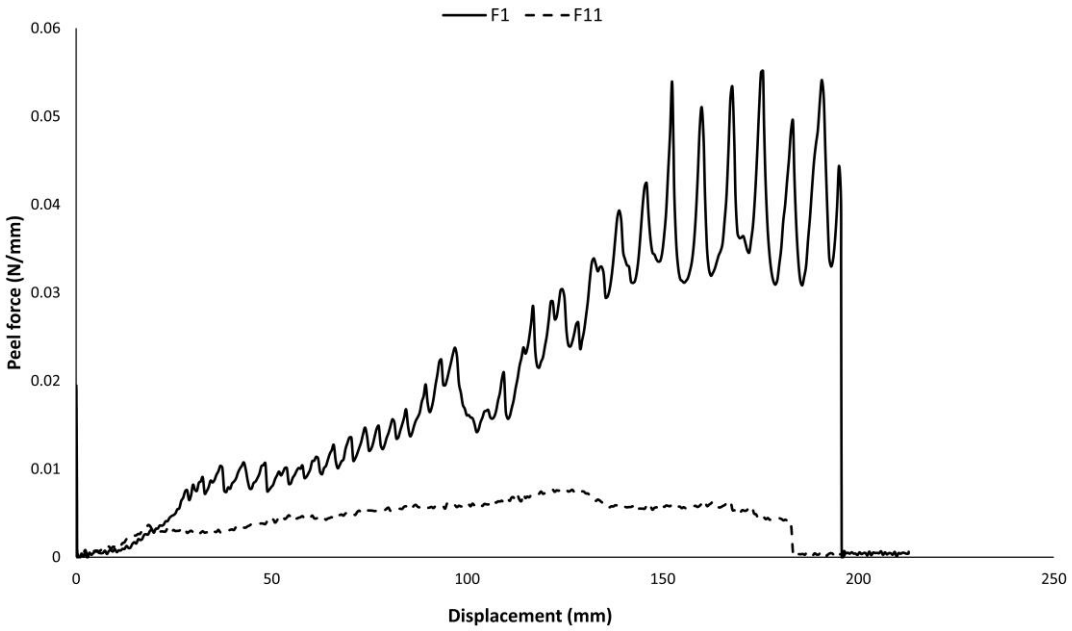

Figure 4.2. Peel force versus displacement curves (protocol A) for placebo formulation (F1, solid line) and loaded with TiO_2 (F11, dashed line).

The anti-sticking role of the TiO_2 loaded ODF on the packaging material was then deepened by using method B The data in **Table 4.2** showed that when pressure was applied on the ODF/packaging material and the detachment angle fixed, the anti-sticking effect of TiO_2 was maintained. Indeed, F11, F12, and F13 were characterized by lower static and dynamic peeling forces, as indicated by the maximum (static) peel force and the dynamic peel force ($p \leq 0.01$), in comparison to formulations F1, F2, and F6, respectively. Moreover, the presence of DNa in the ODF synergized the effect of TiO_2 on the two peeling forces (F11 versus F12 and F13, $p \leq 0.01$). In other words, the presence of TiO_2 favoured the peeling from the primary packaging, an indication of ODF handling without damage.

4.4.2 Drug content and in vitro dissolution properties

DNa, 25 mg equivalent of diclofenac, was successfully loaded in the ODF (**Table 4.3**), and the drug content complied with the pharmacopeia limits. Nevertheless, heating at 95 °C, as required by the preparation protocol, caused the formation of the impurity A of DNa [Ph. Eur.

Monograph on Diclofenac sodium (01/2017:1002)], which, in any cases, represented less than 0.2 %w/w (**Table 4.4**) for F2 and F13. The dissolution profiles of formulations F2, F6 and F13 were superimposable in deionized water **(Figure 4.3A)**, and pH 5.7 SSF (**Figure 4.3B)**, with $t_{80\%}$ approximately 3 min in all three formulations. Based on these results, F2 and F13 were considered suitable for an accelerated stability study.

Table 4.3. Drug contents and different dose strengths in ODF with different area

ODF area (cm^2)	F13 Drug Content	
	DNa (mg)	*DNa (%)*
1	3.90±0.01	11.44±0.53
2	9.43±0.42	11.13±0.17
6	25.66±1.51	11.73±0.71

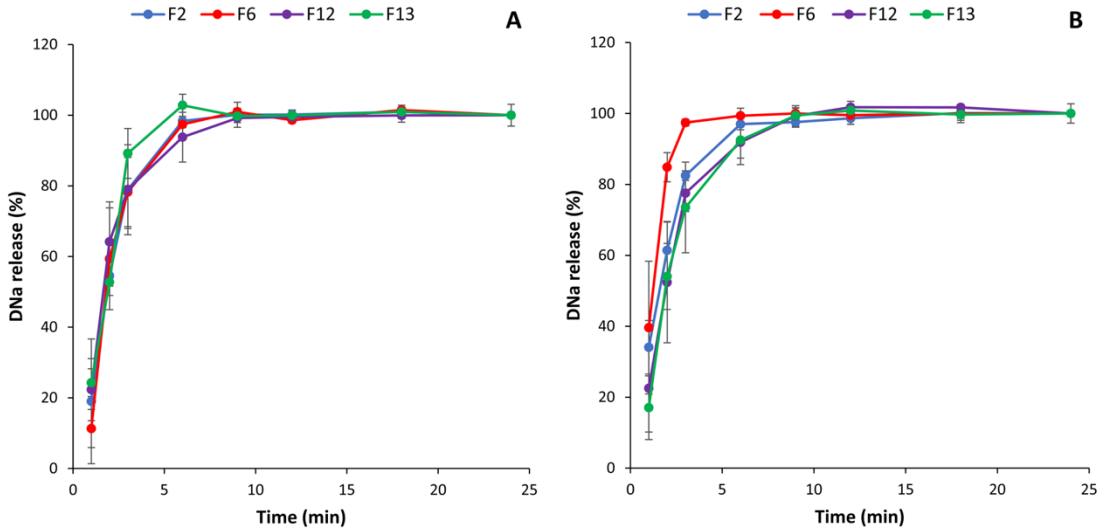

Figure 4.3. *In vitro* dissolution profiles of DNa only loaded ODF (F2), DNa plus TMA loaded ODF (F6), DNa plus TiO_2 (F12), DNa plus TMA and TiO_2 (F13) ODF in deionized water **(A)** and pH 5.7 SSF **(B)** (Time zero).

4.4.3 ODF accelerated stability study

After six months of storage of the ODF in accelerated conditions, the physical appearance was unaffected: ODF were non-sticky and remained easy to handle without fractures. The drug content and the impurity A of DNa remained within the acceptable range over time according to the Ph. Eur. specifications (**Table 4.4)**. The *in vitro* dissolution profiles of DNa loaded in F2 or F13 were superimposable over time (**Figures 4.4A** and **4.4B)**, confirming the t_{80} detected at

time 0 within 3 min. Moreover, in all cases, the complete drug release was achieved in less than 10 min.

Table 4.4. ODF drug content and impurity A level from the accelerated stability study

Sampling time (months)	F2		F13	
	DNa (%)	*Impurity A (%)*	*DNa (%)*	*Impurity A (%)*
0	10.43±0.09	0.17±0.00	11.73±0.71	0.11±0.06
1	10.72±0.26	0.15±0.05	11.19±0.12	0.18±0.03
3	10.17±0.05	0.16±0.01	11.00±0.08	0.18±0.01
6	11.03±0.24	0.11±0.04	11.13±0.17	0.14±0.01

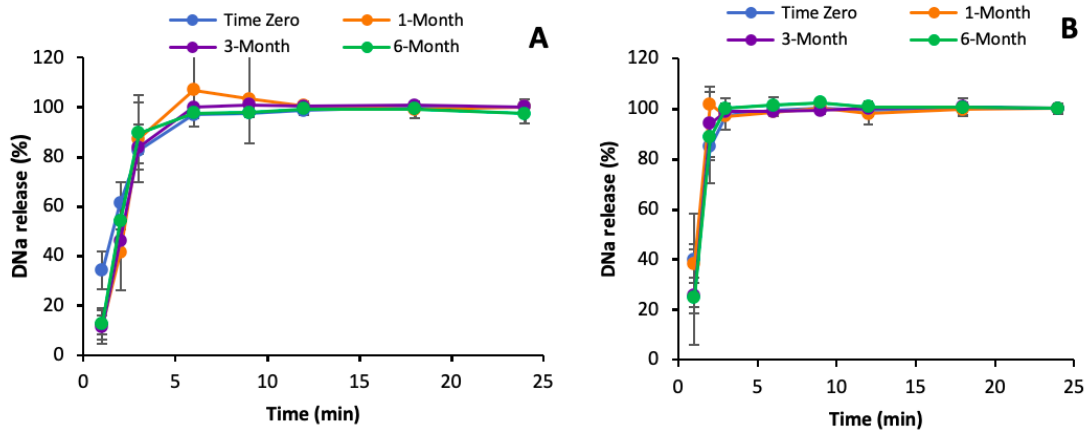

Figure 4.4. *In vitro* dissolution profiles of DNa loaded ODF (F2) **(A)**, DNa plus TMA+TiO_2 loaded ODF (F13) **(B)** in pH 5.7 SSF at time 0, 1, 3 and 6-month stability tests.

The overall results confirmed that hot-melt ram printing is a versatile method for the extemporaneous preparation of ODF made of maltodextrins. Indeed, the formulation space given by such a technology permits to load in the ODF with different TMA to mitigate the unpleasant taste of drugs, like DNa, without altering the ODF technological properties. However, this is not a rule of thumb, as several authors reported that the addition of TMA may influence ODF tensile properties and this aspect is evident in ODF prepared by solvent casting, regardless of the matrix-former excipient used in the preparation. As an example, an irregular pattern of tensile strength was reported for hydroxypropyl methylcellulose-corn starch-based films loaded with donepezil hydrochloride and different TMA (i.e., aspartame, sucralose, saccharin sodium, and pineapple flavour) [17]. A significant alteration of tensile properties was also reported in the case of ODF made of maltodextrins and loaded by nicotine [6]. On the

contrary, the TMA effect on the tensile properties seems lower for the ODF obtained by hot-melt printing than for those with the same formula but prepared by the casting technique [10]. This feature can be attributed to the absence of solvent(s) in the proposed printing technology, which permits to obtain ODF with a slightly higher thickness.

Regarding the presence of TiO_2, which was selected as a colour additive to enhance ODF aesthetic appearance, this excipient significantly improved the film mechanical properties. The addition of 0.1% is sufficient to reinforce the ODF, as demonstrated by the significant increase of the tensile strength (F1 versus F11, **Table 4.2**). This effect has already been described when TiO_2 was loaded as a functional filler in pharmaceuticals and foods [18, 19, 20]. Interestingly, TiO_2 also exhibits anti-sticking properties; the peel forces required to detach the ODF from the primary packaging material was significantly reduced (**Table 4.2**). Thus, TiO_2 could be considered a functional excipient to control the ODF tackiness and, therefore, avoid failures during patient handling.

Finally, despite DNa is classified in the BSC Class II [21], all the studied formulations allowed a fast *in vitro* drug release in both media (i.e., deionized water and pH 5.7 SSF); t_{80} was attained within 3 min, and a complete drug release was achieved in less than 10 min in all cases. Thus, ODF formulations can be described as 'rapidly dissolving' dosage form according to the EMA guidelines for new drug products [22].

It should also be mentioned that even if DNa is a thermosensitive drug, its degradation during the printing procedures is minimal, since the impurity A was the only one detected and remained below the maximum limit set by the Ph. Eur. (< 0.2%). Most importantly, the DNa degradation pattern, namely additional impurities or significant changes of preparation-related ones, was not modified over time. Moreover, the *in vitro* dissolution profiles for the selected formulations were superimposable during the accelerated stability study period.

This data suggests that the period of stability of ODF produced by the hot-melt approach could be compliant with the requirements for compounding in pharmacy settings. Indeed, pharmacy preparations are assumed by the patients in a shorter time than industrially prepared medicinal products: their expiration period is within six months from the preparation.

Tuning the area (1 cm^2 and 2 cm^2 or 6 cm^2) of the optimized formulation (Formulation F13, **Figure 4.5, Table 4.3**), it would be possible to make available personalize dosage forms to manage acute migraines [23] and pain [24, 25] in paediatric patients. This aspect could be of interest for children, since to the best of our knowledge, there is not commercially available paediatric dosage form (e.g., syrup or suspension) of DNa due to its stability issues. Moreover, the high acceptability of ODF as a drug delivery platform has already been demonstrated in

infants and children and caregivers [3] since they are a non-invasive and easy to administer, combining the advantages of liquid (e.g., immediate drug release) with those of solid dosage forms (e.g., API stability) [1]. All the formulation components are within the regulatory framework for acceptable daily intake (ADI) [26, 27]. For example, TiO_2 is a colour additive approved by the Food and Drug Administration (FDA) for use in drugs for humans [27]. Furthermore, the amount incorporated (i.e., 0.1%) in the formulation, which is enough to enhance its aesthetic appearance, is far below the ADI recommended by both the FDA and the EU report on Dietary Food Additive Intake [26, 27].

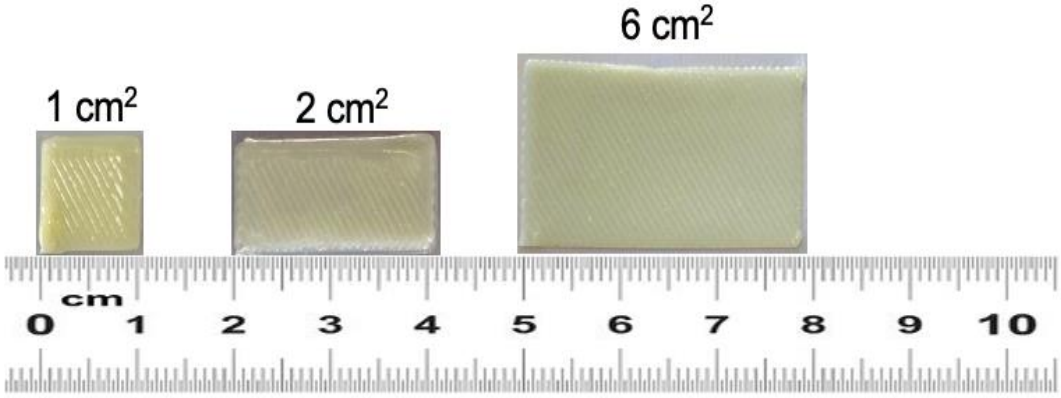

Figure 4.5. DNa ODF with different surface area containing different dose strengths of DNa

4.5 Conclusions

Within the current regulatory frameworks for stability and critical quality attributes of ODF in compliance with the EMA and ICH guidelines [28], the feasibility of loading diclofenac sodium and the combination of TMA in the printed ODF without affecting the drug stability was demonstrated. The tensile properties were mainly dominated by the loaded drug, and not significantly affected by the TMA. Moreover, TiO_2, which improved the ODF aesthetic appearance, also favoured the ODF detachment from the primary packaging material. Therefore, hot melt printing can be proposed to prepare palatable ODF loaded by a bitter thermosensitive drug. The technology could be advantageously used in hospital pharmacy settings to allow a precise personalization of dose.

References

[1] Cilurzo F, Musazzi UM, Franzé S, et al. Orodispersible dosage forms: biopharmaceutical improvements and regulatory requirements. Drug Discov. Drug Discov. Today. 2018; 23: 251-259.

[2] Visser JC, Woerdenbag HJ, Crediet S, et al. Orodispersible films in individualized pharmacotherapy: The development of a formulation for pharmacy preparations. Int. J. Pharm. 2015; 478: 155-163.

[3] Orlu M, Ranmal SR, Sheng Y, et al. Acceptability of orodispersible films for delivery of medicines to infants and preschool children. Drug Deliv. 2017; 24: 1243-1248.

[4] Slavkova M, Breitkreutz J. Orodispersible drug formulations for children and elderly. Eur. J. Pharm. Sci. 2015; 75: 2-9.

[5] Selmin F, Musazzi UM, Cilurzo F, et al. Alternatives when an authorized medicinal product is not available. Med Access @ Point Care. 2017;1(1):16–21.

[6] Cilurzo F, Cupone IE, Minghetti P, et al. Nicotine fast dissolving films made of maltodextrins: A feasibility study. AAPS PharmSciTech. 2010; 11: 1511–1517.

[7] Krampe R, Visser JC, Frijlink HW, et al. Oromucosal film preparations: points to consider for patient centricity and manufacturing processes. Expert Opin. Drug Deliv. 2016; 13: 493-506.

[8] Nishigaki M, Kawahara K, Nawa M, et al. Development of fast dissolving oral film containing dexamethasone as an antiemetic medication: Clinical usefulness. Int. J. Pharm. 2012; 424: 12-17.

[9] Khadra I, Obeid MA, Dunn C, et al. Characterization and optimization of diclofenac sodium orodispersible thin film formulation. Int. J. Pharm. 2019; 561: 43-46.

[10] Cilurzo F, Cupone IE, Minghetti P, et al. Diclofenac fast-dissolving film: Suppression of bitterness by a taste-sensing system. Drug Dev. Ind. Pharm. 2011; 37: 252-259.

[11] Musazzi UM, Khalid GM, Selmin F, et al. Trends in the production methods of orodispersible films. Int. J. Pharm. 2020; 576. doi: 10.1016/j.ijpharm.2019.118963.

[12] Musazzi UM, Selmin F, Ortenzi MA, et al. Personalized orodispersible films by hot melt ram extrusion 3D printing. Int. J. Pharm. 2018; 551: 52-59.

[13] Visser JC, Wibier L, Kiefer O, et al. A pediatrics utilization study in the Netherlands to identify active pharmaceutical ingredients suitable for inkjet printing on orodispersible films. Pharmaceutics. 2020;12(2):1–10.

[14] Cupone IE, Selmin F, Cilurzo F, et al. Amino acids as non-traditional plasticizers of maltodextrins fast-dissolving films. Carbohydr. Polym. 2014; 115: 613-616.

[15] Franceschini I, Selmin F, Pagani S, et al. Nanofiller for the mechanical reinforcement of maltodextrins orodispersible films. Carbohydr. Polym. 2016; 136: 676-681.

[16] Lai F, Franceschini I, Corrias F, et al. Maltodextrin fast dissolving films for quercetin nanocrystal delivery. A feasibility study. Carbohydr Polym. 2015; 121: 217-223.

[17] Liew KB, Tan YTF, Peh KK. Characterization of oral disintegrating film containing donepezil for Alzheimer's disease. AAPS PharmSciTech. 2012; 13: 134-142.

[18] Bonsu MA, Ofori-Kwakye K, Kipo SL, et al. Development of Oral Dissolvable Films of Diclofenac Sodium for Osteoarthritis Using Albizia and Khaya Gums as Hydrophilic Film Formers. J. Drug Deliv. 2016; 1. doi: 10.1155/2016/6459280.

[19] Li W, Zheng K, Chen H, et al. Influence of nano titanium dioxide and clove oil on chitosan-starch film characteristics. Polymers. 2019; 11. doi:10.3390/polym11091418.

[20] Zhang X, Xiao G, Wang Y, et al. Preparation of chitosan-TiO 2 composite film with efficient antimicrobial activities under visible light for food packaging applications. Carbohydr. Polym. 2017;169: 101-107.

[21] Chuasuwan B, Binjesoh V, Polli JE, et al. Biowaiver monographs for immediate release solid oral dosage forms: diclofenac sodium and diclofenac potassium J. Pharm. Sci. 2009; 98: 1206-1219.
[22] European Medicine Agency (EMA), 2000. EMA/CPMP/ICH/367/96/2000.
[23] Barbanti P, Grazzi L, Egeo G. Pharmacotherapy for Acute Migraines in Children and Adolescents. Expert Opin. Pharmacother. 2019; 20: 455-463.
[24] Boric K, Dosenovic S, Jelicic Kadic A, et al. Interventions for Postoperative Pain in Children: An Overview of Systematic Reviews. Paediatric Anaesthesia. 2017; 27: 893-904.
[25] Wright J. An update of systemic analgesics in children. Anaesth. Intens. Care Med. 2019; 20: 324-329.
[26] European Commission (EC), 2001, https://publications.europa.eu/en/publication-detail/-/publication/26105dba-6d8f-4515-a641-0e43fe3f5498/language-en. Accessed 25 August 2020.
[27] Food and Drug Administration (FDA), 2019, https://www.fda.gov/industry/color-additive-inventories/summary-color-additives-use-united-states-foods-drugs-cosmetics-and-medical-devices. Accessed 25 August 2020.
[28] European Medicine Agency (EMA), 2004, EMA/CHMP/ICH/167068/2004.

Chapter 5

A comparison of preparation methods on the *in vitro* performances of olanzapine orodispersible films

5.1 Introduction

In recent years, new drug delivery platforms have been proposed to meet the increasing demand of dosage forms to address specific needs of patient populations. For instance, the design of drug products to be administered to geriatric and paediatric patients should consider the presentation of the treatment to the end-user (i.e. patient, care giver, health care provider) which includes the dosage form, formulation, dose, dosing frequency and packaging [1]. Patient centric drug products would also avoid the practice of manipulating tablets or capsules which may compromise the dose accuracy, patient safety and the treatment efficacy [2]. In this context, orodispersible films (ODF) have been reported to improve ease of administration, compliance and medication adherence in patients having difficulties with swallowing [3]. Tailored dose can be obtained from the same formulation cut into different sizes and shapes, thus, ODF have been also proposed for patient-focused therapy [4] [Chapter 2].

Generally speaking, the main ODF production processes can be referred to solvent-based or heating-based technologies [6]. The first entails that the drug substance can either be suspended or dissolved in an aqueous polymeric dispersion comprising all the other excipients. Then, the slurry is subsequently cast, or jetted, onto a release liner, or edible substrate, and dried. Alternatively, in the attempt to produce small batches or to compound personalized therapies, printing technologies have been proposed. Some of them avoids the use of solvents, mainly water in the case of ODF and can limit the risk of unintended drug phase transformations, which could directly affect the dissolution rate of the loaded drug and limit its bioavailability.

Olanzapine (OLZ), an anti-psychotic drug available on the market as 10 mg orodispersible tablets to improve the patient's adherence in the treatment of schizophrenia could represent one of these cases. It is a poorly water soluble drug which presents an intricate polymorphism since OLZ can crystallize in several forms, including various anhydrates, solvates and hydrates [7]. In particular, the exposure to different moisture or direct contact with water promotes the conversion to the hydrate forms [8] and this reduces the possibilities to develop OLZ ODF since the hydrate forms are poorly water soluble.

This work aims to compare the technological performances of ODF loaded by OLZ prepared by two different methods, namely solvent casting and hot-melt ram printing. The latter was proposed for personalized therapy since it consists of (I) the melting of a mixture made of the active

ingredient, the film forming material and other excipients and (II) the printing of the ODF of the desired size and shape directly on the primary packaging [9].

5.2 Materials

Maltodextrin, with a dextrose equivalent equal to 6 (MDX, Glucidex® IT6), was obtained from Roquette (F). Olanzapine (OLZ) was a courtesy gift from Deafarma (Azelis, I). Glycerol was purchased from VWR International, (B), Span® 80 (Croda, E).
All solvents were of analytical grade unless otherwise specified.

5.3 Methods

5.3.1 ODF preparation

ODF were prepared by hot-melt ram printing and solvent casting according to the composition reported in **Table 5.1**. Regarding the printing, a paste of the various excipients was transferred into the extruding chamber heated at 95±1 °C for 10 min. The melt was extruded to print the ODF of the desired dimensions (2×3 cm) on a 20×20 cm aluminium primary packaging foil kindly provided by IBSA Spa (I). The printed ODF were sealed with another packaging aluminium foil without further manipulations. The ram speed (12 mm/min) and the chamber temperature were controlled by Repetier-Host 2.0.1 software (Hotword GmbH, G); the film dimension and number per each print were designed by 3D Builder® (Microsoft, USA) and converted in G-code.
For ODF prepared by solvent casting; the aqueous dispersion was prepared by dissolving maltodextrin, glycerol and Span® 80 (**Table 5.1**) in distilled water maintained at 80 °C and stirred with a magnetic stirrer. The obtained dispersion was cooled down to 40 °C and stirred overnight and cooled down to room temperature. Specific amount of olanzapine was added to the slurry and stirred for 1 h 30 min. after a rest period to remove the air bubbles, the films were obtained by using a laboratory-coating unit Mathis LTE-S(M) (CH). The aqueous dispersion was cast onto a polyester release liner with a thickness selected to obtain films with a thickness of about 120 μm. The coating rate was fixed at 1 m/min, and the cast dispersion was dried in the oven at 60 °C for 15 min with a horizontal air circulation of 1200 rpm. The films were then cut into desired shape and size and packaged individually in airtight seal and stored at 25 ± 1 °C until use.

5.3.2 Physical and technological characterizations

Film thickness

The film thickness was measured by using a micrometre MI 1000 μm (ChemInstruments, USA). The accuracy of the instrument was 2.5 μm ± 0.5%.

ODF water content

Loss on drying (LOD): the LOD was assayed gravimetrically using a thermobalance (Gilbertini, Italy). Film samples were kept at 100±2 °C until constant weight, and the percentage of moisture loss was calculated.

Water content: An ODF exactly weighted was transferred into an empty glass vial of a Karl-Fisher apparatus (Mettler Toledo, CH). After adding 1.5 mL anhydrous methanol, the sample was sonicated for 30 min and an aliquot of 0.5 mL was injected into the titration chamber. The water content was calculated according to Equation (1):

$$\text{water content (\%)} = \frac{Ms - Mm}{Mo} \times 100 \quad (1)$$

where:

M_s is the mass of water in the sample introduced into the titration chamber;

M_m is the mass of water in the anhydrous methanol;

M_0 is the initial mass of the ODF.

Drug content

ODF specimen of 2×3 cm was dissolved in the mobile phase containing a mixture of phosphate buffer pH 6.7 and acetonitrile (60/40 %v/v). The drug concentrations were quantified by HPLC analysis (Agilent HP 1100, Chemstation, Hewlett Packard, Santa Monica, USA). The following chromatographic conditions were used: column: InterClone™ (5 μm ODS, 100 Å, 150×4.6 mm, Phenomenex®, USA); flow rate: 1.5 mL/min; wavelength: 258 nm; temperature: 40 ºC; injection volume: 20 μm. The drug concentrations were determined from a known standard curve in the 6–600 μg/mL range (R^2 = 0.999).

Thermal analysis

Differential scanning calorimetry (DSC): DSC analysis was performed using a Mettler Toledo CH (Mettler Toledo, CH) operating with a Stare software using (4–6 mg) samples in 40 μL aluminium pans with pierced lids at heating rate of 10 °C min^{-1} and nitrogen purge at 80 $mLmin^{-1}$. The system was calibrated using an indium standard.

Thermogravimetric analysis (TGA). The mass loss of the sample as a function of temperature was determined using a Mettler Toledo 851e TGA/SDTA (Mettler Toledo, CH). Samples were placed in open alumina crucibles and heated at a rate of 10 °$Cmin^{-1}$ under a nitrogen purge (80 $mLmin^{-1}$).

X-Ray diffraction (XDP)

X-ray powder diffraction data were obtained using a Bruker D8 diffractometer with graphite monochromatized CuKα radiation source (λ: 1.541874 Å). The unit-cell parameters, refined from powder data using the UNITCELL software [9]. The 2θ range were at 5.120° to 60.100° for OLZ Form I raw material, 5.000° to 49.980° for OLZ loaded ODF made by casting and 3D printing, respectively.

Disintegration test

The disintegration test was carried out in deionized water according to specifications of the monograph on the "Disintegration of tablets and capsules" reported in the Ph. Eur. The results complied with the Ph. Eur. requirements for orodispersible tablets if the disintegration time was lower than 3 min.

In vitro dissolution test

Preliminarily, the dissolution test was carried out in simulated salivary fluid (SSF) at pH 6.8 for 6 min; afterwards, the pH was shifted to simulated gastric fluid (SGF) pH 1.2 adding 1N hydrochloric acid. Based on these results, the dissolution behaviour was also tested in both SSF at pH 6.8 and SGF at pH 1.2 for 30 min.

In all cases, the medium volume was set at 900 mL maintained at 37±1 °C and stirred at the speed of 25±1 rpm in Ph. Eur. apparatus type I (SR8 PLUS Hanson Research, Chatsworth, USA) equipped with basket. Aliquots of 3 mL were taken at 1, 2, 3, 6, 9, 12, 18, 24 and 30 min and immediately replaced with fresh buffers. OLZ concentrations were assayed spectrophotometrically

at 257 nm (UV–Vis spectrometer, Lambda 25, Perkin Elmer, I). The calibration curves were in the range of 0.4–45 μg/mL (R^2 = 0.999).

The results are expressed as the mean and standard deviation of three replicas for each formulation.

5.3.3 Statistical analysis

The performances of the ODF were compared by paired t-test analysis using IMB SPSS Version 25. The level of significance was taken as $p < 0.05$. Outliers were rejected, according to Dixon's t-test.

5.4 Results and discussion

The OLZ did not elicit a plasticizing effect on maltodextrin used (MDX6), therefore, the operative conditions adopted for the placebo formulations permitted to obtain OLZ loaded ODF without visual defects with both the preparation methods. The range of ODF thickness was suitable for the patient's handling (**Table 5.1**). As expected from previous experiences, cast film were thinner with respect to printed ODF even if they contained the similar drug contents from the same superficial area of 6 cm^2. The residual water content observed was acceptable for this type of dosage form (**Table 5.1**). Some differences also reflected in disintegration time which, in all cases, complied the Ph. Eur. specifications (**Table 5.1**).

The drug content resulted uniform HPLC analyses did not evidence any degradation peak despite of the differences in processing temperature.

The overall dissolution of orodispersible dosage form is considered substantially similar to those of conventional oral dosage form. Indeed, after disintegration in the mouth, insoluble drug substances disperse in the saliva, they are swallowed and reach the stomach in about 5-10 min [11]. Based on this consideration, the dissolution test on cast and printed ODF was carried out in pH 6.8 for 6 min and then, the pH value was dropped down to 1.2. To make the dissolution condition reproducible, the use of the basket apparatus (USP type I) was preferred since ODF can easily float, stick on the paddle or vessel [12] [Chapter 2]. As shown in **Figure 5.1**, OLZ ODF made by casting formed a precipitate at pH 6.8 SSF which was readily re-dissolved at lower pH.

To better elucidate the different behaviour, dissolution tests at a specific pH, namely pH 6.8 SSF and pH 1.2 SGF, were carried out (**Figure 5.2**). In agreement with previous results, ODF prepared by hot-melt ram printing promptly released OLZ and the film was completely dissolved within 6 min independently on the dissolution media (**Figure 5.2**). A similar result was obtained by cast

ODF in pH 1.2 SGF, but in pH 6.8 SSF a yellow precipitate was evident in the bottom of vessel after 3 min. The pH dependence in dissolution profile of OLZ was expected considering the basic nature

Table 5.1. Compositions (% w/w) of the placebo and olanzapine (OLZ) loaded ODF by printing and solvent casting. ODF thickness, weight, loss on drying (LOD), moisture content (MC), disintegration time (Disint), weight (mg), and drug content are presented as mean ± standard deviation (SD).

Technology	Components (%)					Thickness (µm)	LOD (%)	MC (%)	Distnt. (s)	ODF weight (mg)	OLZ content (mg)
	OLZ	MDX6	Glycerol	Water	Span®80						
Printing	-	78.00	20.00	2.00	-	220±27	3.4±1.2	10.4±0.6	38±2	333±26	-
	6.29	73.09	18.74	1.87	-	278±13	4.4±0.6	10.3±0.4	44±2	203±5	12.6±0.2
Casting	-	46.41	10.56	41.27	1.76	126±4	7.0±0.1	10.0±0.5	76±0	101±1	-
	5.07	44.05	10.04	39.18	1.67	140±5	5.6±0.7	10.0±1.7	38±12	121±5	9.4±0.1

of this drug (dissociation constants: pK_{a1} = 4.01 and pK_{a2} = 7.24) [13]. Indeed, when the pH was shifted from 6.8 to 1.2, OLZ was completely dissolved (**Figure 5.1**).

Considering the peculiar polymorphic behaviour of this drug, qualitative analysis of OLZ polymorph was carried out by DSC and XRDP. The DSC curve of raw material evidenced a single endothermic event with the onset at about 194 °C (ΔH=128±9 J/g) (**Figure 5.3**) which was attributed to the melting of Form I (**Figure 5.4a**) according to the XRDP pattern [7]. This structure was found to be anhydrous as the baseline of the thermogram is perfectly horizontal at lower temperature. MDX DE6 presents glass transition temperature (T_g) at about 103 °C [14] and the mixing with plasticizer(s), i.e. water or glycerol, caused a massive drop in its value [15]. The binary mixture of OLZ and MDX presented a broad endothermic peak at about 90-100 °C, meanwhile the melting event of Form I was preserved in terms of temperature indicating the maintenance of the crystalline phase (**Figure 5.3**). Hence, these preliminary results suggest that 95 °C might be a suitable temperature for the ram-extrusion of the OLZ–MDX formulation.

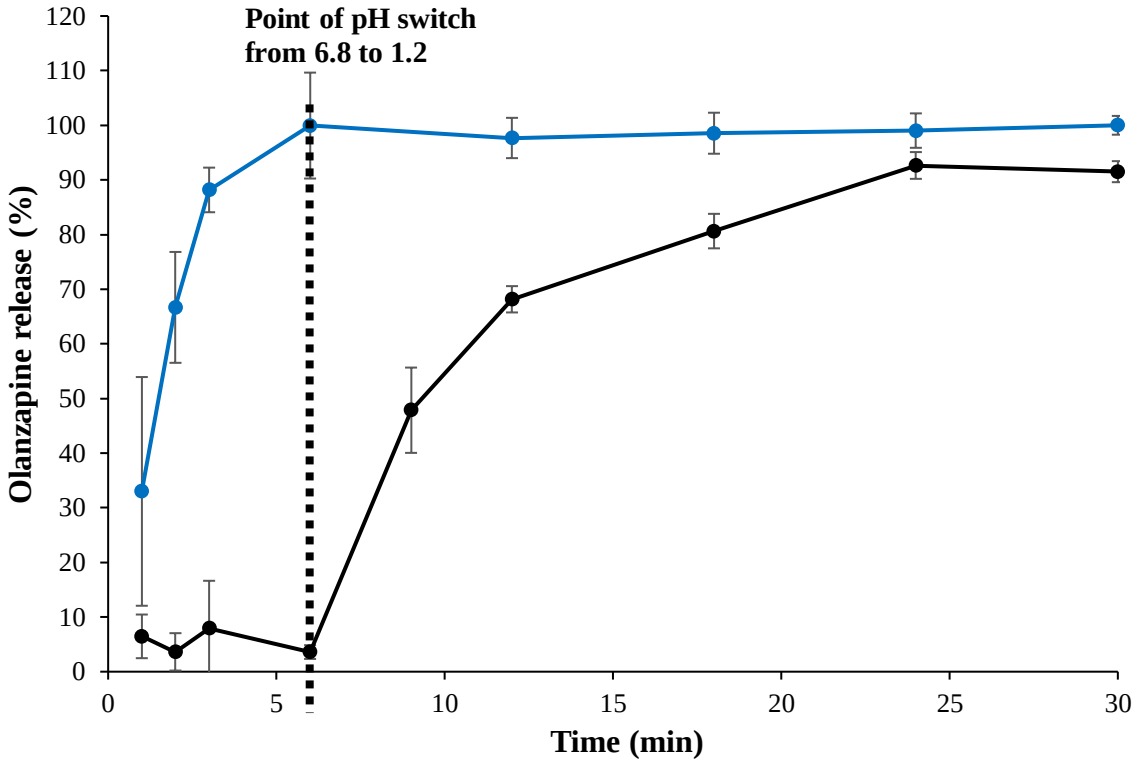

Figure 5.1 – Dissolution profile OLZ from printed (blue line) and cast (black line) ODF at pH 6.8. The switch of pH occurred after 6 min.

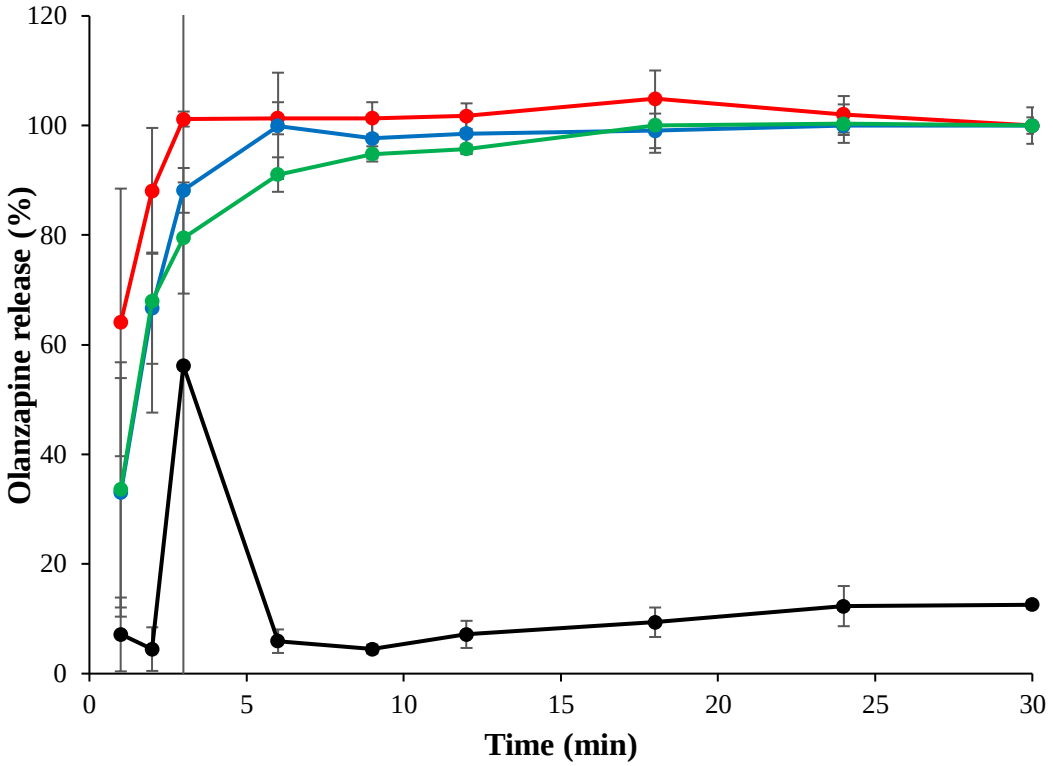

Figure 5.2 – *In vitro* dissolution profile OLZ ODF; printed OLZ ODF in SGF pH 1.2 (red line), printed OLZ ODF in SSF pH 6.8 (blue line), cast OLZ ODF in SGF pH 1.2 (green line), and cast OLZ ODF in SSF pH 6.8 (black line).

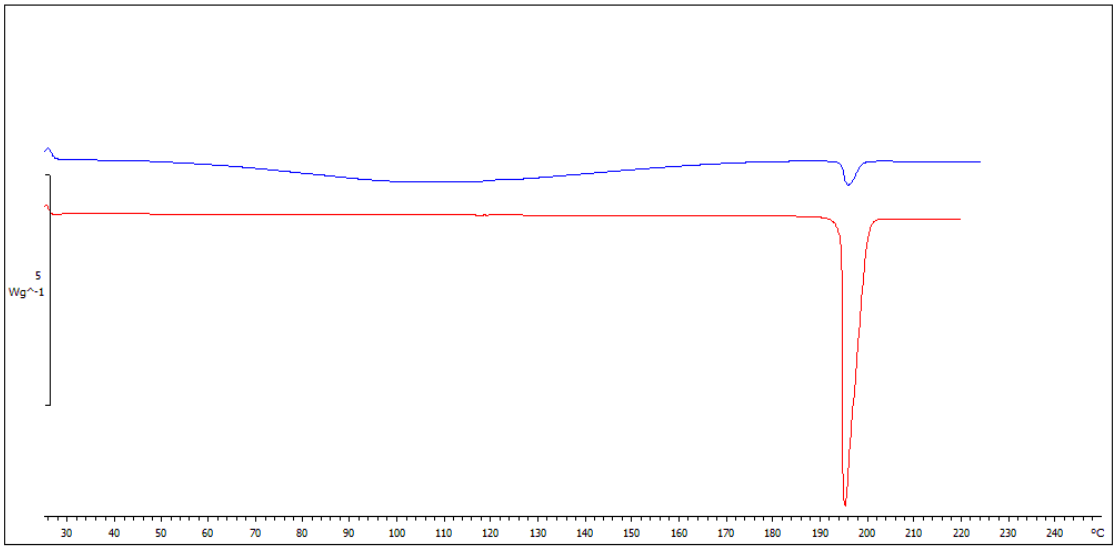

Figure 5.3 – DSC trace of pure OLZ (red line) and physical mixture OLZ and MDX (blue line).

In case of ODF (cast and printed), the presence of glycerol determined several endothermic events up to 130 °C which were ascribed to the thermal degradation of the film and did not permit to

describe the melting behaviour of OLZ (data not shown). XRPD studies that showed the presence of crystalline OLZ. In case of cast ODF, although the peaks at 2θ values of about 9°, 14.4° and 18.7° were relatively broad and with significant background noise associated, it is still possible to confirm the correspondence to Form I (**Figure 5.4b**). In contrast, printed ODF showed only two sharp diagnostic peaks corresponding to 2θ values at about 9° and 18.5° (**Figure 5.4c**).

Indeed, Form I OLZ is reported to be obtained exclusively from dry non-solvate forming organic solvents; meanwhile the hydrate forms usually and readily crystallize when water is present [16]. In line with these considerations, XRDP and TGA was carried out on the OLZ precipitate recovered during in vitro dissolution in SSF pH 6.8 without further purification steps. First, it was noticed that the XRPD pattern was not superimposable to that of OLZ Form I, but some shifts in the 2θ values of the most characteristic peaks were evident (**Figure 5.4d**) and during the thermal treatment a mass loss of about 2% corresponding to about 0.5 mole of water was measured. Based on this result, it can be confirmed that the casting method, which included the preparation of an aqueous slurry, favours the conversion from Form I to a pseudo-polymorphic one.

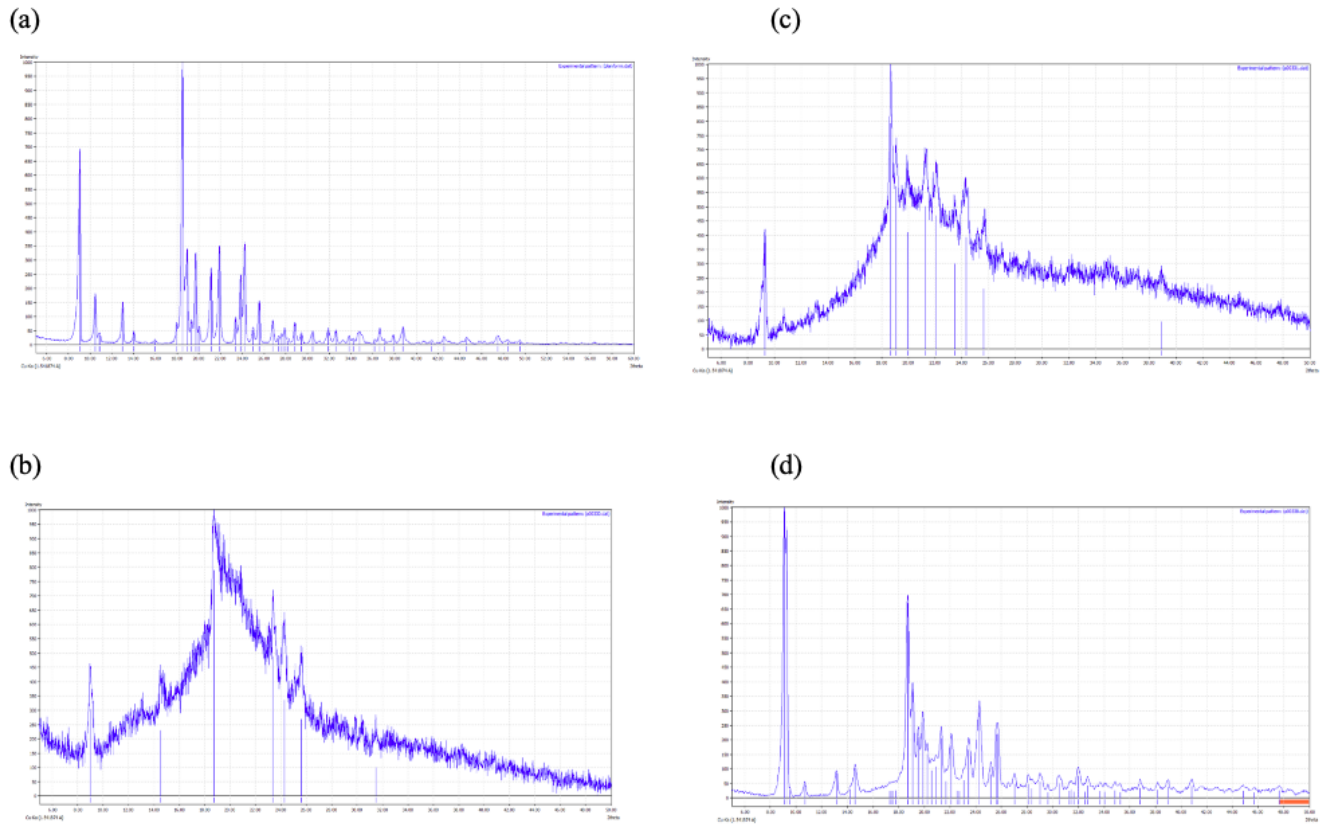

Figure 5.4 – XRDP of (a) OLZ form I, (b) OLZ loaded ODF obtained by casting, (c) OLZ loaded ODF obtained by printing, and (d) precipitated OLZ from cast ODF during the dissolution study at pH 6.8 SSF.

ODF presents an important innovation in the field of pharmaceutical dosage forms for several reason. First, ODF allows to make available dosage forms suitable for those who experience swallowing difficulties. Therefore, it is possible to address clinical needs of dysphagics, geriatrics and paediatrics, with a concomitant improvement in adherence.

Then, ODF can be obtained by different platforms which are of interest both of industry and pharmacies. The most used technologies can be roughly divided on the use of solvent or heat to obtain the mass containing the film forming polymer, the plasticizer, other functional excipients, and the drug substance. It implies that both formulation and the process could be optimized also in relation with the chemical or physical instability of the drug substance. For instance, ibuprofen, which undergoes sublimation, can be formulated as ion-pair complexes in cast ODF [17]. In case of loperamide, when hydroxypropyl cellulose was selected as film-forming polymer, the transformation from polymorph I to polymorph II occurred over time [18].

In the current study, OLZ was selected as model drug because the pseudo-polymorphic transition, resulting in a change of its physico-chemical properties, is triggered by humidity [16] and such conversion towards the hydrate forms caused problems in bioavailability due to the variation on drug solubility of olanzapine [19,20]. Paisana et al. provided some criteria to choose excipients helping on avoiding the formation of metastable phases that may affect the quality of the final product [8]. Among them, thanks to the ability to form specific interactions with drugs, PVP was able to protect OLZ from undergoing hydrate transformation, both in environment at different levels of residual humidity and in solution [21]. Further, a PVP derivative (i.e. PVP VA64) in association with PEO, P188 and P407 was proposed as film forming material to load an amorphous dispersion of OLZ by hot-melt pneumatic extrusion at 160 °C [22].

Beside the physicochemical properties of the choice polymer, the physical structure of the extruded systems prepared with OLZ are a consequence of the drug loading and the processing temperature [23]. Interestingly, no clear relationship was found between dissolution and drug crystallinity or indeed with processing temperature and the Authors concluded that, in this case, the behaviour of the polymer may determine dissolution performance rather than the physical state of the drug [23]. Here, the qualitative composition of ODF was maintained constant, but two different manufacturing processes were selected to investigate the which rule the biopharmaceutical feature of the final dosage form. As expected, the manufacturing process itself can rule a physical transformation in drug solid state. Clearly, the amount of water present in the casted slurry and paste to be extruded is an important factor of OLZ polymorphic conversion and, therefore, dissolution behaviour. It is worthy to underline that those differences were evident only using different dissolution media due to the nature of the drug.

5.5 Conclusion

Based on these results, it is clear that the solvent casting technique favoured the solid-state transition of olanzapine in the prepared ODF, affecting its *in vitro* dissolution patterns which is directly related to its biopharmaceutical performance. On the contrary, the potential of hot-melt ram extrusion printing as ODF preparation method to load drugs that can undergo solid-state modification after exposure to aqueous media, was demonstrated.

References

[1] Menditto E, Orlando V, De Rosa G, et al. Patient centric pharmaceutical drug product design—the impact on medication adherence. Pharmaceutics. 2020;12:1–23.

[2] Casiraghi A, Musazzi UM, Franceschini I, et al. Is propranolol compounding from tablet safe for pediatric use? Results from an experimental test. Minerva Pediatr. 2014;66:355–362.

[3] Cilurzo F, Musazzi UM, Franzé S, et al. Orodispersible dosage forms: biopharmaceutical improvements and regulatory requirements. Drug Discov. Today. 2018;23.

[4] Visser JC, Woerdenbag HJ, Hanff LM, et al. Personalized Medicine in Pediatrics: The Clinical Potential of Orodispersible Films. AAPS PharmSciTech [Internet]. 2017;18:267–272. Available from: http://link.springer.com/10.1208/s12249-016-0515-1.

[5] Khalid GM, Selmin F, Musazzi UM, Gennari CGM, et al. Trends in the Characterization Methods of Orodispersible Films. Current drug delivery (under review)

[6] Musazzi UM, Khalid GM, Selmin F, et al. Trends in the production methods of orodispersible films. Int. J. Pharm. 2020;576.

[7] Polla GI, Vega DR, Lanza H, et al. Thermal behaviour and stability in Olanzapine. Int. J. Pharm. 2005;301:33–40.

[8] Paisana MC, Wahl MA, Pinto JF. Role of moisture on the physical stability of polymorphic olanzapine. Int. J. Pharm. [Internet]. 2016;509:135–148. Available from: http://dx.doi.org/10.1016/j.ijpharm.2016.05.038.

[9] Musazzi UM, Selmin F, Ortenzi MA, et al. Personalized orodispersible films by hot melt ram extrusion 3D printing. Int. J. Pharm. 2018;551:52–59.

[10] Demartin F, Campostrini I, Ferretti P, et al. Fiemmeite Cu2(C2O4)(OH)2•2H2O, a new mineral from Val di Fiemme, Trentino, Italy. Minerals. 2018;8:1–10.

[11] Seager H. Drug-delivery products and the Zydis fast-dissolving dosage form. J. Pharm. Pharmacol. 1998;50:375–382.

[12] Preis M, Woertz C, Kleinebudde P, et al. Oromucosal film preparations: classification and characterization methods. Expert Opin. Drug Deliv. [Internet]. 2013;10:1303–1317. Available from: http://www.tandfonline.com/doi/full/10.1517/17425247.2013.804058.

[13] National Center for Biotechnology Information. PubChem Compound Summary for CID 135398745 Olanzapine. https://pubchem.ncbi.nlm.nih.gov/compound/Olanzapine. Accessed Oct. 11, 2020.

[14] Selmin F, Franceschini I, Cupone IE, et al. Aminoacids as non-traditional plasticizers of maltodextrins fast-dissolving films. Carbohydr. Polym. 2015;115.

[15] Roussenova M, Murith M, Alam A, et al. Plasticization, antiplasticization, and molecular packing in amorphous carbohydrate-glycerol matrices. Biomacromolecules. 2010;11:3237–3247.

[16] Reutzel-Edens SM, Bush JK, Magee PA, et al. Anhydrates and Hydrates of Olanzapine: Crystallization, Solid-State Characterization, and Structural Relationships. Cryst. Growth Des. 2003;3:897–907.

[17] Liu J, Guan J, Wan X, et al. The Improved Cargo Loading and Physical Stability of Ibuprofen Orodispersible Film : Molecular Mechanism of Ion-Pair Complexes on Drug-Polymer Miscibility. J. Pharm. Sci. 2020;109:1356–1364.

[18] Woertz C, Kleinebudde P. Development of orodispersible polymer films with focus on the solid state characterization of crystalline loperamide. Eur. J. Pharm. Biopharm. [Internet].

2015;94:52–63. Available from: http://dx.doi.org/10.1016/j.ejpb.2015.04.036.
[19] Galarneau D. A Case of Teeth Discoloration Upon Transition From Zyprexa to Generic Olanzapine. Ochsner J. 2013;13:550–552.
[20] Samuel R, Attard A, Kyriakopoulos M. Mental state deterioration after switching from brand-name to generic olanzapine in an adolescent with bipolar affective disorder , autism and intellectual disability : a case study. BMC Psychiatry. 2013;13:244.
[21] Paisana MC, Wahl MA, Pinto JF. Effect of polymers in moisture sorption and physical stability of polymorphic olanzapine. Eur. J. Pharm. Sci. [Internet]. 2017;97:257–268. Available from: http://dx.doi.org/10.1016/j.ejps.2016.11.023.
[22] Cho H, Baek S, Lee B. Orodispersible Polymer Films with the Poorly Water-Soluble Drug , Olanzapine : Hot-Melt Pneumatic Extrusion for Single-Process 3D Printing. Pharmaceutics. 2020;12:692.
[23] Pina M, M Z, Pinto JF, et al. The Influence of Drug Physical State on the Dissolution Enhancement of Solid Dispersions Prepared Via Hot-Melt Extrusion : A Case Study Using Olanzapine. J. Pharm. Sci. 2014;103:1214–1223.

Final remarks

All together the collected results demonstrated that hot-melt ram extrusion printing is a suitable technology to design small batches of maltodextrins based ODF, permitting to overcome some limitations associated with the conventional solvent casting and other ODF printing techniques. First, the possibility to prepared ODF in few steps without requiring extra-materials (e.g., drug-loaded filaments, pre-formed ODF substrates, and/or an ink solution) would allow its use with different drug substances, and also in pharmacy setting. The basic formulation can be easily adapted to load high dose drugs in combination with taste masking agents, and/or opacifier. The possibility to use the same basic formulation to design ODF differing in surface area, from 1 to 6 cm^2, would make available personalized doses both for children and adults.

The printing of a single ODF directly on the packaging material also reduces the costs associated to the material waste and time required to cut different sizes, along with the manipulation of the final printed ODF. Among tensile properties, the evaluation of peeling remains one of the most important aspect to correctly handle and administer the films. Beside the possible tests to evaluate this property, it was also proposed the use of a nanofiller, namely titanium dioxide, used as an opacifier, to lower the forces required to peel-off ODF

Being a solvent-free technology, hot-melt ram extrusion printing can also be used to load drugs that can undergo solid-state modifications after exposure to a solvent system, as demonstrated using olanzapine as a model drug. At the same time, the use of relatively low temperature allows to prepare ODF with drug sensitive to thermal stress, such as diclofenac.

However, to make this technology a real opportunity in the field of dose personalization, the focus should now be towards the development of non-destructive methods carried out without the need of intensive training or specialized equipment. As an example, thumb tack test and folding endurance can be proposed to guarantee the mechanical quality of ODF prepared on-demand, since these tests can be easily performed by a well-trained pharmacist. Meanwhile, many efforts are still required to have tools to identify and determine the uniformity of drug content in small batches of ODF extemporaneously prepared.

Acknowledgements

Acknowledgements

Those that cannot remember the past, are condemned to repeat it! I, therefore, dare not to forget all those that contributed to the success of this Ph.D.

I would like to start by thanking my supervisor, Professor Francesca Selmin, for her thoughtful guidance. Your objective critiques made me became not only an independent researcher but also independent in so many spheres of life. Special gratitude also to the person whose thoughts and a strong belief in my humble ability kept me on the track of this Ph.D. journey right from day one. This is no other person but Professor Paola Minghetti, you inspired me from my first day of admission to the end, thus, I dedicate this entire Ph.D. to your memory. Professor Francesco Cilurzo, you represent such a humble personality, sharing knowledge and experience with the students in a very simple manner. I thank you most sincerely for the special weekly lessons you organized for me on biopharmaceutics and many aspects of pharmaceutical technology. Thank you, Professor Antonella Casiraghi, for your help with some documents on EU regulations regarding paediatric formulations at the onset of my Ph.D. program. Dr. Paulo Rocco, I enjoyed your lessons on EU Institutions and EU Pharmaceutical Laws, thank you for the virtual tour.

To the people I was actively engaged with within the lab, special thanks to Dr. Umberto Musazzi, I have learned a lot from you. You should know that little compliment “good work” you used to say whenever I achieved some experimental results, means so much to me; it’s like a recipe for motivation. Thank you, Dr. Chiara Gennari, Dr. Silvia Franzè, Dr. Gaia Quaroni, and Dr. Giulia Magri for your active supports. You helped me in so many ways, I enjoyed most especially those ends of the year dinners. To all the undergraduate lab students I worked with from 2017 to 2020, big thank you for the company and friendship.

I will not close this part without thanking Professor Francesco Demartin and Professor Marco A. Ortenzi of the Department of Chemistry, Università Degli Studi di Milano, for the remarkable multidisciplinary collaboration we had on this project.

Family means a lot in our lives, therefore, special thanks and gratitude to my mum and dad for your moral and spiritual support. To my brothers, sisters, and friends, your valuable support is undoubtedly most cherished.

Finally, to my lovely wife Hauwa, and our adorable daughter, Fatima Zahra, thank you for your patience and understanding. I am very proud and blessed to have you as my inner circles especially during my Ph.D. study.